The Mitochondrial Role in Calcium Metabolism and Differential Calcium Buffering Capacity of Amyotrophic Lateral Sclerosis (ALS) Vulnerable and Resistant Motoneurons from Mice

Dissertation
zur Erlangung des Doktorgrades
der Mathematisch-Naturwissenschaftlichen Fakultäten
der Georg-August-Universität Göttingen

vorgelegt von

Saju Balakrishnan

aus Ollur, Kerala (Indien)

Göttingen 2006

D7
Referent: **Prof. Dr. Reinhold Hustert**
Koreferent: **Prof. Dr. Friedrich-Wilhelm Schürmann**

Tag der mündlichen Prüfung:

Dedicated to my Parents & Sister

Contents

Abbreviations

aCSF	artificial Cerebrospinal Fluid
ALS	Amyotrophic Lateral Sclerosis
AM	Acetoxy Methyl
AMPA	α-amino-3-hydroxy-5-methyl-4-isoxazole propionic acid
ATP	Adenosine Triphosphate
BAPTA	1, 2-bis (o-aminophenoxy) ethane-N,N,N',N'-tetraacetic acid
$[Ca^{2+}]i$	Intracellular Calcium concentration
CCD	A charge-coupled device
CCS	Copper chaperone for SOD1
CN	Cyanide
CNQX	6-cyano-7-nitroquinoxaline-2, 3-dione disodium salt
COX	Cytochrome c oxidase
CPA	Cyclopiazonic acid
^{o}C	Grade Celsius
D-AP-5	D(-) 2-amino-5-phosphonopentanoic acid
DMSO	Dimethylsulfoxide
DNA	Deoxyribonucleic acid
et al	et alteri (and others)
FCCP	Carbonyl cyanide 4-trifluromethoxyphenylhydrazone

FMN	Facial motoneuron
GluR2	Glutamate Receptor 2
G93A	Glycine to alanine at position 93
GΩ	Giga Ohm
HEPES	4-(2-Hydroxyethyl)piperazine-1-ethanesulfonic acid
HMN	Hypoglossal Motoneuron
kDa	Kilodalton
kHz	Kilo Hertz
max	maximum
min	minimum
MNs	Motoneurons
mosmol	milliosmol
mRNA	messenger Ribonucleic Acid
mSOD1	mutant Superoxide dismutase 1
mV	millivolts
μ	micro,-$(_x 10^{-6})$
NF	Neurofilament
nm	nanometer
nM	nanomolar
NMDA	N-methyl D-aspartate
OMN	Oculomotor Neuron
ONOO-	peroxynitrite ion
Rhod-123	Rhodamine-123
ROI	Region Of Interest
ROS	Reactive Oxygen Species

s	second
SOD1	Superoxide Dismutase 1
TMN	Trochlear Motoneuron
TTX	Tetrodotoxin
UV	Ultraviolet

Chapter 1

Introduction

1.1 Motoneurons and Amyotrophic Lateral Sclerosis (ALS)

Motoneurons innervate muscle cells and thereby regulate different body muscles. They are organized in the central nervous system into definite motor nuclei along the brainstem and spinal cord (Lower Motoneurons, LMN). A motoneuron supplies its axon to a specific muscle where it innervates a few muscle fibers. This aggregate, a motoneuron and the muscle fibers it innervates, is called a 'motor unit'. Spinal and brainstem motor units are capable of performing and coordinating most of the complex motor patterns, but the neurons of the cerebral motor cortex are also needed to yield an accurate motor behaviour. These neurons which send their axons either to the medulla region of the brain stem or to the ventral horn of the spinal cord are called the Upper Motoneurons (UMN). They represent the center for coordinating the motor function ensemble to produce a well poised and goal-oriented output.

Amyotrophic Lateral Sclerosis (ALS) is a lethal neurodegenerative disease that specifically affects the upper and lower motoneurons. ALS was first described in 1869 by the French neurobiologist Jean Martin Charcot. It involves motoneuron loss in the brainstem and spinal cord, leading to progressive muscle weakness and atrophy. Generally ALS is a late onset disease; the age group involved being 50 to 60 years, though there are rare reports of juvenile onset. The prevalence of ALS is 1-2 in 100.000 persons per year. ALS is also commonly known as Lou Gehrig's Disease after the famous U.S baseball player who fell victim to the disease. The word *amyotrophic* is derived from Greek meaning 'no nutrition for the muscles'. *Lateral sclerosis* indicates the 'atrophy and hardening of the lateral parts of the spinal cord' as a result of massive motoneuron death.

The salient clinical feature of ALS is the loss of muscle strength due to neurogenic muscle atrophy leading to difficulties in performing voluntary and involuntary movements including locomotion, breathing, swallowing and speech. As the disease progresses, extreme muscle wasting and spasticity develop in arms, legs and oropharyngeal muscles. The symptoms of ALS depend on the variable percentage of involvement of upper and lower motoneurons. LMN involvement results in weakness, fatigue, muscle atrophy and loss of reflex reaction, whereas UMN damage causes untimely reflex responses, stiffness and slowing of movements. 'Sporadic' ALS (SALS) is the most prevalent form of ALS, and the genetic

variant (Familial ALS or FALS) represents a minor fraction (~10%) of all ALS cases. There are no apparent differences in the onset and disease progress between both types. Hence it is plausible that both forms of ALS have common etiology (Brown & Robberecht, 2001). In both forms of ALS, death usually results from respiratory failure and survival possibilities are not dependent on either age or gender.
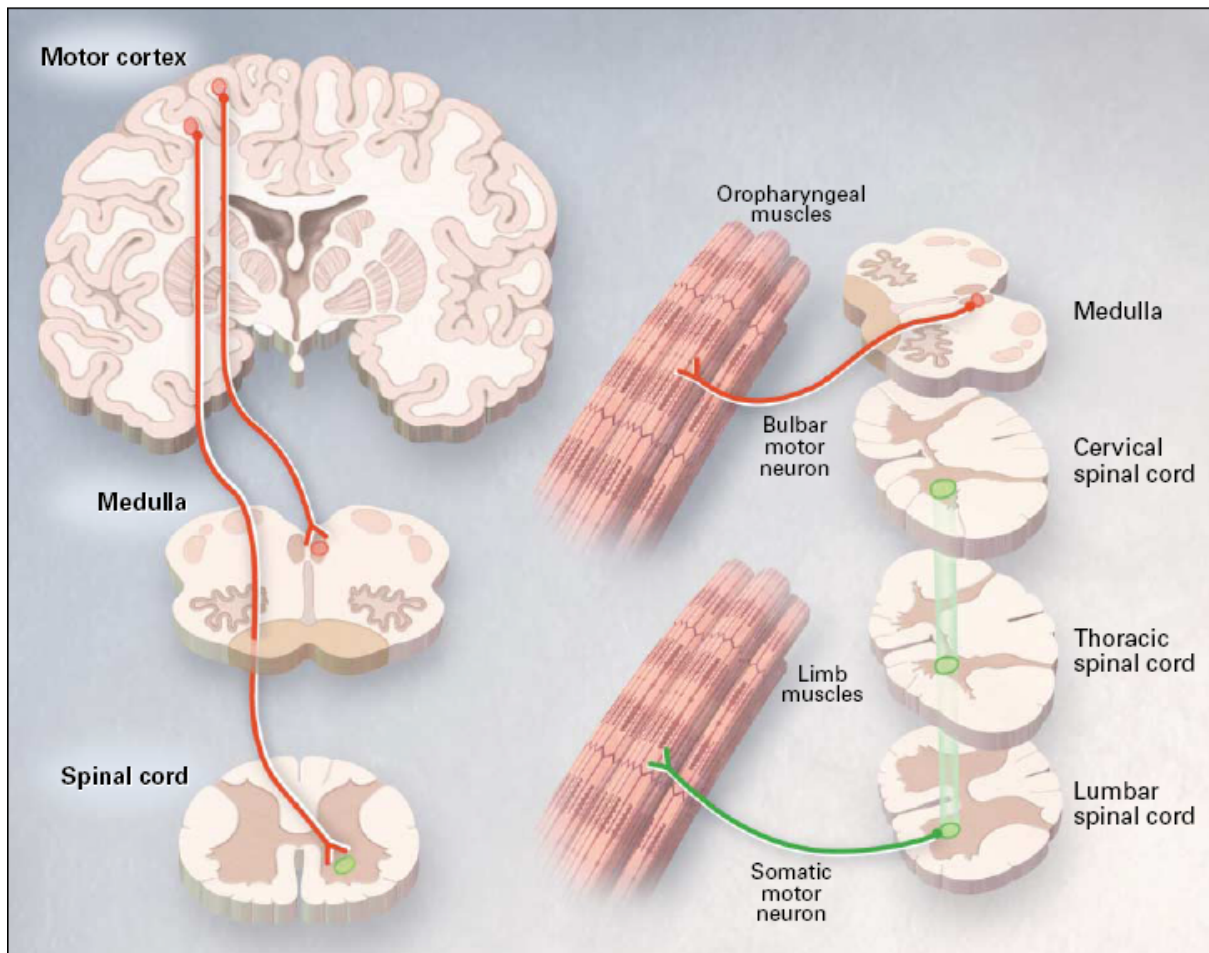
Fig 1.1. The motoneurons in the motor cortex, brainstem motoneurons in the motor nuclei and motoneurons of the ventral horn of spinal cord are seen to degenerate in ALS. (adapted from Rowland & Schneider).

1.1.1 Sporadic ALS (SALS)

Most forms of ALS lack an abnormality in the genetic constitution of the patient. The trigger for sporadic neurodegeneration is still evading scientific research and the reason for motoneurons being specifically targeted is also yet to be understood. Several possible

pathomechanisms have been put forward by several research groups around the world, namely Glutamate excitotoxicity (Rothstein et al, 1992; Heath and Shaw, 2002; Guo et al 2003), Disruptions in the Ca^{2+} Metabolism (Llinas et al, 1993; Appel et al, 1994, 1995), Mitochondrial Malfunction and Deformities (Bowling et al, 1993; Kong & Xu, 1998) and Disorganisation and Atypical Accumulation of Neurofilaments in the Cytoplasm in soma as well as in the axonal branches (Figlewicz et al, 1994). Motoneuron damage in sporadic ALS is also accompanied by prominent reactive gliosis. Gliosis is an evident phenomenon in many of the neurological disorders including stroke; as the neurons die through damage, they are replaced by glial cells.

1.1.2   Familial ALS (FALS)

Approximately 10% of all ALS cases are inherited as an autosomal dominant family trait. Among this genetic form of ALS, ~20% is characterized by one or more of the several known mutations of the ubiquitous reactive oxygen radical scavenging enzyme, Cu/Zn Superoxide Dismutase, SOD1 (Rosen et al, 1993, 1994). At present more than 60 mutations are reported for SOD1, leading to specific motoneuron degeneration. Although it represents only ~10% of incidences, the familial form of ALS is more studied as a model, as the obvious genetic factors involved have already been discovered. The only animal model available at present for the study of ALS pathogenesis is based on the SOD1 mutations. The first such mouse model was developed by Gurney et al in 1994 through the over expression of human SOD1 carrying a mutation of glycine to alanine at position 93. However, the alanine 4 to valine mutation on exon1 of the SOD1 gene is described as the most commonly detected and one of the most clinically severe mutations reported in ALS cases (Rosen et al, 1994).

1.2 Pathology of ALS- Details of Metabolic Malfunction

1.2.1 Glutamate excitotoxicity

Studies conducted in the middle of the last century have discovered glutamate as the major neurotransmitter for fast-signal conduction in the spinal cord and major brain areas. At present, glutamate is known as the dominant excitatory neurotransmitter in the central nervous system. In the neurons, glutamate is synthesized and stored in the synaptic nerve components and is released in response to a depolarization of the neuron. In general, upon release into the synaptic cleft, the glutamate excites the receptors on the post synaptic neuron thus conducting the excitatory signal. The excess glutamate present in the synaptic cleft is actively removed by specialized transporters on the perisynaptic glial cells to terminate the excitatory signal. Glutamate clearance transporters are also found on neurons. To date several glutamate transport molecules have been identified. The human types of these transporters are called Excitatory Amino Acid Transporters (EAAT) 1-5, of which EAAT-2 is the most important one and is exclusively located in the glia.

The participation of glutamate transporters in the etiology was shown by the findings in which rats expressing anti-sense oligonucleotides for GLT-1 (homologue of EAAT-2) displayed elevated extracellular glutamate concentration and suffered from neuronal injuries along major regions of the brain. The glutamate transporter knockout-mice also had high glutamate levels in the synapses, suffered from spontaneous lethal seizures and showed poor motor control (Cluskey & Ramsden, 2001). Significant reduction (30-90%) of the EAAT-2 protein synthesis has been reported in most sporadic ALS post-mortem samples as compared to normal specimens. As an adaptive response to the building imbalance in the glutamate metabolism, it has been observed that both EAAT-1 and EAAT-2 expression increased in astrocytic feet attached to the degenerating motoneurons during early stages of the disease. The specific loss of EAAT-2 type glutamate transporters in ALS cannot be attributed to the betiding cell death, as no damage to the astroglial cells is obvious and there is even gliosis prevailing in response to motoneuron death. On the other hand the knock down of EAAT-2 expression was able to cause neuronal deterioration and resulted in a motoneuron disease

phenotype. It is confirmed that EAAT-2 reduction is not because of the reduction of the synthesis of corresponding mRNA; rather, the causal factor lies in the abnormalities of translation or post-translational processes (Morrison et. al 1999).

Excessive activation of glutamate receptors succeeds the event of over accumulation of glutamate in the synapses. The situation is further aggravated in ALS by the denoted abnormal rearrangement of glutamate receptor components which result in erroneous ionic influx. The motoneurons are densely supplied with NMDA (N-methyl D-aspartate) and AMPA (α-amino-3-hydroxy-5-methyl-4-isoxazole propionic acid) glutamate receptors. The NMDA receptor mediated neurotransmission is characterized by a slow rise time and relatively slow decay and are involved in functions like rhythmic motor activity, the embryonic nervous system development and in learning and memory functions (LTP generation). AMPA receptors undertake most quick excitatory transmissions required especially for active motor function. The component subunits constituting the AMPA receptor are of particular interest with regard to pathology in ALS. AMPA receptors are comprised of four subunits termed GluR 1-4. In usual conditions the GluR2 subunit is a component in the AMPA receptor complex, which renders them particularly impermeable to calcium. On the other hand AMPA receptors lacking the GluR2 subunit are permeable to calcium and thereby can allow the massive calcium entry. These AMPA receptors which lack the GluR2 subunit are reported to be expressed and distributed on the motoneuron plasma membrane and are projected to be the major factor determining the selective vulnerability of motoneurons by causing excessive Ca^{2+} entry leading to excitotoxic injury even at normal extracellular concentrations of glutamate.

1.2.2 Mitochondrial abnormalities

Mitochondria play a pivotal role in determining the life and death of a cell inhabiting them. Mitochondrial functional abnormalities and swelling has been reported in sporadic ALS motoneurons (Beal MF, 2000). Dysfunction of the mitochondria can trigger motoneuron death through Ca^{2+} accumulation and Ca^{2+} mediated excitotoxicity by offensive build up of reactive oxygen species and by initiating apoptotic pathways. Complicated morphological and biochemical abnormalities of mitochondria in motoneurons and muscles are observed in

sporadic human ALS cases. Malfunction of the electron transport chain as well as compromised mitochondrial DNA structure and quantity have also been detected in ALS biopsies (Vielhaber, 2000). It is known that neuronal metabolism is extremely sensitive to ischemia. As mitochondria are the energy sources for cellular activities, their impairment can lead to lethal energy deficits resulting in compromised neuronal functions. Lack of supply of required energy can result in the loss of integrity of neuronal cell membranes, leaving them permeable to ions and water to cause damage. Detailed studies on mouse models of ALS also revealed the presence of wide mitochondrial swelling and loss of structural and functional integrity. Although the precise mechanism through which mSOD1 causes mitochondrial swelling and malfunction has still to be ascertained, the presence of mSOD1 in the mitochondrial intermembrane space and within the mitochondria has opened a wide range of fields to explore. In spinal cord sample studies of sporadic ALS victims, diminished activity of Cytochrome c oxidase (COX) and therefore impaired mitochondrial respiration was denoted (Fujita et al, 1996; Borthwick et al 1999). Localization of a significant fraction of SOD1 into intermitochondrial space thereby causing toxicity, and the inhibition of mitochondrial respiratory metabolism is also reported in transgenic ALS mice models (Higgins et al 2002, Mattiazzi et al 2002, Liu & Cleveland, 2004)   A recent research report exemplifies the submitochondrial abnormality in G93A mice. Cytochrome c in the brain of G93A mice shows a reduced association with the inner mitochondrial membrane as per this investigation (Kirkinezos & Moraes, 2005). This study also points out the increased peroxidation of mitochondrial lipids (e.g. Cardiolipin) in this mSOD1 mouse line. The prevailing instability of mitochondrial proteins can be significant in determining the 'switching on' and progression of neuronal apoptosis, as apoptotic pathways employing mitochondrial changes have been associated with the neurodegeneration in G93A mice and in sporadic ALS events (Guegan et al 2001).

1.2.3 Mutation of Copper-Zinc superoxide dismutase (SOD1)

Superoxide dismutase 1 (SOD1) is a ubiquitously expressed copper & zinc containing homodimeric enzyme with a molecular weight of 17 kDa. SOD1 is predominantly a cytosolic protein but some exceptional localization of SOD1 to the intermembrane space of mitochondria was reported in the seventies. Even though this discovery was controversial

recent works on different mouse models provide evidences for a localization of endogenous SOD1 protein as well as exogenously expressed normal and mutant SOD1 protein within mitochondria in the CNS (Higgins et al 2002).
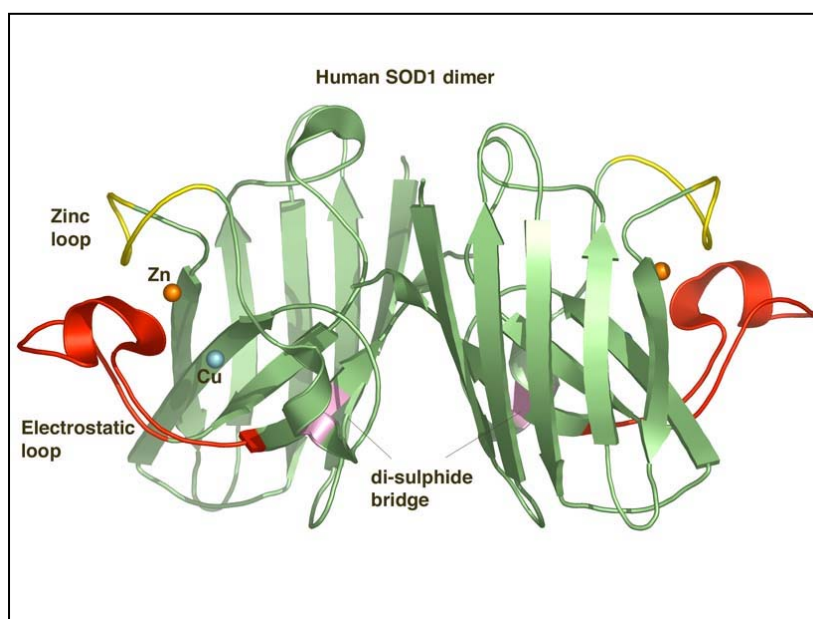
Fig 1.2.3. Superoxide Dismutase is a homodimeric metalloenzyme with each monomer containing 153 amino acids, one Copper and one Zinc ion. The molecule is folded into 'beta barrel' structure consisting of eight anti-parallel twisted beta sheets. The copper and zinc ions are each held in place by hydrogen bonding to four amino acid side chains in a roughly tetrahedral arrangement.

SOD1 forms the crucial component in the detoxification of reactive oxygen radicals. The critical enzymatic reaction catalyzed by SOD1 converts the toxic superoxide radical into hydrogen peroxide (which is detoxified by the enzyme catalase) and molecular oxygen.

$$2O_2^- + 2H^+ \xrightarrow{\text{Cu Zn SOD1}} O_2 + H_2O_2$$

The gene encoding SOD1 in human beings is located on chromosome 21q22.1. SOD1 is an abundant protein in the central nervous system contributing about 1% of the total brain protein. To date more than 100 point mutations of human SOD1 gene has been reported in familial ALS spanning all five coding exons of the gene. According to Ramsden & Cluskey, approximately 35% of the familial disease occurrence is due to either Guanine (G) to Adenine (A) or Adenine to Guanine mutations on the sense strand. Further 10% can be accounted to similar mutations on the antisense strand and consequent modification (Cytosine (C) to Thymine (T) and Thymine to Cytosine) of the sense strand by DNA repair enzymes. Mutant SOD1 transgenic mice that develop a disease pattern which clinically and pathologically resembles human ALS are developed and widely used for ALS research. The most extensively studied are mice with G93A, G85R (Glycine to Arginine at position 85) and G37R mutations. Transgenic rats carrying G93A or H46R (Histidine to Arginine at position 46) SOD1 mutations are also developed and show ALS phenotype. There was an early focus on a 'loss of activity' of the SOD1 enzyme as a result of these mutations to be responsible for the disease. This was disproved by the studies revealing the intact functional activity of the mutant SOD1 enzyme. Different transgenic mouse lines expressing familial ALS linked human SOD1 mutations and one transgenic line expressing mutation in the mouse SOD1 gene clearly showed that the disease in mouse is not due to loss of function, but rather from a gain of new toxic functions. This was further supported by the absence of motor neurone disease in SOD1 knock out mice.

There are some proposed hypotheses about the toxic property gained by the mSOD1. Beckman et.al (1990) proposed that the mutant SOD1 is not folded correctly that it uses peroxynitrite (ONOO-) as the substrate instead of superoxide and converts it to highly reactive nitronium (NO^{2+}) intermediate which can readily react with tyrosine residues of proteins and damage them. This mechanism is suggested as nitric oxide production can occur through the activation of nitric oxide synthase during injury. Further supportive evidence comes from the data showing an elevated oxidative damage to proteins and in sporadic ALS patients (Bowling et at, 1993), familial ALS patients (Said Ahmed et al, 2000), in transgenic G93A-SOD1 mice (Liu et al, 1998, 1999) as well as in cell cultures expressing the G93A mutant vector (Liu et al 1999). Reactive oxygen radicals also target the mitochondrial DNA and cause damage as shown by Warita et al (2001) in the spinal cord of transgenic ALS mice. A second hypothesis proposed by Bredesen et al focuses on the capacity of mSOD1 to use hydrogen peroxide as a

substrate to generate highly toxic hydroxyl radicals that can destroy mitochondrial membranes by lipid peroxidation and glutamate transporters by oxidation. Oxidative stress in the mutant SOD1 expressed environment also can lead to abnormal accumulation of mSOD1 molecules as shown in an exogenously expressed model of *Caenhorabditis elegans* (Oeda et al, 2001). High population of oxidative radicals also can lead to the inhibition of degradation of mutant SOD1 leading to the formation of aggregates (Bruijn et al, 1998). Reduced affinity of mSOD1 for binding the Copper atoms has also been proposed to be involved in exaggerating the oxidative stress, as free copper ions can participate in abnormal oxidative reactions (Carri et al 2003) and peroxidation reactions (Bush et al, 2002). However the participation of copper bound to the active site of SOD1 in the pathogenesis is disproved.

1.2.4 Erroneous neurofilament assembly and accumulation

Neurofilament (NF) aggregation in the motoneurons is also a pathological hallmark of sporadic ALS. Neurofilaments are major structural elements of the neuronal cytoskeleton which determines the cell shape and structure and the calibre of neuronal projections and are also thought to confer some selective pathological mechanism in ALS causing the demise of motoneurons specifically. Neurofilament subunits are synthesized and organised in the cell body and are transported along the axon by slow component of the axonal transport. Martinez et al (2005) has reported the observation of cytoplasmic inclusions and high immunoreactivity for all the neurofilament subunits in the perikarya of atrophic and preserved motoneurons from ALS autopsy specimens. They also demonstrate the occurrence of dilated axons with neurofilament heavy chain immunoreactivity. It is proposed long ago that in sporadic ALS the motoneurons with large calibre axons are at particular risk (Kawamura et al 1981). The discovery of accumulation and aberrant assembly of neurofilaments as salient pathological features of both familial and sporadic ALS (Hirano et al, 1984; 1991) pointed out that neurofilament disarray can contribute to the onset and development of the disease. Wide genetic manipulative research using over expression or deletion of various neurofilament subunits in mutant SOD1 mice have confirmed the role of neurofilament abnormalities in ALS.

Study on G93A mutant SOD1 mice spinal motoneurons revealed that there is increased population of neurofilaments and mitochondria in the axon hillock and initial segment of these motoneurons and proves that this abnormality continues as the transgenic mice ages, as compared to normal mice (Sasaki & Iwata, 2005). These findings suggest that there is impairment in both slow transport of neurofilaments and fast transport of mitochondria in the axonal hillock and initial segment of the G93A mutant SOD1 even before the onset of disease.

1.2.5 Protein aggregation

Presence of atypical protein aggregates is a hallmark of major neurodegenerative diseases, amyloid and tau in Alzheimer's disease, α-synuclein in Parkinson's disease and huntingtin in Huntington's disease. Wide occurrence of well noticeable cytoplasmic inclusions are a typical characteristic of motoneurons and surrounding non-neuronal cells in human ALS and the established mouse models of ALS (Bruijn et al 1998). Further interesting is the high immunoreactivity of these aggregates for SOD1 protein in the mouse model samples. The mutated SOD1 is sufficiently unstable and it precipitates to form aggregates. This undesirable property is of significance as SOD1 is expressed in abundant levels in a cell, representing approximately 1% of cytosolic protein. There is intense debate over whether this aggregate accumulation contributes to the death of motoneurons or they represent the cell's protective machinery in the ALS pathology. There are suggestions that these protein clumps formation is beneficial to the cells by binding potentially toxic mutant or ill folded proteins, or they could be harmless bystanders. On the other hand there are several hypotheses out forward to prove that these aggregates are toxic to the cell. These aggregates may sequester other normal functional proteins required for cellular function. For example presence of CCS (copper chaperone for SOD1) in these aggregates indicate that there could be a depletion of this protein in the cytoplasm thereby leaving the SOD1 molecules copper depleted and possibly the build up of free copper ions. The rigorous misfolding of SOD1 molecules can reduce the availability of chaperone proteins required for the proper folding and structural completeness of vital proteins. This immense accumulation of erroneous protein molecules also can push the protein turn over machinery (proteasome) to the limits. Inhibition of intracellular organelles like

mitochondria by the SOD1 containing inclusion through accumulation within or on the organelles is also suggested.

1.2.6 Calcium related abnormalities in ALS

Calcium ions serve the function of second messenger in many neuronal signal transduction pathways. A precise regulation of the calcium signals and the following cellular pathways are achieved through spatial localization, proper extrusion mechanisms, uptake by intracellular organelles and the endogenous buffering of these calcium ions. Compromised Ca^{2+} homeostasis is one of the major pathophysiological abnormalities evidently involved in neurodegeneration in ALS. It has been proposed that glutamate induced excitotoxicity mediated by uncontrolled elevation of cytosolic calcium, is a predominant factor underlying motoneuron degeneration in ALS (Roy et. al., 1998), (Schinder et al., 1996). Williams et al (1997) have shown that the spinal motoneurons affected by ALS lack the GluR2 subunit of AMPA receptors, which makes them particularly permeable to calcium. A more detailed investigation has revealed an exceptionally low concentration or lack of a number of calcium-binding proteins, such as Calbindin-D(28kDa) and particularly parvalbumin in ALS-vulnerable motoneurons (Alexianu et al,1994; Elliot & Snider, 1995; Dekkers et al, 2004), which can be a risk factor leading to pathological signal cascades triggered by calcium. Furthermore, there is evidence of a differential calcium buffering capacity in vulnerable and resistant motoneurons in ALS. Vanselow & Keller (2000) has reported a comparatively higher calcium buffering capacity in oculomotor neurons which are spared in ALS than in the vulnerable hypoglossal motoneurons (Lips & Keller, 1998). Although precise molecular factors responsible for the disease are still unknown, disrupted calcium homeostasis has been shown in both clinical and animal models of the disease. It is proposed that in sporadic ALS, the accumulation of several of these pathomechanisms occurs from the birth of an individual and the disease commences when these errors can no longer be contained.

1.3 Mitochondria and Ca^{2+} metabolism

The influx of calcium through the different types of voltage and ligand gated calcium channels and the induction of calcium release from the intracellular organelles contribute to the generation of an intracellular calcium signal. On the other hand, the extrusion mechanisms, represented by the plasma membrane calcium ATPase and the Na$^+$/Ca^{2+} exchanger, and accumulation by intracellular organelles contribute to the removal of calcium ions. Apparently, in the last decade, the attention was drawn to the role of mitochondria as an efficient regulator of cytosolic calcium signals (Rizzuto et al 1992; Rutter et al 1996; Mostafapour et al 1997; Shishkin et al 2002; Gunter et al 2004). Mitochondria in neurons are now shown to accumulate considerable amounts of calcium ions during or immediately after a cytosolic calcium transient, even though the calcium content of mitochondria in resting cells is thought to be low (Babcock et al., 1997; Pivovarova et al., 1999; Wang et al., 2002; Ward et al., 2005). Measurements with mitochondrially targeted calcium probes indicate a rapid, dramatic increase in free intramitochondrial calcium (Rizzuto et al. 1992, 1993; Rutter et al. 1993). This uptake by mitochondria has an immense effect on the metabolic state of the cell as it can upregulate the activity of the enzymes in the oxidative metabolism (Rizzuto. 1994, 2003; Rutter et al. 1996).

1.4 Mitochondria and ALS

Chronic mitochondrial membrane potential depolarisation due to Ca^{2+} entry can cause the release of pro-apoptotic proteins and activate the enzymes involved in apoptotic pathways (Murphy et al., 1999; Budd et al., 2000; Darios et al., 2003; Rosenstock et al., 2004; Pivovarova et al., 2004; Henry-Mowatt et al., 2004). Motoneurons contain both NMDA and non-NMDA glutamate receptors and are found to be particularly vulnerable to calcium influx following glutamate receptor activation. The damage culminates through an increase in mitochondrial calcium load leading to the build up of toxic reactive oxygen species (ROS) from boosted mitochondrial metabolism (Carriedo & Weiss, 2000; Hongpaisan et al., 2004; Kahlert et al., 2005), which act on intracellular as well as extracellular targets and have varied and devastating consequences (Fig 1.4). Abnormalities in mitochondrial structure have been

found to be one of the cellular changes in the post mortem human ALS samples (Sasaki & Iwata, 1996). Kong and Xu have revealed the existence of massive vacuoles derived from degenerating mitochondria in the motoneurons of G93A SOD1 mutant mice as an early event in the motoneuron degeneration.
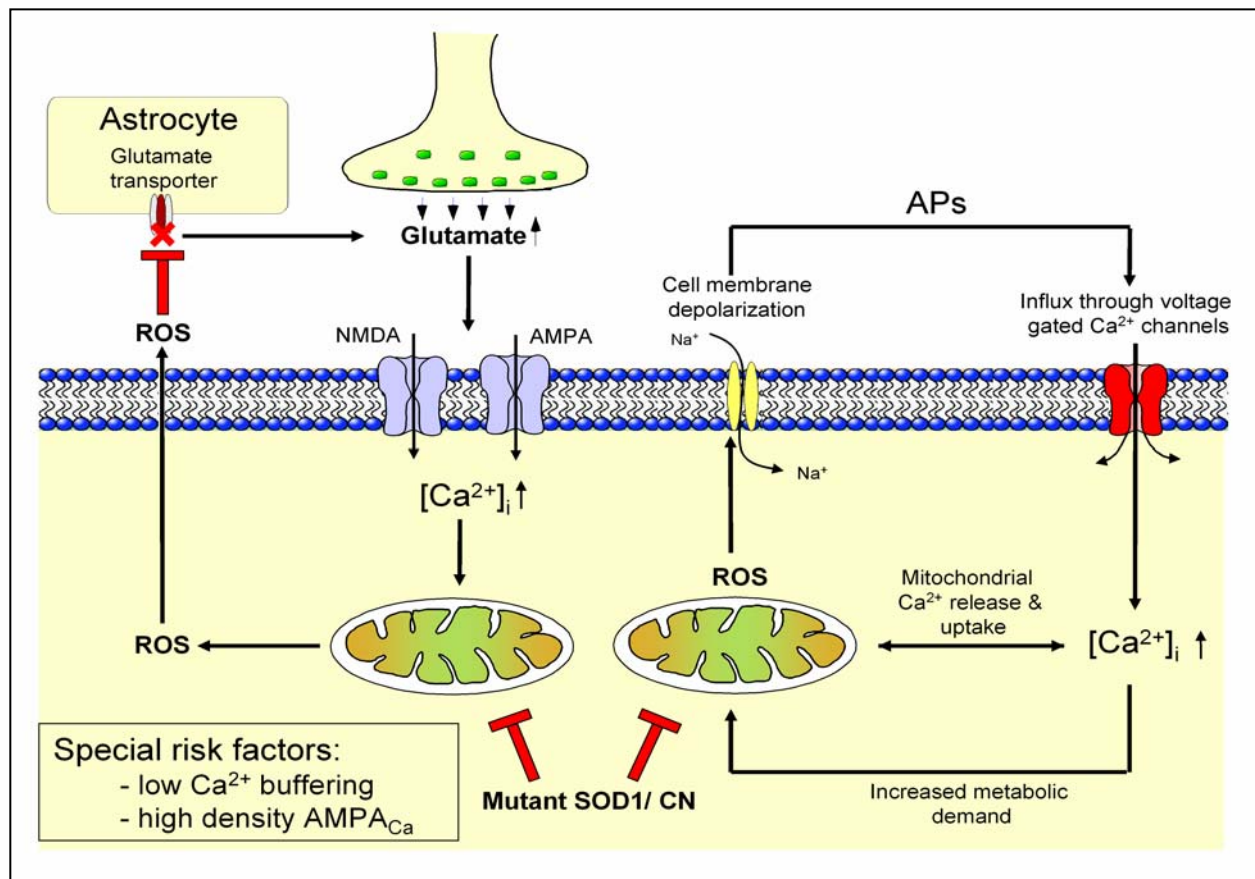
Fig 1.4. Mitochondrial disturbance is predicted to be the key trigger to the ALS etiology. The rampant production of reactive oxygen species (ROS) by disturbed mitochondrial metabolism can be readily cytotoxic as ROS can destroy the membrane integrity by averting the specificity of membrane channels or triggering the opening of particular leak channels as well as by destroying the lipid components of the membrane. It is also hypothesised that ROS produced in motoneurons can escape to the extracellular environment and can damage the glutamate transporters on astrocytes (Rao & Weiss, 2004).

1.5 Objective of the study

The present study endeavours to gain more information about the intricacies of calcium metabolism of brainstem motoneurons in general and to study the prowess which permits particular neurons to resist damage, making the neurodestruction in ALS selective. Previous results have revealed the differential calcium buffering capacity in ALS vulnerable and resistant motoneurons (Lips & Keller, 1998; Vanselow & Keller 2000), the buffering capacity being low in vulnerable types (e.g. HMNs). This indicates the existence of some other mechanism in effectively controlling and synchronising the calcium transients during neuronal activity. The plausible role of mitochondria in calcium control was closely examined by conducting whole cell patch clamp recordings and CCD Ca^{2+} imaging on neonatal mouse brainstem slice preparations. The impact of mitochondria in controlling cytosolic Ca^{2+} was investigated using FCCP as an effective drug to avert mitochondrial potential and metabolic pathways. Expansion of the buffering capacity studies into other brainstem motoneuron populations like facial, trochlear and dorsal vagal neurons was conducted with the aim of understanding their survival differentiability in the ALS attack.

Chapter 2

Materials and methods

2.1   Experimental set-up

All the experiments were performed using the set-up installed in the physiology institute in Göttingen. The set-up consists primarily of an upright microscope (Axioscope, Zeiss, Göttingen Germany), a monochromator as light source for imaging (Till photonics, Graefelfing, Germany), a CCD camera for fluorescence signal detection (Till photonics, Graefelfing, Germany), and instruments for patch clamp recording. The holding chamber for brain slices was fixed on the microscope stage and it allowed X&Y axis manipulations. In addition to that the microscope table was also mobile in the XY axis allowing further flexibility to observe the preparation. Dye loaded brainstem slices were exposed to the excitation wavelength from monochromator through an optic cable directed to the suitable dichroic mirror and filters. The camera was fitted on the microscope allowing direct emitted light capture from the sample under the microscope objective. The microscope and associated instruments were mounted on an air-suspension table surrounded by a Faraday cage in order to prevent vibration and electric noise. The holding chamber was provided with tubing (Tygon®) for continuous perfusion with aCSF (artificial cerebrospinal fluid). The imaging experiments and optical manoeuvres were conducted using a 63X water immersion objective (Achroplan, Zeiss).

2.2   Preparation of slices

Brainstem slices were obtained from 1-4 days old NMR1 mice. Animal experiments were carried out in accordance with the guidelines of the Ethics Committee of the University of Göttingen. Animals were decapitated; brains were carefully dissected out and were quickly transferred to cold (4^0C) aCSF (in mM: 118 NaCl, 3 KCl, 1 $MgCl_2$, 25 $NaHCO_3$, 1 NaH_2PO4, 1.5 $CaCl_2$, and 30 Glucose), pH 7.4, 325 mosmol l^{-1}; and was bubbled with carbogen (95% O_2, 5% CO_2). Transverse slices of the brain stem with a thickness of 200-250μm were cut using a Leica VT 1000s vibroslicer (Leica instruments GmbH, Nussloch, Germany). Slices were cut with extreme care and were maintained at optimal conditions to preserve the intactness of the cells at slice surface. Mechanical disturbances during slice preparations were minimized by performing slicing at low temperatures and optimizing the

metabolic conditions by sufficient oxygen supply. All the experiments were conducted at 24-27^{0}C.

2.3   Identification of brain stem nuclei

Different motoneuron areas were visually identified by their location close to other prominent brain areas with the help of 'the Mouse Brain' atlas by Franklin & Paxinos (Academic press) while cutting the brainstem transversely. Nucleus hypoglossus (12) and dorsal vagus nucleus (10) being located close to the fourth ventricle / central canal; oculomotor nucleus and trochlear nucleus-close to aqueduct and red nucleus, and facial nucleus being at the level of fourth ventricle opening. During patch clamp experiments suitable MNs were identified by their general morphology and/or extensive dendritic arborisation, and their ability to fire action potentials in TTX free solution (Bergmann & Keller, 2004).
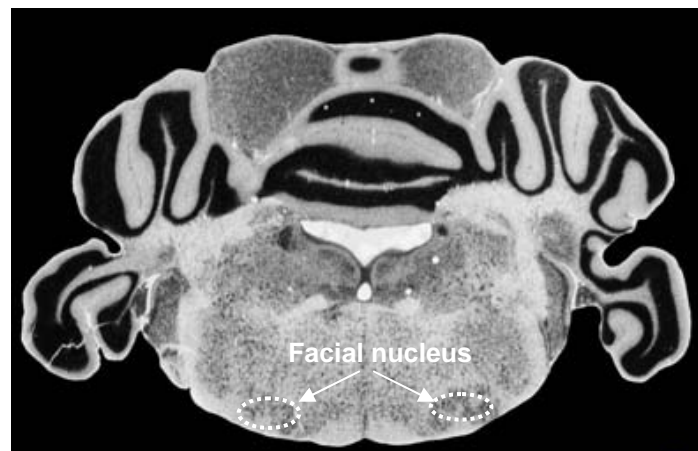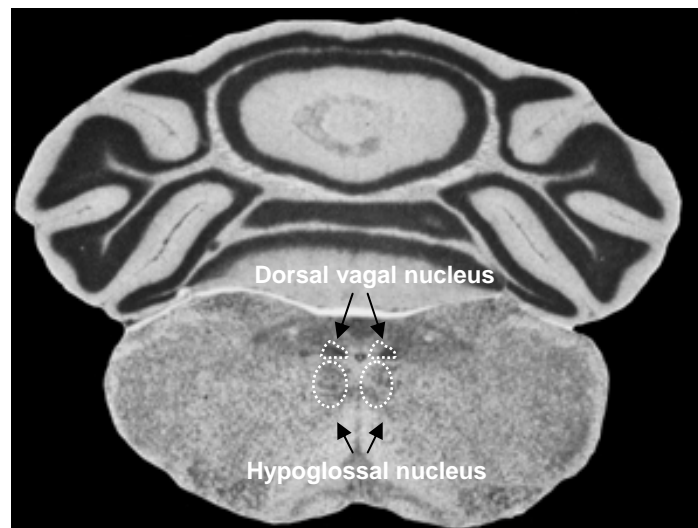
C
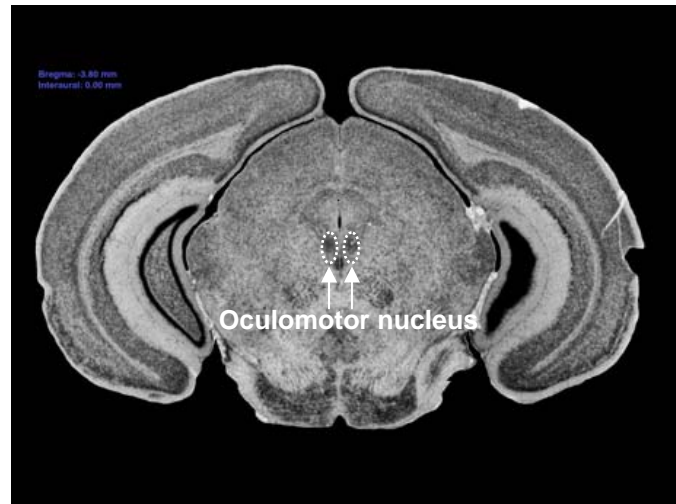
D
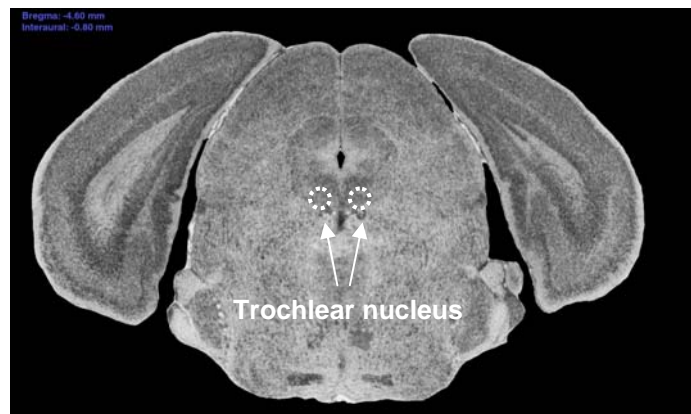
Fig 2.3. Location of different motor nuclei under study in the brainstem sections of mouse. (Adapted from Mouse Brain Library, www.mbl.org). *A,* Facial nucleus, *B,* hypoglossal and dorsal vagal nucleus, *C,* Oculomotor nucleus, D, Trochlear nucleus.

2.4   Patch clamp recording

Whole cell patch clamp experiments were performed with intracellular pipette solutions containing (in mM)**:** 140 KCl, 10 HEPES, 2 $MgCl_2$, 4.4 Mg-ATP, and 0.4 Na-GTP (adjusted to pH 7.3 with KOH). Synaptic blockers were used in the appropriate concentration (CNQX, 10µM; D-AP5, 100µM; Bicuculline, 10µM; and Strychnine, 10µM) in order o prevent spontaneous activity during measurements. Fura-2 was purchased from Molecular probes (Eugene, OR, USA) and was used at concentrations of 50-1000µM for the buffering capacity studies; otherwise the fura-2 concentration used for patch clamp experiments was 100µM. Patch pipettes were pulled from borosilicate glass tubing (KIMAX-51, Kimble products, USA). When filled, they displayed resistances of 2.0-3.5MΩ Recordings were performed with EPC-9 amplifier (HEKA electronik, Lambrecht, Germany). Cells were selected for study if they had membrane resistance >1GΩ in the cell attached mode. Whole-cell currents were recorded with sampling frequencies of 4–10 kHz and filtered (Bessel filter, 2.9 kHz) before analysis. Analysis of signals was performed off-line using Igor (Wavemetrics, Oregon, USA), Origin-7 and pulse and pulse-fit software (HEKA). Unless and otherwise stated, during voltage clamp, a depolarizing voltage step from a holding potential of $^-$60mV to $^+$10mV, for 0.5 sec was applied to activate plasma membrane Ca^{2+} channels and increase cytosolic Ca^{2+}. 30mM K^+ solution was used to achieve the depolarization induced Ca^{2+} entry in fura-2AM imaging experiments.

2.5   CCD camera imaging

As previously described (Ladewig & Keller 2000, Bergmann & Keller 2004) a modified version of a CCD camera system (TILL photonics, Graefelfing, Germany) was employed in experiments. Motoneurons are patch clamped and filled with definite concentration of fura-2 (Fig 2.5) and defined regions of interest (ROI) to measure the Ca^{2+} signals from the cell soma. Background fluorescence was measured in corresponding out-of-focus ROIs, containing no obvious cellular structures emitting fluorescence in this wavelength range and subtracted from each image. Calculations and analysis of intracellular Ca^{2+} concentrations were subsequently performed off-line with Igor or Origin-7 analysis software.
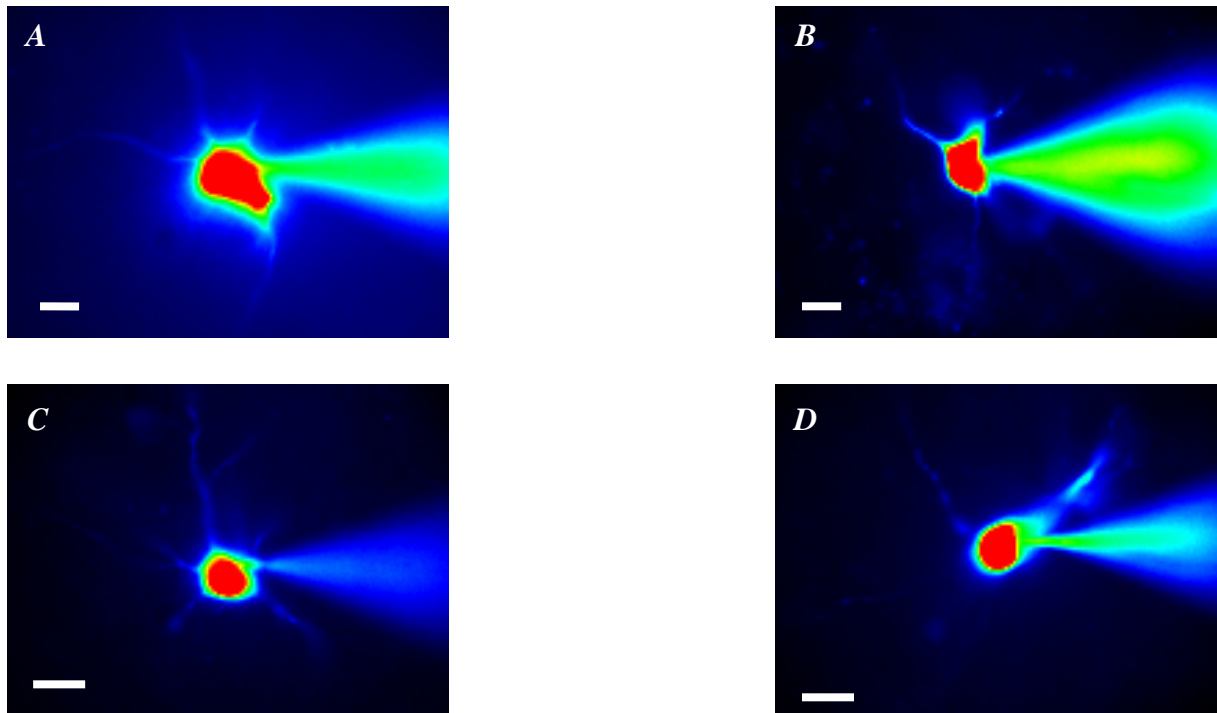
Fig.2.5. Different motoneurons are patch clamped and filled with 50-1000μM fura-2 and the Ca^{2+} transients are monitored by imaging with water cooled CCD camera. *A*, FMN, *B*, HMN, *C*, OMN, *D*, TMN. All the neurons are filled with 500μM fura-2. Scale bar =10μM

2.6   Membrane potential measurements

Rhodamine123 is used as an indicator of intactness of mitochondrial membrane potential (Mostafapour et al. 1997). Briefly, brainstem slices were incubated in ACSF containing 0.5μg/ml rhodamine123 at room temperature for 20 min. Slices were rinsed and placed in the perfusion chamber for fluorescence analysis. The excitation wavelength for rhodamine-123 was 480 nm and a dichroic mirror with mid reflection at 510 was used to collect emission signal.

2.7   Intracellular Ca^{2+} measurements

Two different methodologies were used for staining the cells with fura-2. In the first, fura-2 was filled through the patch pipette in whole cell configuration and Ca^{2+} measurements were performed after fura-2 concentration equilibrates between cell and pipette. In the second procedure, briefly the brainstem slices were incubated in oxygenated artificial cerebrospinal fluid (ACSF) containing 5μM Acetoxy Methyl (AM) ester form of fura-2 (Molecular probes, Eugene, OR, USA) at 27^{0}C for 30 min. The slices were rinsed and incubated for further 30 min in ACSF for de-esterification of fura-2AM. Fura-2 was alternately excited with 360 nm and 390 nm UV light and emitted light was directed to a dichroic mirror with mid-reflection at 425 nm and filtered by a band pass filter (505-530 nm). The absolute Ca^{2+} values were calculated according to Grynkiewicz et al (Grynkiewicz et al, 1985).

$$[Ca^{2+}]_i = Kd(\,R_{max}\,/\,R_{min})(R\text{-}R_{min})\,/\,(R_{max}\text{-}R)$$

Where $[Ca^{2+}]_i$ is the intracellular calcium concentration, Kd is the the dissociation constant of the calcium indicator dye, which was 241nM under our experimental conditions, R$_{max}$ is the Maximum Fluorescence Ratio and R$_{min}$ is the Minimum Fluorescence Ratio. The fluorescence ratios R$_{min}$ and R$_{max}$ were determined 'in vivo' by patch clamping neurons either with intracellular solutions containing no calcium but 10 mM BAPTA (R$_{min}$) or 10mM Ca^{2+} (R$_{max}$).

Fluorescence values in the figures are given as F/F$_0$ (where F denotes the fluorescence values at different time points of experiment and F$_0$ denotes the first fluorescence value. For each of the motoneuron types, Ca^{2+} concentrations corresponding to 0.1 unit of F/F$_0$ value are as represented in table 2.7.

Motoneuron	0.1 division of F/F_0 =
Facial	96.38 ± 5.58 nM Ca^{2+}
Hypoglossal	85.50 ± 15.42 nM Ca^{2+}
Oculomotor	84.58 ± 9.56 nM Ca^{2+}
Trochlear	83.74 ± 6.64 nM Ca^{2+}

Table 2.7. Conversion of the Fura-2 fluorescence measurements expressed in F/F_0 values to calcium concentrations for each of the four motoneuron populations under study.

2.8 Calcium homeostasis studies

The calcium binding ratio K_s of the endogenous buffers is given by:

$$\kappa_s = \Delta[CaS]_i \; / \; \Delta[Ca^{2+}]_i$$

where $[CaS]_i$ and $[Ca^{2+}]_i$ denote the concentration of calcium bound to endogenous buffers and the intracellular free calcium concentration, respectively. Endogenous calcium buffering capacity of facial motoneurons and dorsal vagal neurons was studied using the 'added buffer' method by Neher & Augustine (1992). In this method cellular Ca^{2+} buffering capacity is probed by competition between 'endogenous' calcium buffers (S) and exogenously added buffer (B). In our experiments fura-2 added through the patch pipette competes with the cellular calcium binding proteins, which affect the amplitude and time course of the Ca^{2+}

changes. The incremental Ca^{2+} binding ratio κ_B' of indicator dyes is given by (Neher & Augustine, 1992; Neher, 1995; Helmchen *et al.* 1996, 1997):

$$\kappa_B' = \Delta[CaB]_i \ / \ \Delta[Ca^{2+}]_i$$

$$= [B]_T \, K_d / ([Ca^{2+}]_{rest} + K_d \,)([Ca^{2+}]_{peak} + K_d),$$

Where $[Ca^{2+}]_{rest}$ is the free calcium concentration at rest and $[Ca^{2+}]_{peak}$ is the maximum calcium increase during a stimulation. $[B]_T$ is the concentration of fura-2 at a particular time point of recording and K_d, the dissociation constant of the calcium indicator dye, which was 241nM under our experimental conditions.

Calcium transient recoveries of 0.5S voltage stimuli were fitted with a single exponential decay curve to determine the decay time constant (τ), approximating that the Ca^{2+} extrusion after a response is linear. The quantitative model of somatic calcium homeostasis predicts that under such experimental conditions decay times of calcium transients are a linear function of fura-2 buffering capacity:

$$\tau = (1 + \kappa_B' + \kappa_S)/\gamma,$$

where γ denotes the effective extrusion rate across the plasma membrane. The measurement of τ as a function of κ_B' permits the determination of K_S, the endogenous calcium buffering capacity of the cell. τ is plotted against κ_B', and the negative *x*-axis intercept of linear regression denotes the value for K_S. The calcium decay time in the absence of exogenous buffers can be calculated by extrapolating the same plot to $\kappa_B' = 0$. Once the K_S is obtained, γ is calculated from the above equation by substituting values for K_S, τ and κ_B'.

2.9   Reagents

ATP (Adenosine Triphosphate)	Sigma-Aldrich
BAPTA	Sigma-Aldrich
Bicuculline	Sigma-Aldrich
CNQX (6-cyano-7-nitroquinoxaline-2, 3-dione disodium salt)	Tocris
Cyclopiazonic acid (CPA)	Sigma-Aldrich
D-AP-5 (D(-) 2-amino-5-phosphonopentanoic acid)	Tocris
DMSO	Sigma-Aldrich
FCCP (Carbonyl cyanide 4-trifluromethoxyphenylhydrazone)	Sigma-Aldrich
Fura-2	Molecular Probes
GTP (Guanosine Triphosphate)	Sigma-Aldrich
Pluronic acid	Sigma-Aldrich
Rhod-123	Molecular Probes
Sodium cyanide	Sigma-Aldrich
Strychnine	Sigma-Aldrich
Tetrodotoxin citrate	Tocris

Stock solutions of chemicals were prepared as follows: FCCP was dissolved in ethanol, CPA in DMSO, and sodium cyanide, bicuculline, strychnine, TTX, CNQX, and D-AP-5 were dissolved in distilled water. The corresponding drug was then included in the bath solution and bubbled with 95% O_2, 5% CO_2, at room temperature, before and during the experiments. Fura-2 pentapotassium salt used for patch pipette filling was dissolved in filtered distilled water to 2mM concentration. Fura-2 AM was dissolved in DMSO + 5% pluronic acid (Pluronic F-127) to a concentration of 1mM. Finally, rhod-123 was dissolved in ethanol (10mg/ml).

2.10 Analysis

Each brain stem slice was used for a single experiment, includes one cell per slice in patch clamp experiments and more than one cell in fura-2 AM and rhodamine-123 imaging experiments. For buffering capacity studies many cells were patch clamped from a slice. All results are expressed as mean ± standard error of the mean, and represent a minimum of 5 patch clamp imaging experiments and at least experiments on three separate slices in the case of fura-2AM staining. The significance after pharmacological intervention was calculated using Student's *t* test.

Chapter 3

Results

3.1 Role of mitochondria in defining the Ca^{2+} metabolism of ALS vulnerable motoneurons.

Among the lower motoneurons affected in human ALS, the most severe pathology is seen in the hypoglossal nucleus with tongue muscles being inactivated even early in the disease progression, as well as in the facial nucleus and trigeminal nucleus. A similar pattern of neurodegeneration has been observed in the mouse models of ALS, carrying mutated SOD1 gene. A rapidly progressive decline of motor function caused by the death of motoneurons within the spinal cord and brainstem is evident in these animals (Morrison & Morrison 1999). At the onset of disease in the mutant SOD1 animal, a sharp decline of muscle strength and the formation of vacuoles derived from degenerating mitochondria in the motoneurons has been reported (Kong & Xu 1998). Severe morphological and biochemical mitochondrial abnormalities are also reported in human ALS cases. Evidently, mitochondrial dysfunction contributes to rapid motoneuron death: by predisposing them to calcium-mediated excitotoxicity, by increasing generation of reactive oxygen species (ROS), and by signalling apoptotic pathways, leading to functional decline of the motor system. A compromised ATP supply from mitochondrial metabolism can have significant effects on the cellular energy status, causing system malfunction. Hence understanding the functions of mitochondria in different motoneurons, and after-effects and relative contribution of mitochondrial disintegration to the ALS pathogenesis is indispensable.

3.1.1 Monitoring mitochondrial function in brainstem slices

Mitochondrial respiratory metabolism and associated proton efflux results in the accumulation of negative charges in the mitochondrial matrix and development of a strong electrochemical gradient across the mitochondrial membrane. In general, the mitochondrial membrane potential ($\Delta\Psi_m$) ranges from -90 to -180mV. $\Delta\Psi_m$ is indispensable in permitting the Ca^{2+} influx into mitochondria, allowing them to serve as Ca^{2+} buffers (Duchen 2000; Ward et al. 2000). FCCP is the widely used drug to dissipate this potential gradient and to cause the release of stored Ca^{2+} from mitochondria (Colegrove *et al* 2000; Brocard *et al*. 2001; Feeney *et al*.2003; Wyatt et al. 2004).
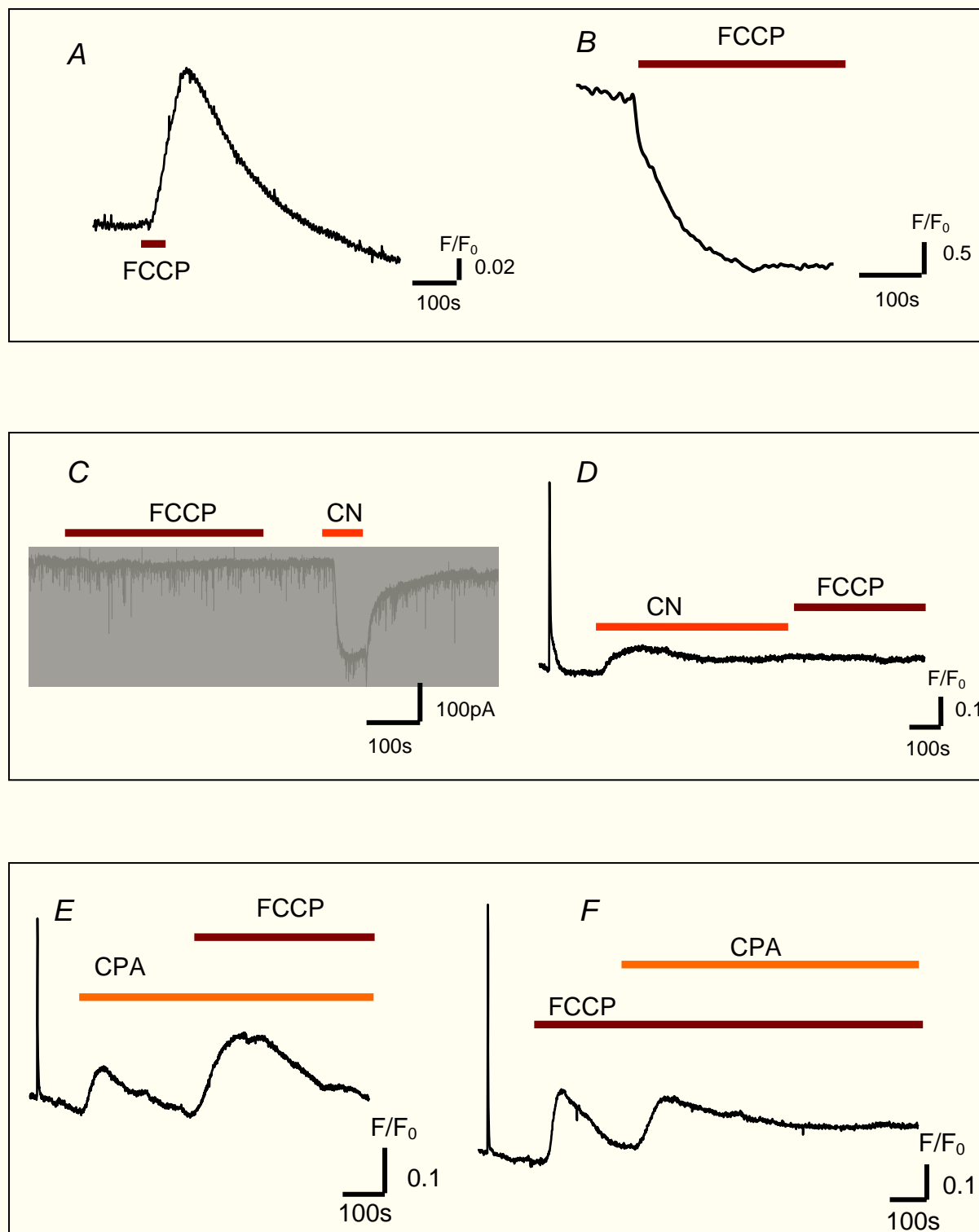
Fig. 3.1.1. *A,* carbonyl cyanide 4-trifluromethoxyphenylhydrazone (FCCP) induced mitochondrial depolarization in hypoglossal motoneurons. Cells were loaded with rhodamine-123 (0.5μg/ml) and superfused with artificial cerebrospinal fluid (aCSF). 2μM FCCP was added to the superfusate for 1 min (indicated by the bar), which quickly released the dye quenched by mitochondria. Data shown represents a single cell from the slice imaged. *B,* Application of 2μM FCCP caused immediate decrease

in the NADH fluorescence (n>25). *C*, presence of FCCP did not result in any change in the basal current through the plasma membrane (n=5); 2mM sodium cyanide was used as a positive control, which induced a prominent inward current in the HMNs. *D*, pre-emptying the mitochondrial Ca^{2+} load further confirmed that FCCP is releasing Ca^{2+} from the same target as cyanide, which are mitochondria. *E & F*, any non-specific action of FCCP to release the ER Ca^{2+} store was checked by pre and post application of ER specific Ca^{2+} releasing drug CPA (50μM) to FCCP; the figures reveal that FCCP is releasing Ca^{2+} from an entirely different store other than ER; it also shows the existence of two different Ca^{2+} stores in these MNs.

To confirm that FCCP depolarized mitochondria of neurons in the brainstem slice preparation, we checked its effect on the mitochondrial membrane potential & metabolism (NADH autofluorescence). To measure ΔΨm, the slices containing nucleus hypoglossus were loaded with rhodamine123, and the corresponding fluorescence changes of HMNs are monitored. The cationic dye rhodamine-123 is readily sequestered by functioning mitochondria and is released in response to the loss of mitochondrial membrane potential. As shown in Fig. 3.1.1*A* (n>25) application of 2μM FCCP for 1 min resulted in the release of quenched rhodamine123 from mitochondria of HMNs, indicating the transient loss of ΔΨ due to proton influx through FCCP. Monitoring the blockade of mitochondrial metabolism is another choice to pin point the action of FCCP. NADH natural-fluorescence is a good experimental measure to monitor energy metabolism of the cell. In the intact cell there is a continuous cycling of NADH produced in the glycolysis and TCA cycle to the electron transport chain where it functions as the electron donor. Besetting the mitochondrial membrane potential adversely affects the production of NADH in the mitochondrial metabolism. 2μM FCCP application caused a sudden decrease in the NADH autofluorescence of these neurons (Fig. 3.1.1*B*, n>25) by specifically and clearly destroying the mitochondrial integrity. Further more, we confirmed against the projected non-specific incorporation of FCCP on the cell membrane by monitoring cell membrane potential during FCCP application. Measurement of the cell membrane current in the whole cell patch clamp configuration revealed that FCCP did not cause any significant ion influx through the cell membrane of HMNs (Fig. 3.1.1*C*, n=5), whereas 2mM sodium cyanide application for 1 min caused a reversible inward current as previously shown by Bergmann & Keller.

The above findings were strengthened by the studies to verify the target specificity of FCCP. Pre-emptying the mitochondria using 2mM sodium cyanide and further application of 2μM FCCP did not result in any calcium release or any further $[Ca^{2+}]i$ response (Fig. 3.1.1*D*, n=7). To validate the specific release of mitochondrial Ca^{2+} by FCCP and to avoid measuring

any ER released calcium, we studied the action of FCCP along with ER specific Ca^{2+} extruding drug CPA (SERCA pump inhibitor). The specificity of FCCP to cause mitochondrial Ca^{2+} release separate from that of the ER stores was revealed by simultaneous application of FCCP and CPA on HMNs. Application of $2\mu M$ FCCP resulted in a separate Ca^{2+} release response even after the complete draining of ER Ca^{2+} stores (Fig 3.1.1*E*, n=7). Besides, ER stores remained to be separate from that released by FCCP (Fig. 3.1.1*F*, n=6), thus clearing out the non-specific action of FCCP on ER Ca^{2+} load, as well as revealing the existence of two separate intracellular Ca^{2+} stores in these MNs.

3.1.2   Mitochondrial disruption differentially affects cytosolic Ca^{2+} transients

The accumulation of Ca^{2+} by mitochondria may have an apparent influence on the lifetime of a $[Ca^{2+}]i$ transient. This effect was studied by following the dynamics of Ca^{2+} signal under control and mitochondria depleted conditions.
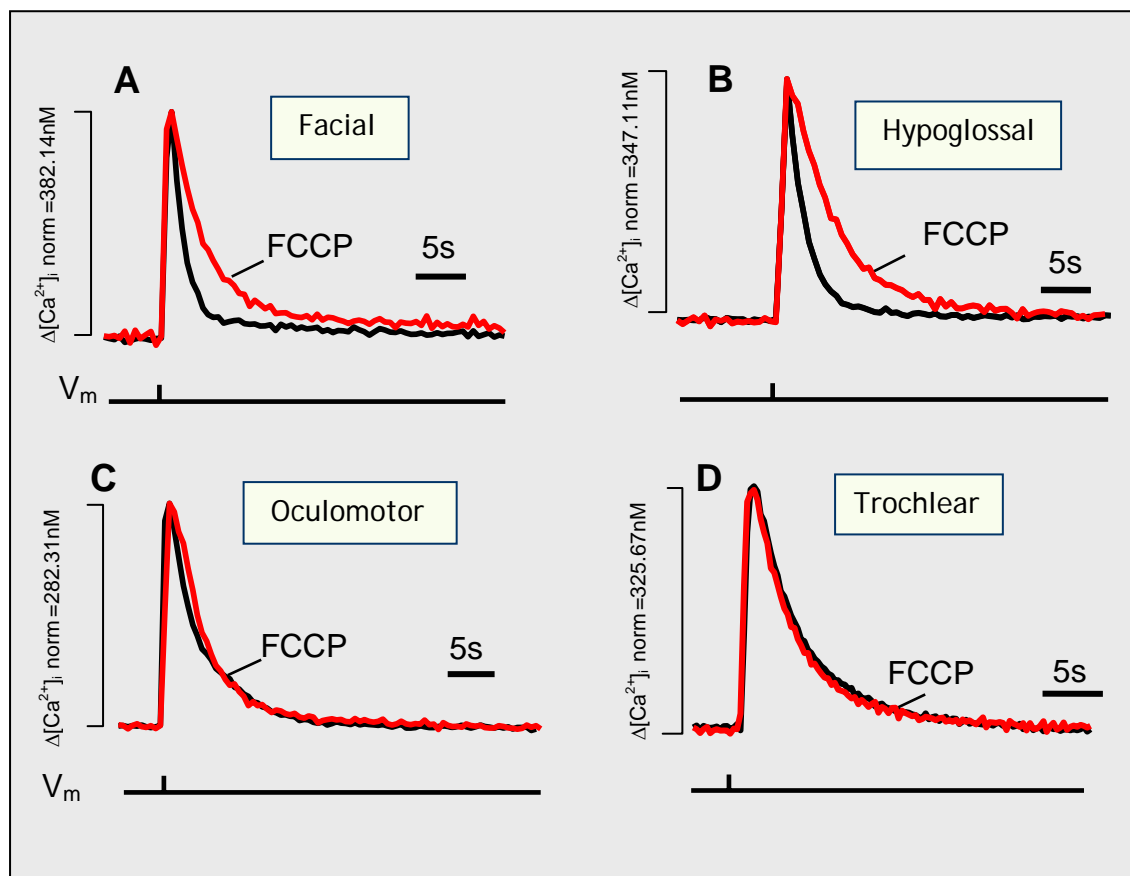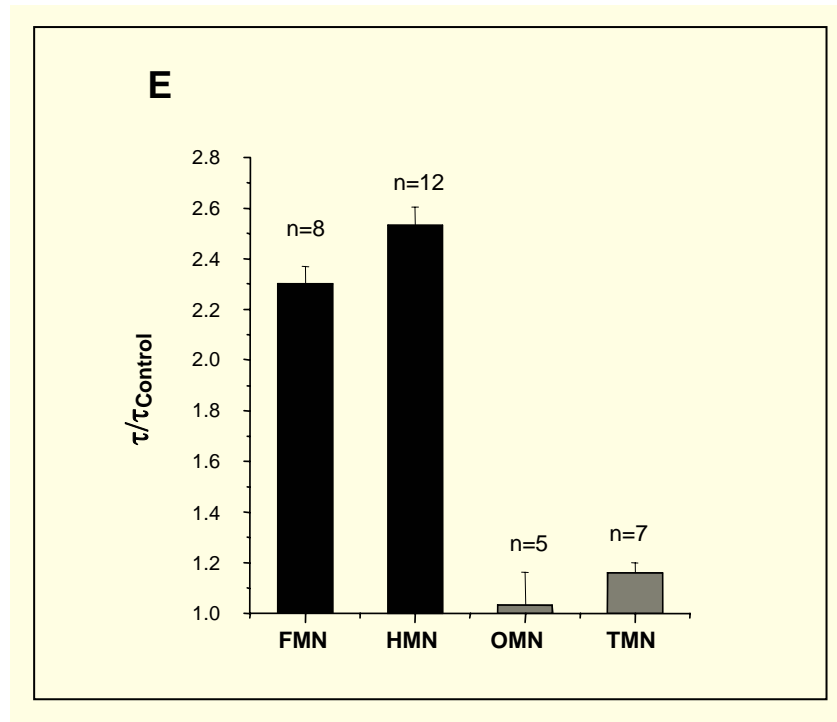
Fig 3.1.2. Monitoring the impact of preventing mitochondrial Ca^{2+} uptake in FMNs, HMNs, OMNs and TMNs. Superposition of voltage stimulated (step depolarization from -60mV to +10mV for 0.5s) Ca^{2+} transients (normalised to the same amplitude) under control conditions and after incubation with FCCP for ~5 min, from facial (*A*), hypoglossal (*B*), oculomotor (*C*) and trochlear motoneurons (*D*). Note that in facial and hypoglossal motoneurons mitochondrial disruption by FCCP prolongs the recovery time constant (τ) of Ca^{2+} transients. The delay in τ was 2.30 ± 0.07 times (n=8, *P*<0.001) and 2.54 ± 0.07 times that of control measurements (n=12, *P*< 0.001) for facial and hypoglossal motoneurons respectively; whereas in OMN (n=5) and TMN (n=9) the delay in τ was 1.03 ± 0.13 times (n=5) and 1.16 ± 0.04 times (n=7) that of control, respectively. This delay in τ is not attributable to any depletion in ATP since 4.4 mM ATP was continuously supplied to the cell. *D*, comparison of delay in τ of FMN, HMN, OMN and TMN is presented.

Blocking the mitochondrial calcium uptake by 2μM FCCP for ~5 min produced contrasting effects on the $[Ca^{2+}]i$ transient decay time constant (τ) of ALS vulnerable or resistant motoneurons. A comparative analysis of the τ of 0.5s voltage stimulus induced calcium transients of facial, hypoglossus, oculomotor neurons and trochlear motoneurons was done, in the presence and absence of FCCP. For these experiments the neurons were voltage clamped, and filled with 100μM fura-2 through the patch pipette and $[Ca^{2+}]i$ transients were triggered once fura-2 concentration equilibrated. Interestingly it was found that in facial and hypoglossal

motoneurons, presence of FCCP significantly delayed the τ . Compared to these neurons, in oculomotor neurons and trochlear motoneurons this effect was of much less significance.

The Ca^{2+} transient decay time for facial and hypoglossal motoneurons under control conditions, were found to be 1.63 ± 0.14s and 1.59 ± 0.14s respectively, whereas in presence of FCCP the decay time increased to 3.75 ± 0.28s (Fig. 3.1.2*A,* n=8, *P<0.001*) and 4.04 ± 0.3s (Fig. 3.1.2*B,* n=12, *P<0.001*). This retardation in the $[Ca^{2+}]i$ transient recovery time was not distinct in the OMNs and TMNs . In the case of oculomotor neurons the Ca^{2+} transient decay time was found to be 5.39 ± 0.96s and 5.57± 0.71s, at control conditions and in presence of FCCP respectively (Fig. 3.1.2*C* ,n=5). Again, in the case of trochlear motoneurons, the decay time under control conditions and in presence of FCCP was 3.53± 0.13s and 4.09 ± 0.61s (Fig. 3.1.2*D,* n=7) respectively.

As evident from these values given above, the decay time increased by 2.30 ± 0.07 times and 2.54 ± 0.07 times in the case of facial and hypoglossal motoneurons, whereas for oculomotor neurons and trochlear motoneurons, this delay was only 1.03 ± 0.13 and 1.16 ± 0.04 times control (Fig. 3.1.2*E*). The slowing down of Ca^{2+} transient decay time is not attributable to ATP depletion in the neurons since 4.4 mM ATP was continuously available by dialysis from the intra-pipette solution. This rules out the possibility that mitochondrial depolarisation retards the Ca^{2+} transients in HMNs and FMNs by depleting cytosolic ATP and thereby inhibiting the Ca^{2+} clearance by plasma membrane calcium ATPase.

3.1.3   FCCP causes differential calcium release from mitochondria

It is clear that mitochondria act as local calcium buffers, thus shaping spatiotemporal aspects of cytosolic calcium signals. The calcium uptake into the mitochondria is undertaken by the Mitochondrial Calcium Uniporter (MCU) located in the inner mitochondrial membrane. Recent data suggest high efficiency and extremely high affinity of this channel to Ca^{2+} (Kirichok & Clapham, 2004).
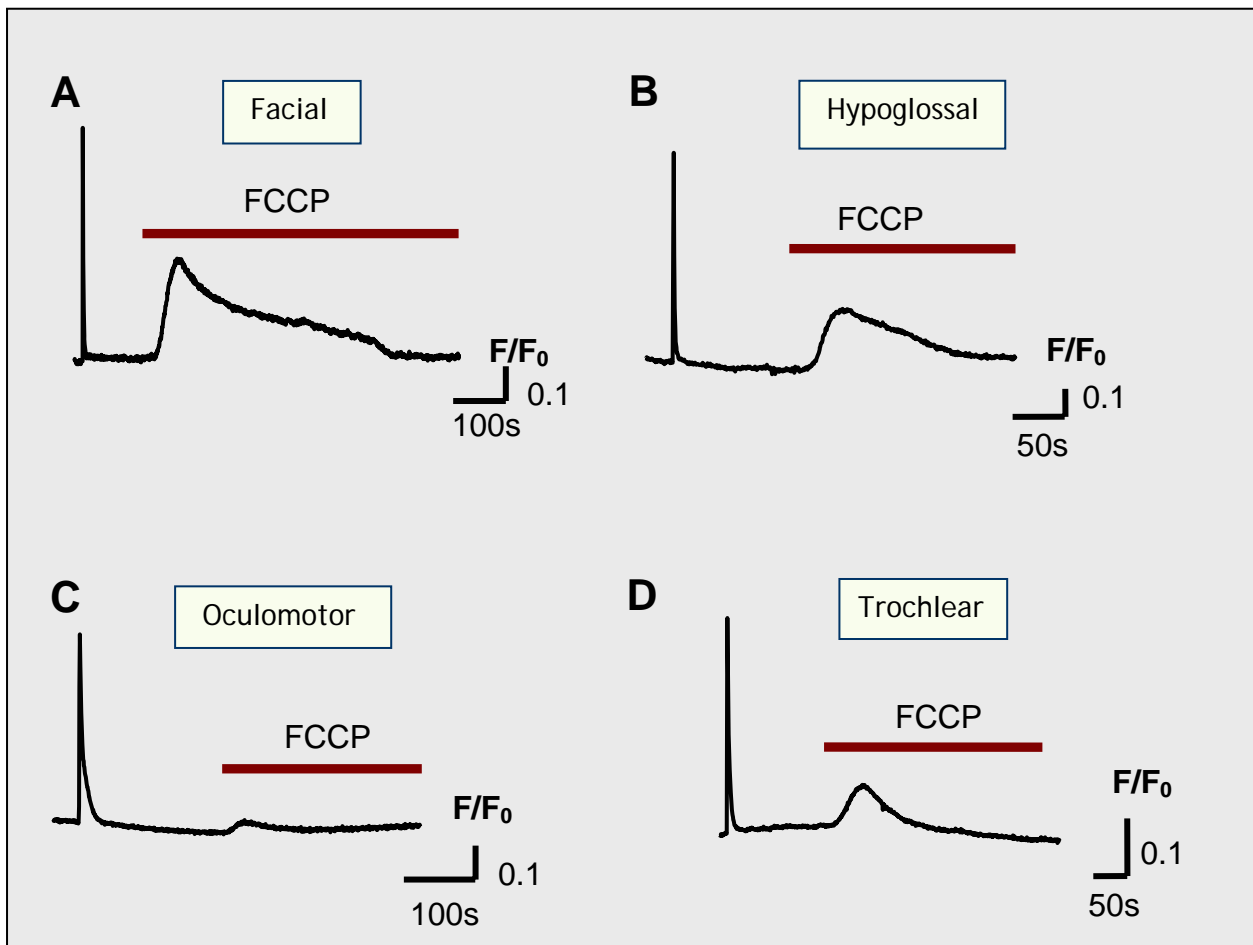
Fig 3.1.3. Evaluation of the ability of mitochondria to accumulate Ca^{2+}, in facial, hypoglossal, oculomotor and trochlear motoneurons is investigated, by rupturing mitochondria after cell stimulation to fill the intracellular Ca^{2+} stores. When $2\mu M$ FCCP was perfused shortly after a voltage induced $[Ca^{2+}]i$ transient, there was an evident Ca^{2+} release from the mitochondria in all four types of neurons.

*A,* In the facial MNs the Ca^{2+} release amplitude was 124.15 ± 11. 83 nM (n=17). *B,* in the hypoglossal motoneurons this amounted to be 99.03 ± 6.1 nM (n=19). *C & D,* in the oculomotor and trochlear motoneurons this release was of much less amplitude; 20.51± 2.73 nM (n=5) & 37.04± 7.99 nM (n=7) respectively.

In the next set of experiments to analyse the comparative efficiency of mitochondria as a Ca^{2+} sequestering organelle, we applied FCCP to evacuate mitochondria after the cell was exposed to an evoked Ca^{2+} load through a depolarizing stimulus. In the case of facial and hypoglossal motoneurons, application of 2μM FCCP within 5 min after a voltage induced depolarization (0.5s) resulted in a calcium release of 124.15 ± 11. 83 nM (Fig. 3.1.3*A*, n=17) and 99.03 ± 6.1 nM respectively (Fig. 3.1.3*B*, n=15). Similar application of 2μM FCCP on oculomotor neurons and trochlear motoneurons, resulted in a calcium release of only 20.51± 2.73 nM (n=5) & 37.04± 7.99 nM (n=7) respectively (Fig. 3.1.3*C&D*), implying, there is a significant difference in the Ca^{2+} accumulation activity of mitochondria in these neurons; the store being several folds lower. Fig. 3.1.3*E* shows the comparative analysis of average calcium release caused by FCCP from all four types of motoneurons studied.

3.1.4 Ca^{2+} uptake and $[Ca^{2+}]i$ transients in fura-2 AM loaded cells

In all these neurones under study, 30mM K^+ stimulation for 30s evoke a rapid and prominent $[Ca^{2+}]i$ signal. Since the above mentioned observations reveal that mitochondria in hypoglossal motoneurons can effectively shape the pattern of the Ca^{2+} transient, experiments were conducted to check whether mitochondrial uptake can affect the peak Ca^{2+} response of these neurons. To determine this, firstly the slices containing facial or hypoglossal motoneurons were stained with fura-2AM, and were exposed to 30mM K^+ for 30s, under normal conditions and in presence of 2μM FCCP. As shown in Fig. 3.1.4(i) *A&B*, for the facial and hypoglossal motoneurons, the peak amplitude of 30mM K^+ induced calcium response increased to 4.1 ± 0.08 (n>25, *P<0.001*) and 2.09 ± 0.1 (n>25, *P<0.001*) folds in presence of FCCP. More over it was observed that the presence of FCCP interfered with the post-depolarization recovery of $[Ca^{2+}]i$, as evident from the disturbance in the decay of $[Ca^{2+}]i$ signal. Thus it is evident that in the absence of mitochondrial Ca^{2+} uptake, the $[Ca^{2+}]i$ signal is more strongly reflected in the

cytoplasm of these neurons; exemplifying that mitochondria can actively sequester Ca^{2+} during an ongoing Ca^{2+} influx as a result of the opening of voltage gated calcium channels and influx.
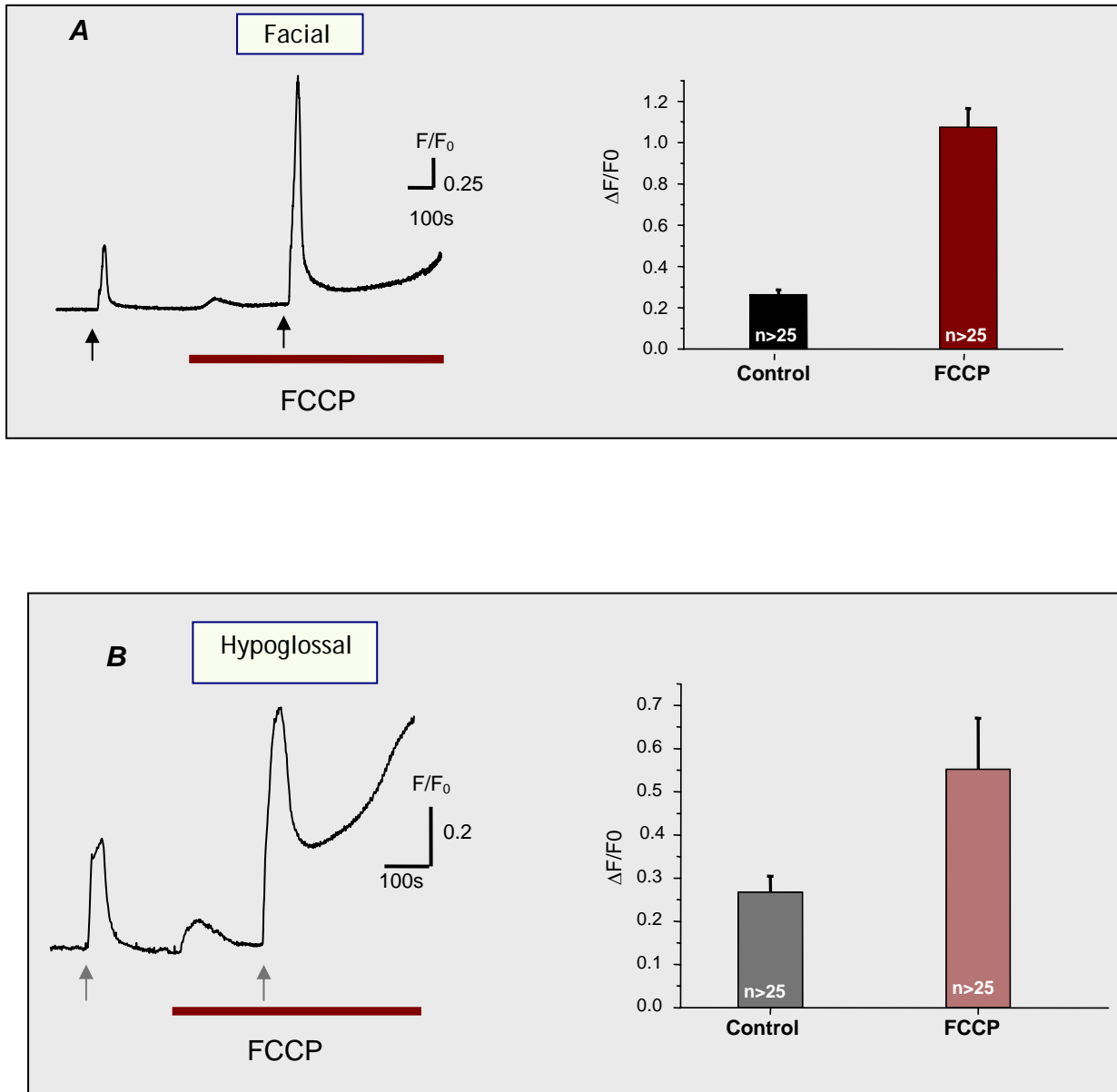
Fig 3.1.4 (i).   Effect of perturbing mitochondrial Ca^{2+} uptake on the calcium transient (evoked by 30mM K^+, 30s, indicated by arrows) amplitudes of ALS-vulnerable MNs (FMNs & HMNs) was studied in 5µM fura-2 AM stained slices, containing facial and hypoglossal nucleus. Lack of mitochondrial Ca^{2+} uptake was readily reflected in the cytoplasm of these MNs, as an increase in amplitude of K^+ induced Ca^{2+} transients. This measured to be 4.1 ± 0.08 (n>25, $P<0.001$) and 2.09 ± 0.1 (n>25, $P<0.001$) times the average control peak (*A* and *B*) for FMNs and HMNs respectively.
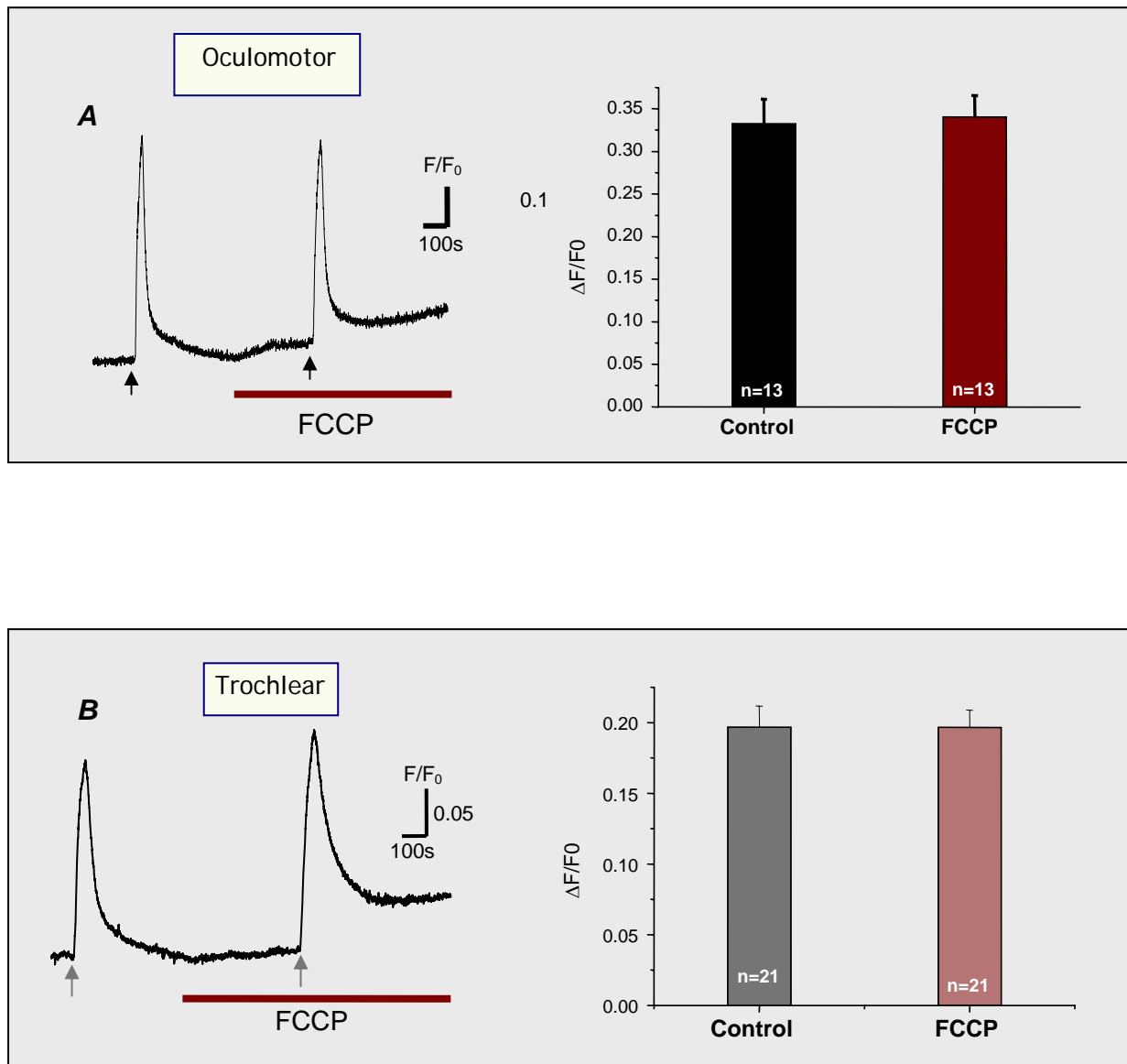
Fig 3.1.4 (ii). Mitochondrial Ca^{2+} uptake and its influence on calcium transient (evoked by 30mM K^+, 30s, indicated by arrows) amplitude was checked also in ALS- resistant MNs (OMNs and TMNs) in 5µM fura-2 AM stained slices containing oculomotor or trochlear nucleus. The oculomotor neurons only showed a very slight increase in Ca^{2+} transient amplitude (1.04 ± 0.03 times control, n=13) after mitochondrial disruption, which was not significant ($P>0.05$) *A*. Further more, in trochlear motoneurons the average amplitude of Ca^{2+} transients in presence of FCCP was similar to control responses *B*.

Secondly, the same experimental protocol was applied to oculomotor neurons and trochlear motoneurons. The disruption of mitochondrial Ca^{2+} accumulation by FCCP did not have any significant effect on the Ca^{2+} transient amplitude of oculomotor neurons, the increase in amplitude was only 1.04 ± 0.03 times the control (Fig. 3.1.4(ii)*A*, n=13, *P*>0.05). In the case of trochlear motoneurons, (Fig. 3.1.4(ii)*B*, n>25); the average amplitude of K^+ induced Ca^{2+} transients in presence of FCCP & in the control conditions were similar. (F/F_0 value of 0.1967 ± 0.01 (control), and 0.1965 ± 0.01 (in presence of FCCP)). There was a slight influence of FCCP on the recovery of the transients in trochlear motoneuron measurements.

3.1.5 Calcium stores of ER in the neurons under study

Endoplasmic reticulum functions as an effective Ca^{2+} storing organelle in many cells including neurons. Active transport of cytosolic calcium into intracellular stores by sarco-endoplasmic reticulum Ca^{2+}-ATPase (SERCA) is important in regulating calcium signalling. (Cavagna et al, 2000). Inhibition of calcium uptake by endoplasmic reticulum has been shown to disrupt Ca^{2+} homeostasis.

In our experiments CPA application resulted in the mobilization of Ca^{2+} in voltage clamped, 100μM fura-2 filled FMNs (26.17 ± 2.83 nM; Fig.3.1.5*A*, n=7), HMNs (34.95 ± 3.19 nM; Fig.3.1.5*B*, n=12), OMNs (52.66 ± 2.08 nM; Fig.3.1.5*C*, n=5), and TMNs (27.55 ± 2.77 nM; Fig. 3.1.5*D*, n=5), preceded by a depolarizing stimuli to fill the intracellular stores. The comparison of average endoplasmic reticular calcium release of FMNs, HMNs, OMNs and TMNs studied has been presented in Fig.3.1.5*E*.
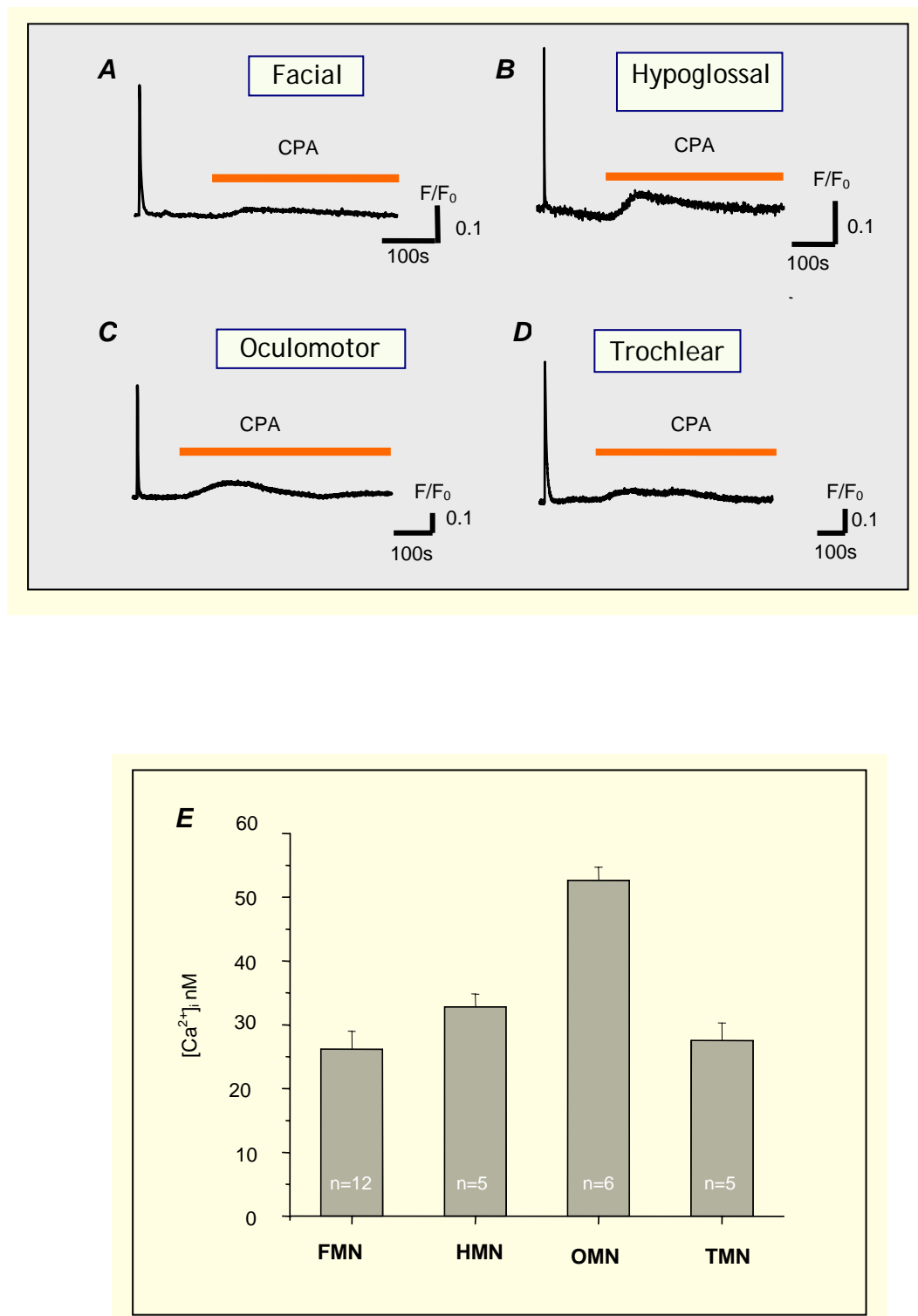
Fig 3.1.5. Slices were incubated with cyclopiazonic acid (CPA) to inhibit ER Ca^{2+} ATPase and thereby to deplete Ca^{2+} content. Application of 50μM CPA after filling the stores with a predepolarization caused measurable Ca^{2+} release from facial (*A*), hypoglossal (*B*), oculomotor neurons (*C*) and trochlear motoneurons (*D*). Comparison of the amplitude of ER calcium release in these four types as a result of SERCA pump inhibition has been presented in *E*.

3.1.6 Nominal role of ER, compared to mitochondria, as a Ca^{2+} sequestering organelle in ALS vulnerable MNs

There was a significant difference in the Ca^{2+} load of the mitochondria and ER in the case of ALS vulnerable motoneurons; the calcium release being high from the mitochondria of these motoneurons. The calcium release from mitochondria of facial neurons was 4.74 ± 0.52 (P<0.0001) times larger than the ER Ca^{2+} release. Similarly in the case of hypoglossal MNs this was 3.17 ± 0.36 (P< 0.0001) times larger than that caused by 50μM CPA. This observation further indicates the importance of mitochondria as a dominant Ca^{2+} store in both motoneurons, Fig. 3.1.6 *A&B*. In the case of ALS resistant model MNs, except in the case of TMNs, the ER was better loaded with Ca^{2+} after a depolarization induced Ca^{2+} transient (Fig 3.1.6 *C*).
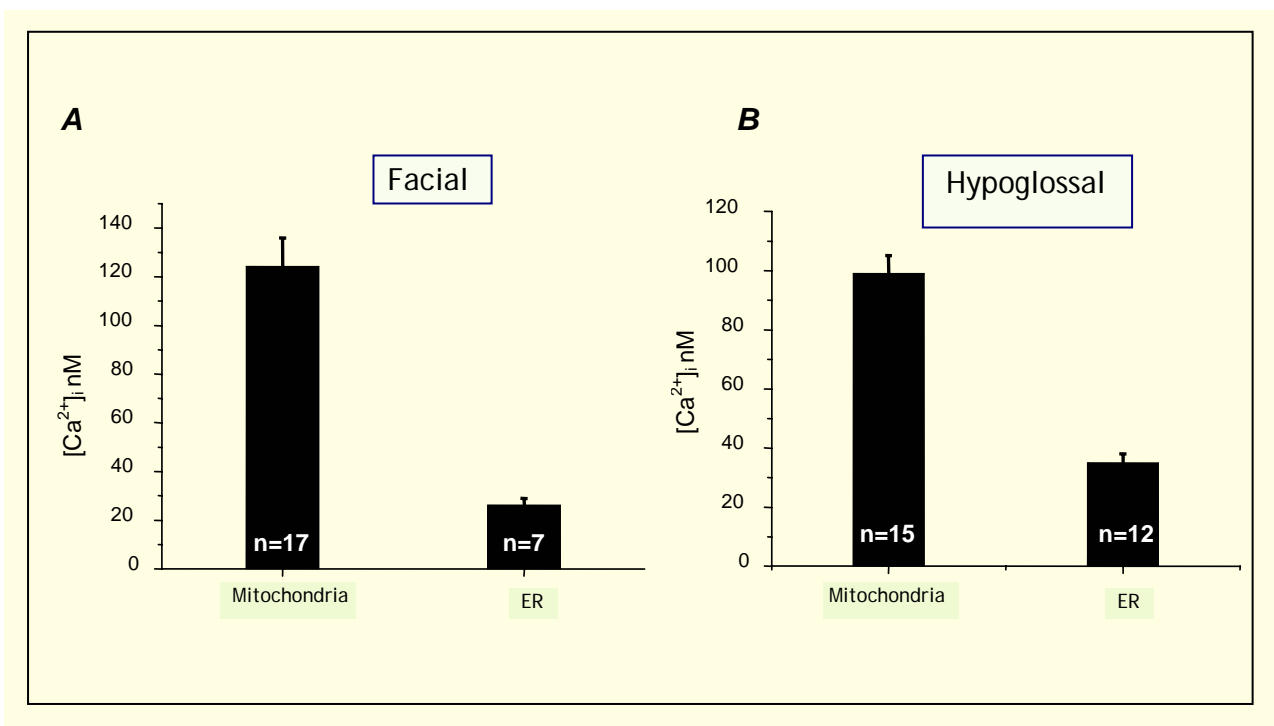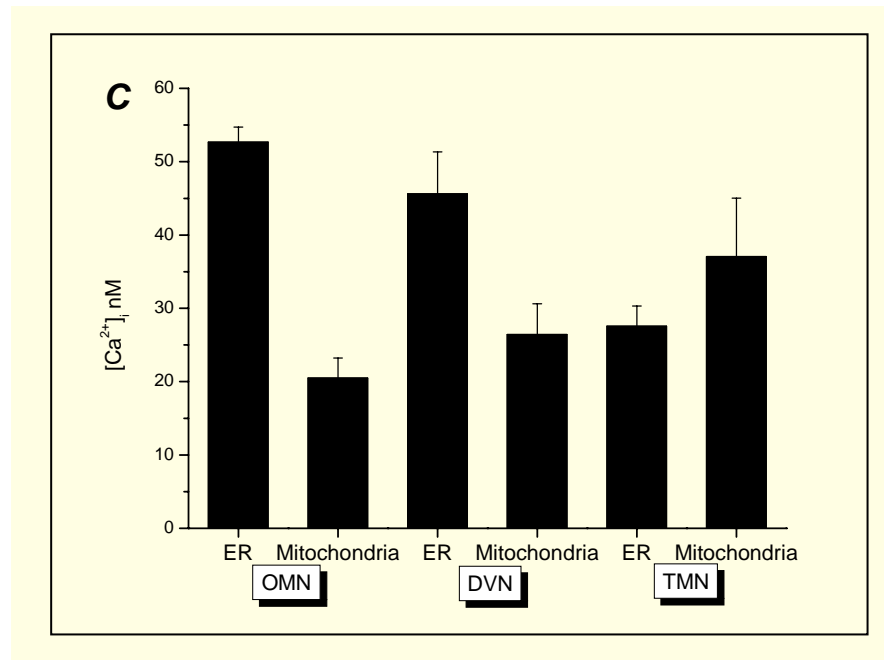
Fig 3.1.6. Comparative analysis of the calcium storing ability of mitochondria and endoplasmic reticulum, in all the model motoneurons under study was done by using specific chemicals interfering with the integrity of these organelles. FCCP and CPA were used to release of the quenched calcium from mitochondria and ER respectively. Quantitative difference between the ER and mitochondrial Ca^{2+} load was evident in FMNs (*A*) & HMNs (*B*); the mitochondrial load being high over the ER loads. *C*. Comparison of ER and mitochondrial Ca^{2+} release from ALS resistant neurons (OMN & TMN) and dorsal vagal neurons is also presented.

3.2 Study on calcium buffering capacity of motoneurons and its significance in Amyotrophic lateral sclerosis etiology

3.2.1 Differential Ca^{2+} buffering capacities of ALS vulnerable and ALS resistant MNs

As we have previously shown the differential buffering capacity of ALS vulnerable (Lips & Keller, 1998; Palecek & Keller, 1999) and resistant motoneurons (Vanselow & Keller, 2000), we pursued further to ascertain the intrinsic calcium buffer concentration of other brainstem neuronal populations, like facial motoneurons and trochlear motoneurons, which show differentiability in their survival in ALS challenge. Buffering capacities (K_S) were plotted for 15 facial MNs from mice aging four days and 10 trochlear motoneurons (day 2-day 5) after filling these neurons with concentrations ranging from 50 to 1000μM of fura-2 by means of whole cell patch clamp. For all cells, fluorescence changes at 360 and 390nm were recorded immediately after attaining the whole cell mode, in order to monitor the fura-2 concentration. Calcium responses were measured by depolarizing the cells from $^-60$ to $^+10$mV for 0.5s. Calculations and plotting of graphs were done as described in the methods.

3.2.2 Calcium buffering capacity of facial (P4) motoneurons

The facial motor nucleus (VII) is located ventrally at the level of pons in the brainstem. The neurons of this nucleus project their axons to constitute the somatomotor (brachialmotor) component of the facial nerve which provides voluntary control of the muscles of facial expression. Signals for voluntary control of the facial muscles originate in the motor cortex and pass via the corticobulbar tract to the facial motor nuclei. Lesions or damage to the facial motor nucleus can result in the paralysis of all muscles of facial expression (including those of forehead). The facial nucleus appears in the mouse brainstem slice as a dark, vast, oval area located ventro-laterally on either side of the middle line. The nucleus contains huge motoneurons of approximately 20μM diameter and showed extensive dendritic span when filled with fura-2 and visualized.

After achieving the whole cell patch clamp configuration, equilibration of the pipette and cytosolic solutions occurred with a time constant of 56.64 ± 8 s (Fig 3.2.2(i)*A* n=20) as indicated from the Ca^{2+} independent fluorescence (F_{360}) measurements of fura-2. Ca^{2+} signals were evoked, at low and high binding affinity of fura-2, through electrical stimulation and the changes in amplitude and decay time constant of these transients were closely monitored. The amplitudes of the Ca^{2+} transients reduced as fura-2 diffused into the cell. This displays the buffering effect of the added fura-2 which progressively binds a higher proportion of the incoming calcium. The recovery time of the Ca^{2+} transients of FMNs became drastically slower as the fura-2 seeped into the cell from the patch pipette, also due to the increasing buffering capacity imparted by the added fura-2 (Fig.3.2.2(i)*B*). The assumption made in the linear model for Ca^{2+} dynamics is that there should be a single exponential time constant for the decay of Ca^{2+} transients. Hence the decay of Ca^{2+} transients in the presented experiments is described by a single exponential fit. Then the measured τ of Ca^{2+} transients were plotted against the Ca^{2+} binding affinity (K_B') of the added buffer (fura-2).

There was unavoidable scatter of the data points most likely representing the variability of the buffering condition in different neurons measured. Subsequently, for facial MNs, the K_S was calculated to be 46 ± 21 from the negative intercept of linear regression line for calcium decay time constant τ versus K_B' (Fig. 3.2.2(ii)). The basal decay time constant, i.e. in the absence of any external buffers (at $K_B=0$) was found to be 0.43 ± 0.20s for FMNs. The extrusion rate constant γ could be calculated from the following equation as the values of K_S, K_B' and τ are known.

$$\gamma = (1 + \kappa_B' + \kappa_S) / \tau,$$

where K_S, K_B' and τ represent the values described in the methods. Accordingly an effective extrusion rate of 113 ± 7s^{-1} (n= 17) was calculated for P4 FMNs.
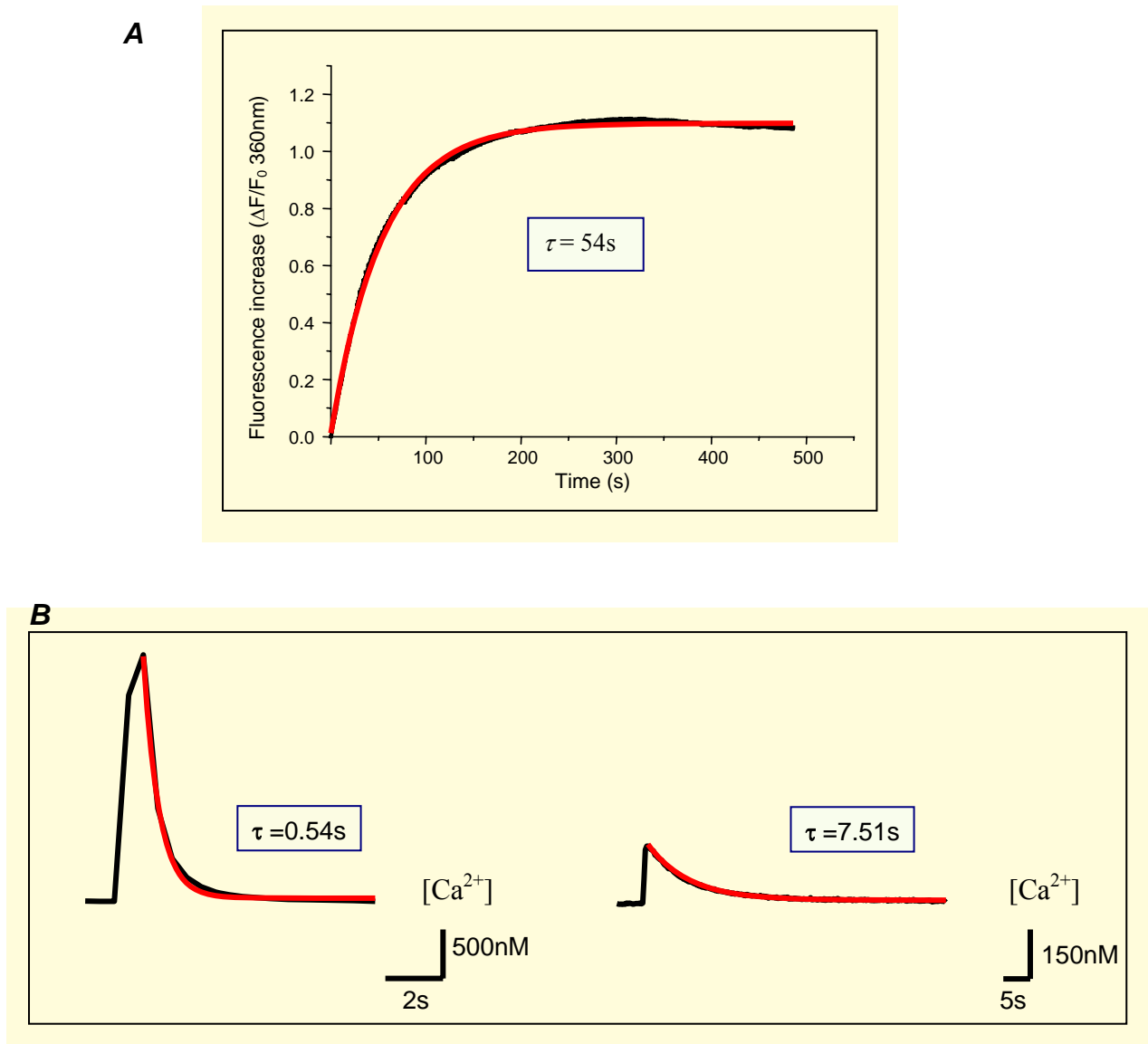
Fig 3.2.2(i). (A) Fluorescence intensity change in the Ca^{2+} independent wavelength F_{360}, of fura-2 after establishing the whole cell patch configuration, for a FMN. The data points are fitted with a single exponential decay function. (B) Ca^{2+} transients of facial MNs evoked by step depolarization to 10mV for 0.5s: the left trace indicates the Ca^{2+} change during stimulation immediately after the cell membrane patch was ruptured for whole cell measurements and the right trace represents the Ca^{2+} signal after the intrapipette solution has equilibrated with the cytosol and fura-2 concentration has increased to saturation.
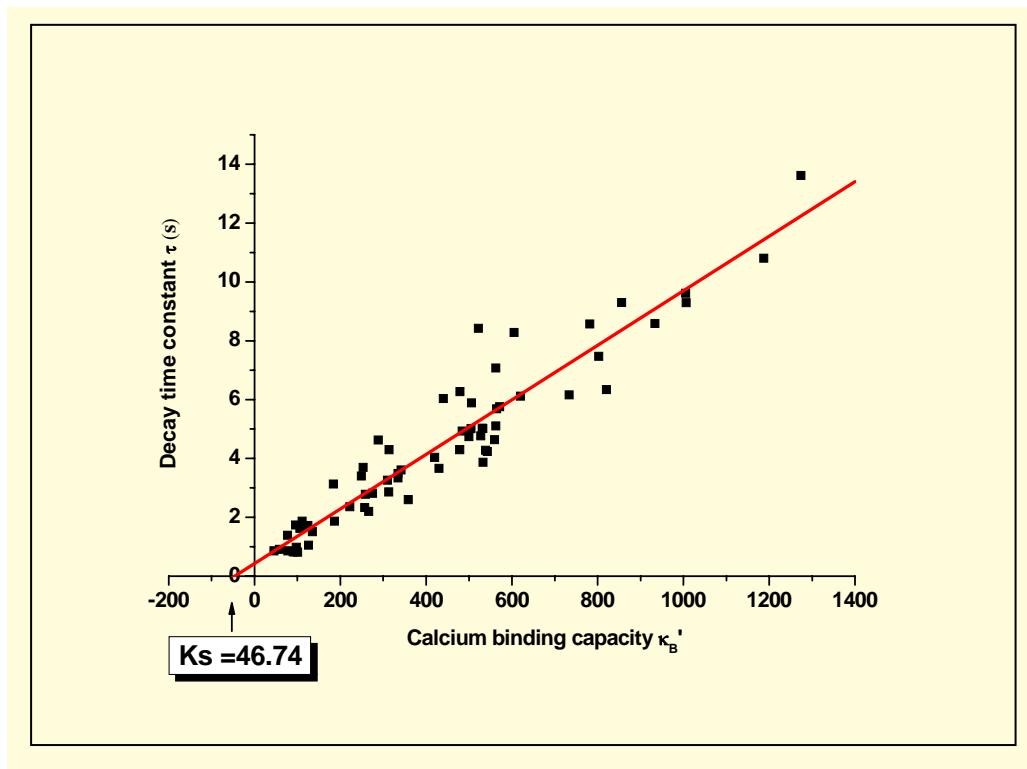
Fig 3.2.2.(ii)   To determine the intrinsic buffering capacity, decay time constants were plotted against κ_B' of fura-2. A linear regression of this plot was drawn. The *x*-axis intercept of the regression line yielded the calcium binding capacity of 46 ± 21 (15cells) for facial motoneurons. Calcium decay time constant at $\kappa_B' = 0$ was determined to be 0.48 ± 0.14s, from the intersection point of *y*-axis with the linear regression line.

3.2.3 Calcium buffering capacity of trochlear motoneurons

Trochlear nucleus is located in the tegmentum of the mid brain roughly at the level of inferior colliculus and the sustantia nigra. The nucleus exists slightly ventral to the aqueduct of sylvius (cerebral aqueduct). The axonal fibers of these motoneurons make up the trochlear nerve (cranial nerve IV) which innervates the superior oblique muscle of the eye orbit. The superior oblique muscle is one of the six extra ocular muscles responsible for the precise movement of the eye for visual tracking or fixation on an object.

When patch clamped with 50-1000µM fura-2 and Ca^{2+} transients were studied, trochlear motoneurons had a characteristic slower decay time for the voltage induced Ca^{2+} transients at lower concentration of fura-2. These motoneurons are shown to express high levels of calcium binding proteins like calbindin-D28K and parvalbumin (Alexianu et al, 1994). Accordingly a much higher K_S of 392 ± 58 (Fig. 3.2.3 *A, B* and *C*) was obtained from the τ versus K_B' plot of trochlear motoneurons. They showed an average τ of 3.0 ± 0.44s for somatic calcium transients at $K_B=0$, indicating the average life time of their Ca^{2+} transients at basal conditions. The Ca^{2+} extrusion rate constant γ for trochlear motoneurons is calculated to be 138 ± 6s^{-1} (n=12).

A

$\tau = 80$s
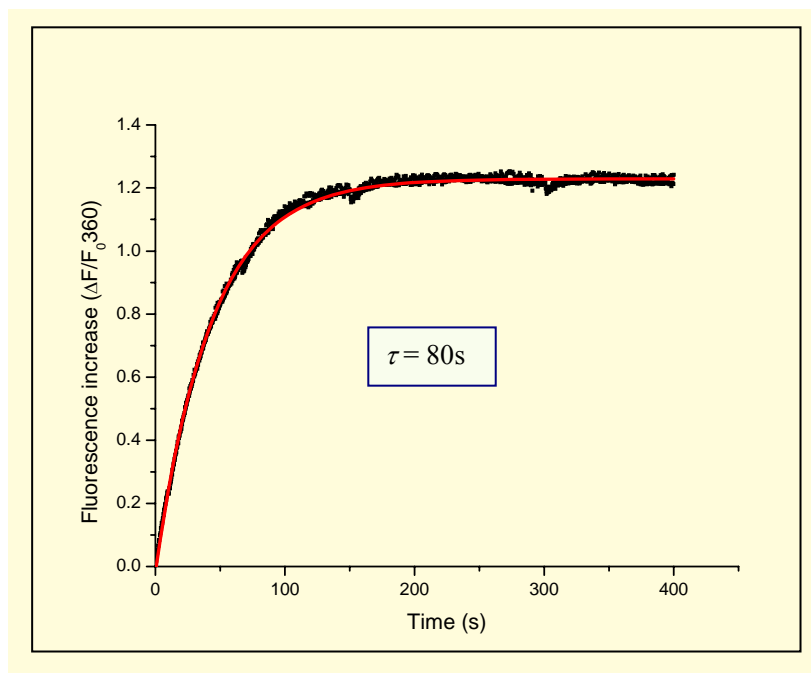
B
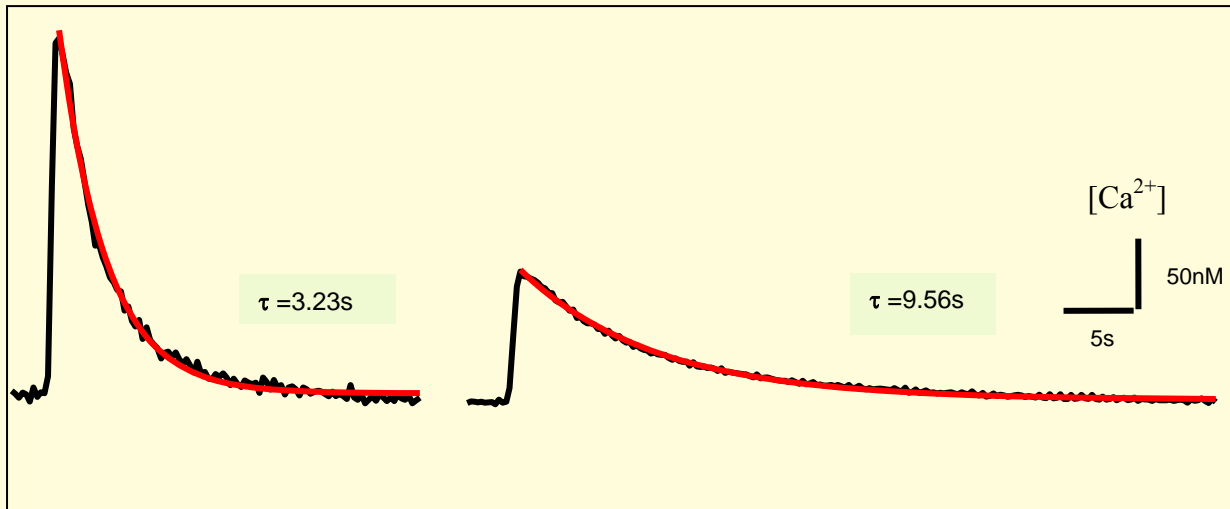
C
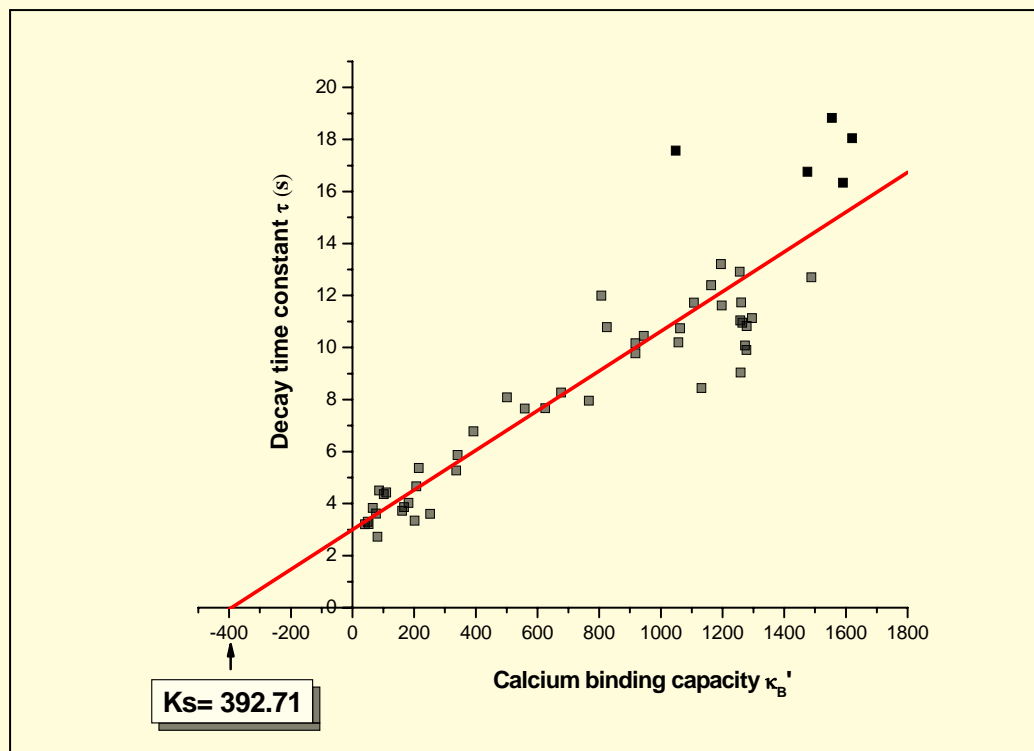
Fig 3.2.3. *(A)* Intensity change in the Ca^{2+} independent fluorescence, F_{360} when trochlear MNs were whole cell patch clamped with 50-1000µM fura-2. The data points are fitted with a single exponential decay function. The average filling time for these neurons is calculated to be 80.74 ± 15s *(B)* Ca^{2+} transients evoked by step depolarization to 10mV for 0.5s for trochlear MNs: the left trace indicates the Ca^{2+} change during stimulation at a low binding affinity of fura-2, i.e. just after the cell membrane patch was ruptured for whole cell measurements, and the right trace represents the Ca^{2+} signal after the cell is fully loaded with a high fura-2 concentration. *(C)* To determine the intrinsic buffering capacity, decay time constants were plotted against κ_B' of fura-2 and a linear regression fit of the data points is made.

The *x*-axis intercept of the regression line yielded the calcium binding capacity of 392 ± 58 (10cells) for trochlear motoneurons. Calcium decay time constant at $\kappa_B' = 0$ was determined to be 3.0 ± 0.44s.

3.3 Developmental aspects of Ca^{2+} metabolism of FMNs

It was observed that FMNs from P0 mouse had a slower Ca^{2+} transient decay time than the FMNs of P4 animal at a similar K_B' (binding affinity of fura). This observation lead to the attempt to find out whether there is any difference in the Ca^{2+} buffering capacity of FMNs at P0 stage to that of later stages. Using the same tools and approaches, study has been done to evaluate the characteristics of Ca^{2+} handling in these neurons. The role of mitochondria in the Ca^{2+} metabolism of P0 FMNs was also checked, using FCCP to release the mitochondrially accumulated Ca^{2+} and studying the Ca^{2+} transients in presence and absence of mitochondrial Ca^{2+} uptake.

3.3.1 P0 FMN has slower Ca^{2+} transient decay times than age P4 and above

FMNs from P0 animals were again studied by patch clamping them with 100μM fura. The decay time constant of the Ca^{2+} transients triggered by step depolarization to +10 from -60mV were analysed by fitting them with single exponential decay.
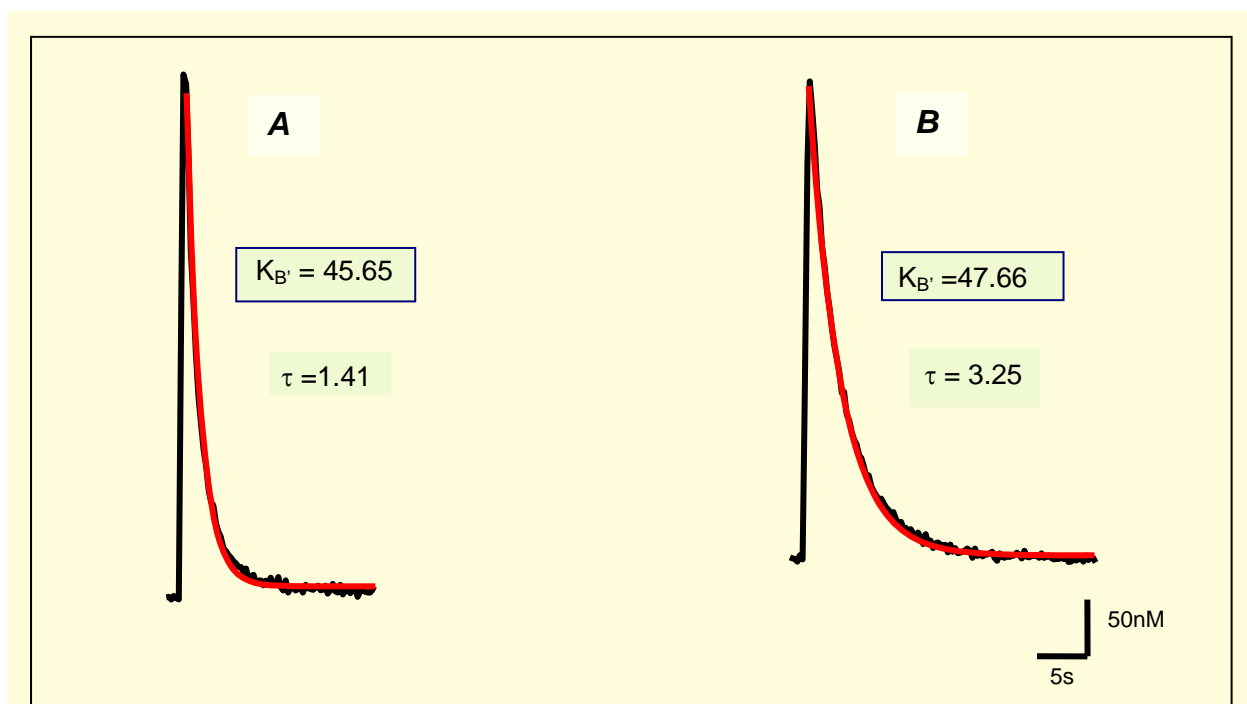
Fig. 3.3.1. FMNs from mice aging 4 days and zero-day were patch clamped with 100μM fura-2 and depolarisations were evoked through the patch electrode. The Ca^{2+} transients in response to these depolarisations had definite decay time period at a particular K_B' of fura-2. when compared among them, P4 (*A*)and P0 (*B*) FMNs showed different decay time constants (τ) for similar K_B'; the decay time being comparatively faster for the P4 FMNs.

This revealed that FMNs from P0 animal to have a much slower Ca^{2+} transient decay time than FMNs from P4 animal. This delay in decay time was presumed to be a reflection of an increased Ca^{2+} buffering molecule concentration in the P0 FMNs. Further analyses were done to elucidate this presumption.

3.3.2 P0 Facial motoneurons have lower calcium release upon FCCP application

Mitochondria act as local Ca^{2+} accumulating organelle in many neuron types during the electrical activity. This pool of Ca^{2+} is releasable by drugs interfering with the mitochondrial membrane potential ($\Delta\Psi$) as ion accumulation by mitochondria is dependent on the electrogenicity of the mitochondrial membrane (Shishkin et al 2002). Previously we have seen that facial motoneurons from mice on postnatal day four has a comparatively low Ca^{2+} buffering capacity and mitochondria have an enhanced role of accumulating Ca^{2+}. This was evident from the experiments where we applied FCCP to release accumulated Ca^{2+} after a depolarizing stimulus in the voltage clamp configuration.
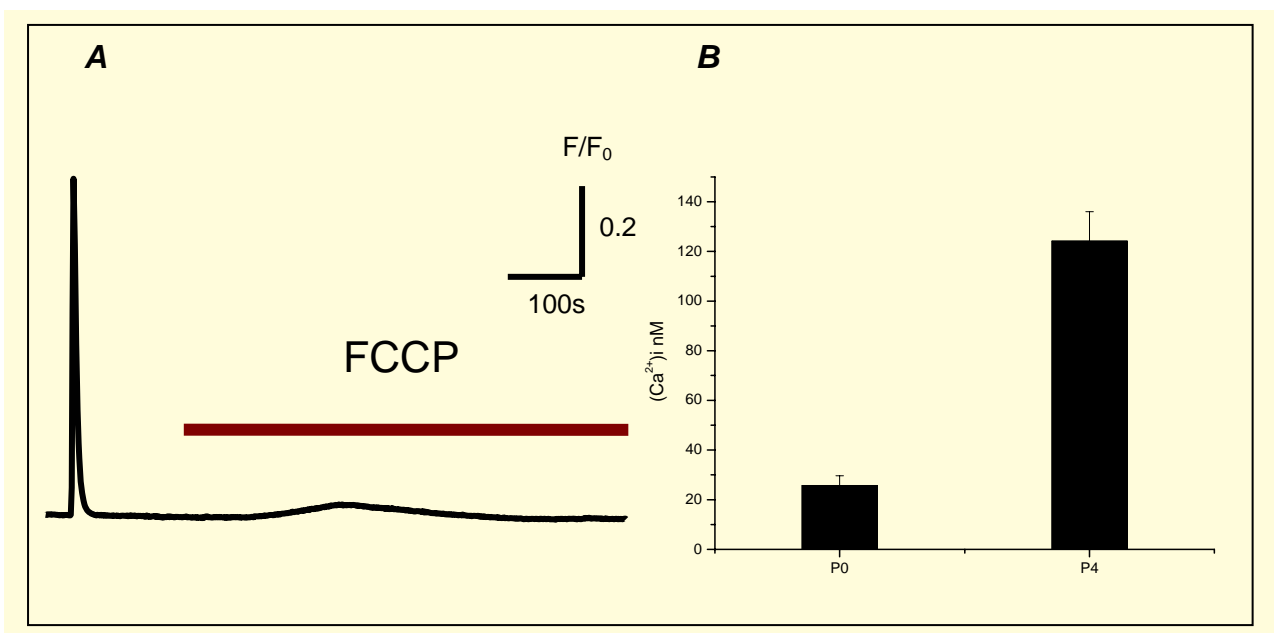
Fig 3.3.2. *A*, whole cell patch clamped P0 FMNs were exposed to 2μM FCCP through circulation to cause the mitochondrial Ca^{2+} release. FCCP was applied shortly after an induced controlled Ca^{2+} influx. *B*, Ca^{2+} release events from P0 FMNs were of much lower amplitude than what was observed in P4 FMNs when treated with FCCP after a short Ca^{2+} activity.

Applying the same experimental approach on the facial motoneurons of postnatal day zero mice resulted in comparatively lower release of Ca^{2+} from the mitochondria. On an average this amounted to be only $25.77 \pm 3.89nM$ (n=10, Fig 3.3.2), which is less than half the amount observed in the P4 animal (data shown in Fig 3.1.3).

3.3.3 Ca^{2+} transient decay delay caused by FCCP application is also smaller in the P0 FMNs

Other than the Ca^{2+} permeable channels on the plasma membrane, intracellular Ca^{2+} sequestering mechanisms have a tremendous influence on the life and amplitude of a Ca^{2+} signal. The role of mitochondria in this aspect could be tested by measuring the decay time constant (τ) of a depolarization induced Ca^{2+} transient of a patch clamped neuron in presence and absence of electrically intact mitochondria.
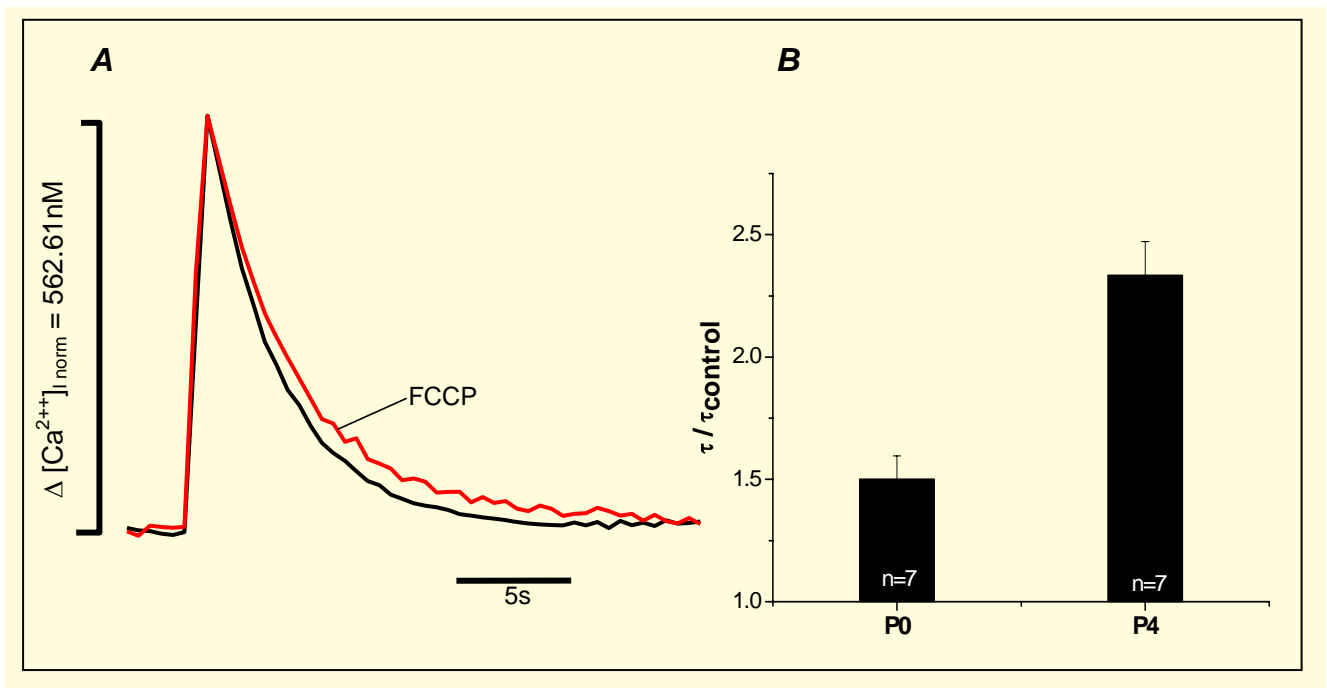
Fig 3.3.3. *A*, decay time constant of depolarisation induced Ca^{2+} transients are not very much influenced by the mitochondrial Ca^{2+} uptake deletion. On average the Ca^{2+} signals in P0 FMNs were delayed only 1.48 times that of the control transients evoked at similar $K_{B'}$ of fura-2. *B*, comparison of Ca^{2+} transient decay time delays caused by FCCP on FMNs at age P0 and P4.

It was seen that the τ of the depolarization induced transient was not much delayed after incubation with $2\mu M$ FCCP (Fig 3.3.3 *A* and *B*). On average the τ of the control transient was

$2.92 \pm 0.17s$ and that in presence of FCCP was $4.32 \pm 0.24s$. These values reveal a delay in the recovery time of 1.48 times for the calcium transients in presence of FCCP.

3.3.4 P0 facial motoneurons has a comparatively higher Ca^{2+} buffering capacity

It is evident from the results above that the mitochondrial participation in the Ca^{2+} buffering of P0 facial motoneurons is to a lesser extent. Further verification of the abundance of Ca^{2+} buffering molecules in these motoneurons was done by the 'added buffer method' (Neher & Augustine, 1992) where motoneurons were patch clamped with varying concentration of the Ca^{2+} indicator dye fura-2 and calcium transients were studied (Fig 3.3.4 (i) *A*). The decay time constants (τ) of depolarization induced Ca^{2+} transients were measured at different binding affinities ($K_{B'}$) of fura-2 and were plotted against each other. An endogenous calcium buffering capacity (Ks) of 134 ± 14 was obtained for P0 facial motoneurons (Fig 3.3.4 (i) *B*). This value is almost three times higher than the value observed for the same neurons at the age of post natal day four (P4).

Similar experiments were conducted to analyse the buffering capacity of facial motoneurons at the age of post natal days 8 to 10. The decay time constants (τ) of depolarization induced Ca^{2+} transients were recorded at different binding affinities ($K_{B'}$) of fura-2 and were plotted against each other like in the buffering capacity studies described for P4 and P0 motoneurons (Fig 3.3.4 (ii) *A*). No significant difference in the Ca^{2+} buffering capability was found at this age points compared to that of postnatal day four. Facial motoneurons from P8-P10 showed a similar endogenous buffering capacity value of 42 (Fig 3.3.4 (ii) *B*), to that of P4 FMNs. The plasma membrane extrusion rate for Ca^{2+} was found to be $70 \pm 3s^{-1}$ (n=15) for P0 FMNs and $101 \pm 5s^{-1}$ (n=13) for FMNs at the age P8-P10.
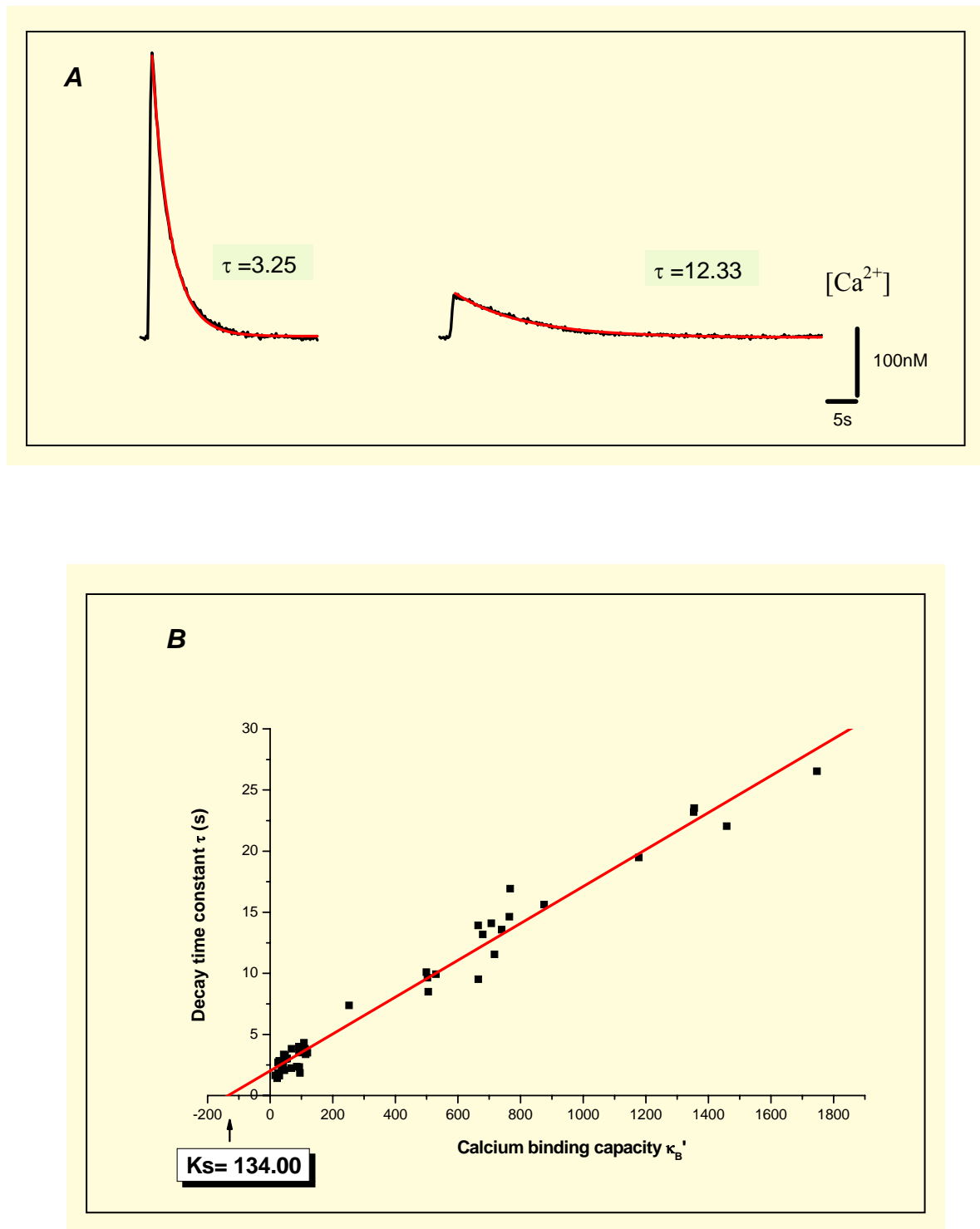
Fig 3.3.4 (i). Ca^{2+} buffering molecule concentration of P0 FMNs was determined by added buffer method. *A*, Ca^{2+} transients evoked at low and high $K_{B'}$ of fura-2. At low $K_{B'}$ (left) the calcium entering the cell is hugely reflected in the cytoplasm as the increase in the fura-2 ratio, where as at high $K_{B'}$ (right) the ratio value is much less due to the high concentration of unbound fura-2. *B*, the τ of the voltage triggered Ca^{2+} transients at different $K_{B'}$ was plotted against one another. Subsequent linear regression fit of this graph resolved the Ca^{2+} binding capacity of these neurons to be 134.00 ± 14.
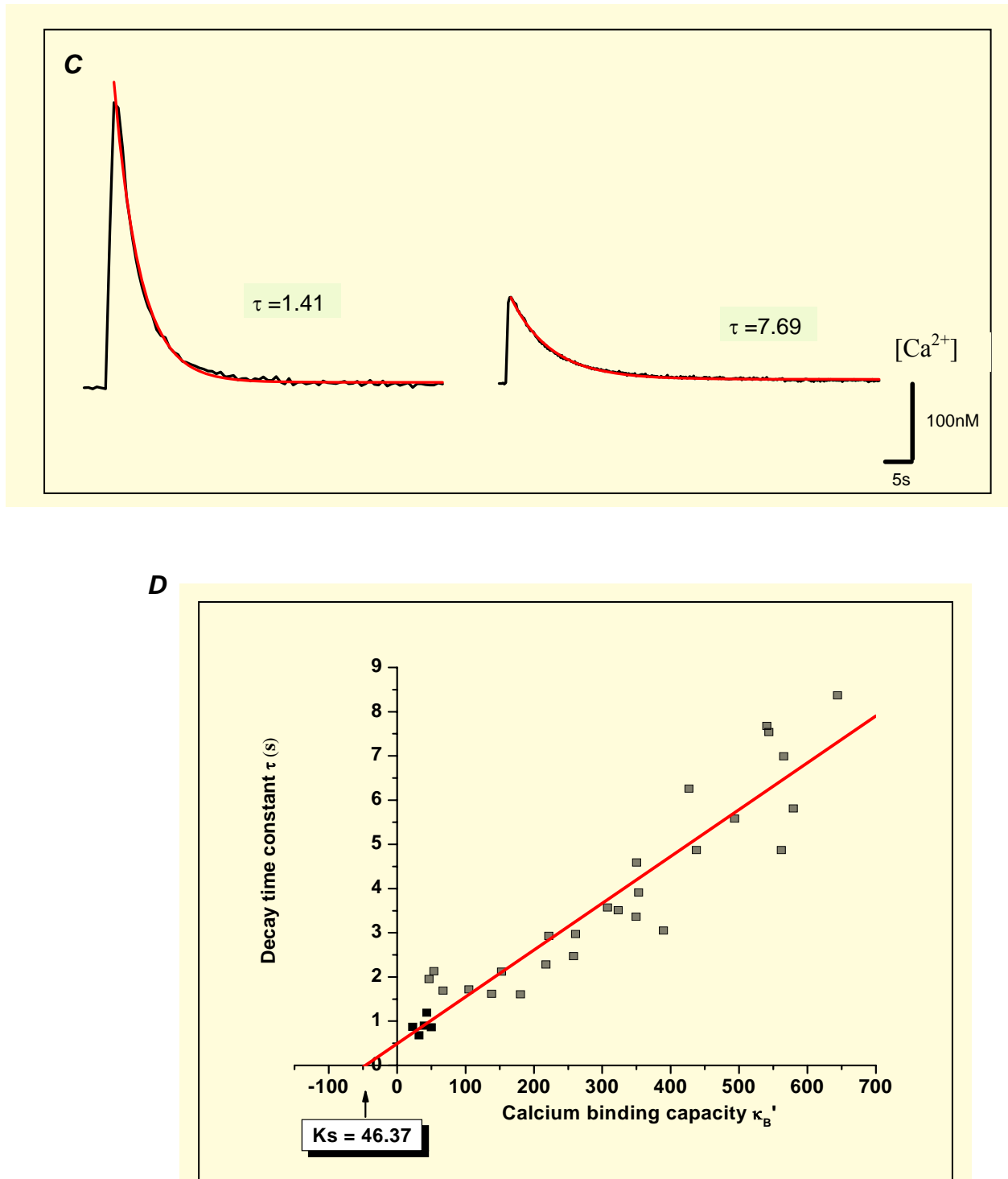
Fig 3.3.4 (ii). *C*, in the P10 FMNs the influence of increasing fura concentration on the decay time of Ca²⁺ transients was more drastic, similar to that in P4 FMNs. The left trace represents a Ca²⁺ peak at a low concentration of fura-2; very early after the whole cell configuration is achieved and the right trace is at a higher concentration of fura-2; some minute after the whole cell is established. *D*, the decay time constant (τ) of these transients measured at different time points during patch clamp measurements is plotted against the increasing fura-2 binding affinity $K_{B'}$. The linear fit for this graph revealed that FMNs at age P8-10 show a Ca²⁺ buffering concentration of 46 as shown by P4 FMNs.

3.3.5 The effective extrusion rate (γ) is slightly but significantly increased as the buffering capacity reduces in the neonatal FMNs

The Ca^{2+} clearance done by plasma membrane channels also determine the life time of Ca^{2+} transients in the cell. The comparison of calcium extrusion rate at P0, P4 and P8-P10 reveals that as the Ca^{2+} buffering capacity of these motoneurons becomes lower with the age, the effective extrusion rate through the plasma membrane Ca^{2+} channels tend to increase slightly but significantly ($P<0.01$). This analysis is represented in the following figure.
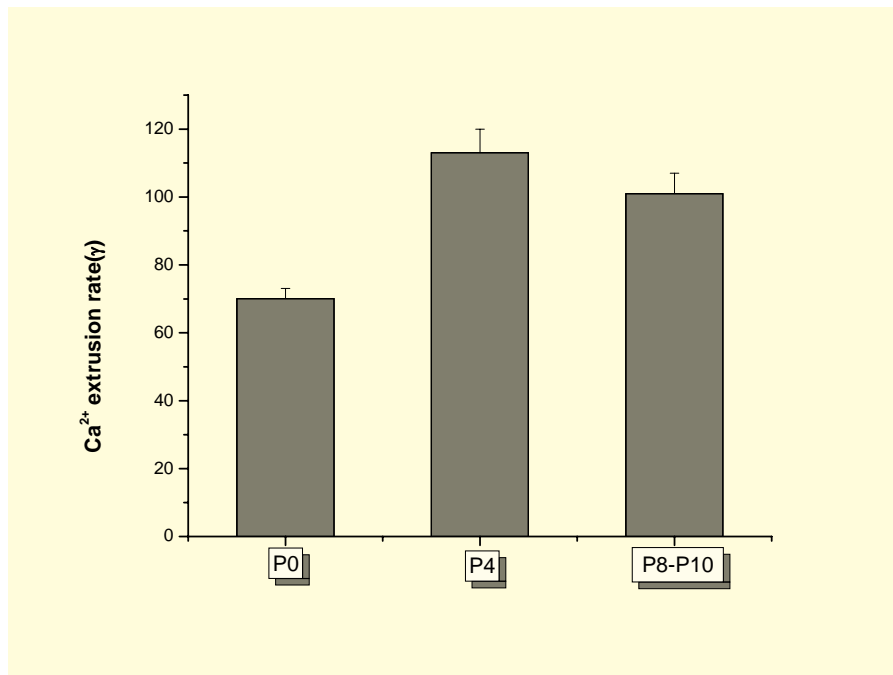
Fig 3.3.5. From the analysis of effective extrusion by the plasma membrane Ca^{2+} channels of facial motoneurons from P0, P4 and P8-P10 ages it is evident that with respect to the reducing Ca^{2+} buffering capacity, there s an increase in the participation of neuronal membrane Ca^{2+} channels to clear Ca^{2+} after a short period of activity.

3.3.6 Oculomotor neurons at P0 age has higher endogenous buffering capacity values

Further investigations were done to find out the buffering capacity of oculomotor neurons at the P0 stage. This was to evaluate whether there is any change happening, regarding the Ca^{2+} buffering capacity of these neurons, during first few days of development, as in the case of facial motoneurons.
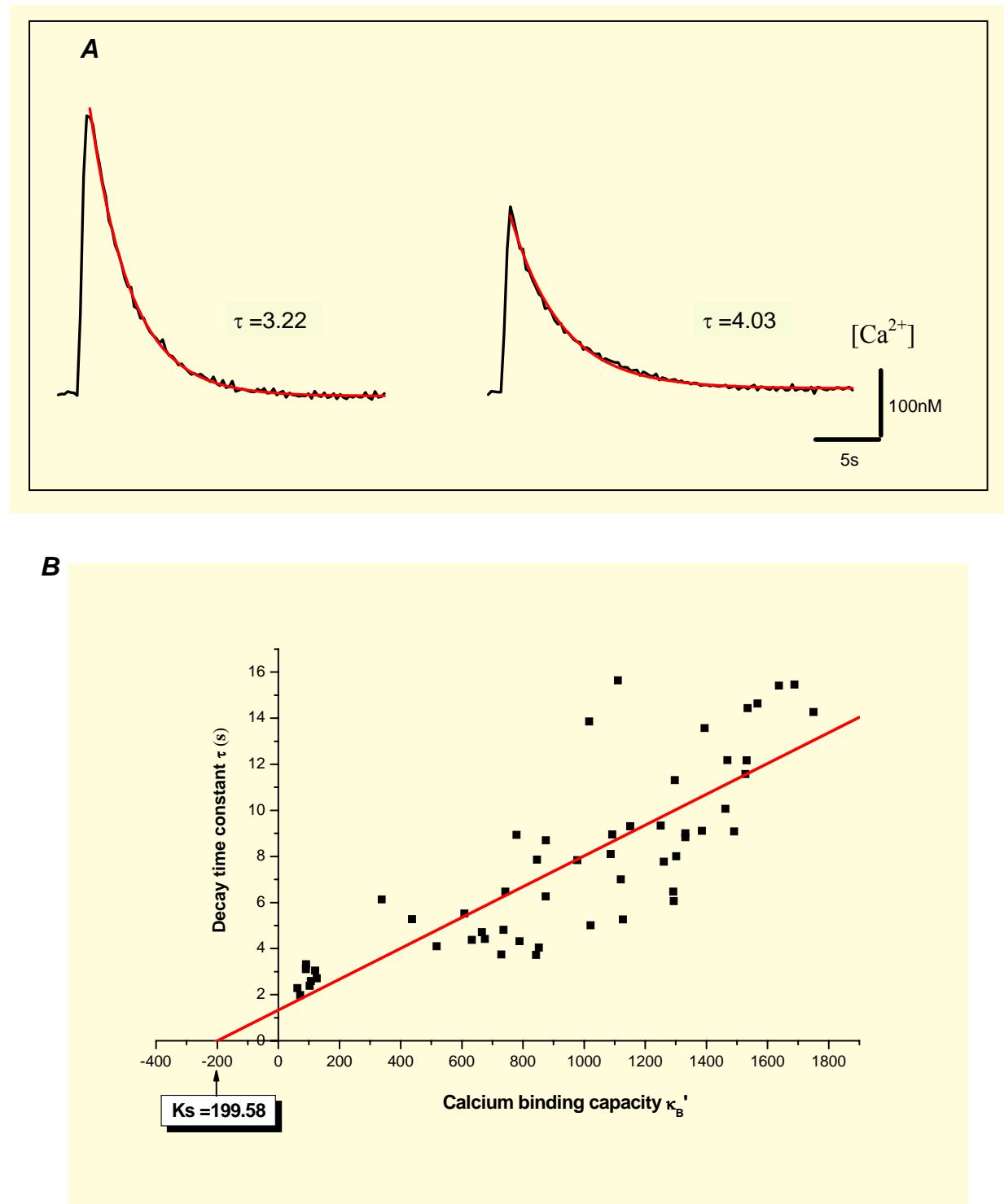
Fig 3.3.6. *A*, voltage triggered Ca^{2+} peaks from P0 oculomotor neurons. It is evident from the figure that the increase in the fura-2 $K_{B'}$ did not have a severe influence on the decay time constant of these neurons as represented in the left (low $K_{B'}$) and right (high $K_{B'}$). Buffering capacity of these neurons was figured out from the plot of decay time constants measured against the varying calcium binding affinity during the whole cell measurements with varied fura-2 concentrations (*B*).

Plotting the decay time constants of Ca^{2+} transients against the $K_{B'}$ of fura-2 revealed a buffering capacity of 199.58 for these neurons at this particular developmental time-point. Previously we have seen a buffering capacity value of 263.8 for oculomotor neurons from P2-P6 mice (Vanselow & Keller, 2000). As evident from the values there is no significant change happening to the Ca^{2+} buffering ability of these neurons during the first few days of development.

3.4   Ca^{2+} metabolism of Dorsal Vagal neurons

Dorsal motor nucleus of the vagus (X) is located slightly dorsal and lateral to the hypoglossal nucleus. The axons arising from the neurons (smooth muscle motoneurons) constituting this nucleus give rise to pre-ganglionic parasympathetic nerve fibers that exit the brain stem dorsal and lateral to the inferior olive. These axons comprise the visceromotor component of the vagus nerve. These fibers activate the post-ganglionic parasympathetic neurons in ganglia supplying pharynx, larynx and oesophagus. These post-ganglionic fibers in turn innervate glands and smooth muscles in these structures. Cardiac branches of the vagus nerve affect the heart rate, and stimulation of this nerve slows down the heart rate. Any unilateral lesion of either (right or left) dorsal vagal nerve can result in an increase in the heart rate. The visceromotor fibers from vagus also reach the stomach and gut, and stimulation of the nerve results in increased peristalsis and increased secretion from the gastric and intestinal glands and the relaxation of sphincters. Thus the dorsal motor nucleus X plays an important role in various visceral reflexes whereby receives and returns information about the 'internal milieu'.

Complimentary study on the Ca^{2+} characteristics of dorsal vagal neurons where carried out in order to understand whether these smooth muscle motoneurons which are spared in the early neurodestruction during ALS (Bergmann & Keller, 2003) are also specially equipped with, to counteract the uncontrolled Ca^{2+} influx. For this we have employed the same experimental protocols as previously described on other neuronal populations. The results attained from these experiments are described below.

3.4.1 Dorsal vagal neurons show only slight delay in Ca^{2+} transient decay time upon mitochondrial inhibition.

The controlling effect of mitochondria on determining the life period of a Ca^{2+} transient was not prominently visible in DVNs. These neurons, when patch clamped and voltage stimulated for Ca^{2+} transient for 0.5s, in the absence and presence of FCCP, did not show any significant difference in their average decay time. The decay time constant for the Ca^{2+} transients after mitochondrial disruption was not significantly larger than that in the control conditions. The decay time under control conditions and in presence of FCCP was 7.78± 0.39s and 9.52 ± 0.65s (Fig. 3.4.1, n=9) respectively at a similar $K_{B'}$ of fura-2. In effect in the case of vagal neurons, this delay was only 1.22 ± 0.06 times control decay time constant.
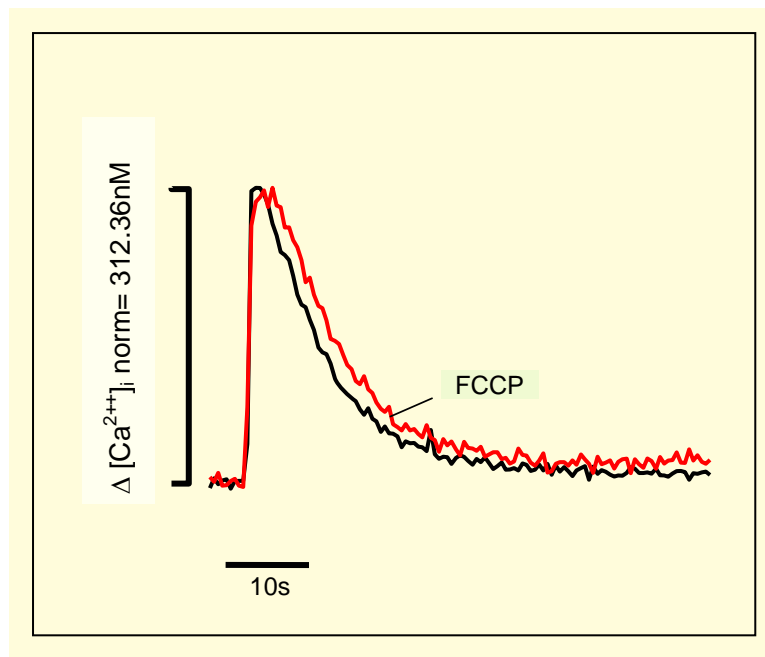
Fig 3.4.1. Depolarisation induced Ca^{2+} signals were invoked in dorsal vagal neurons in presence and absence of intact functioning mitochondria to evaluate FCCP's effect on the rate of Ca^{2+} clearance by mitochondria. The average delay caused by >5 min application of FCCP was only 1.22 times that of the average control response.

3.4.2 DVNs show only very low Ca^{2+} release upon FCCP application

The mitochondrial take up of Ca^{2+} during the increase in the cytoplasmic Ca^{2+} concentration accompanying a controlled voltage stimulus was assessed by simultaneously applying FCCP within 5 minutes of the stimulus. Dorsal vagal neurons showed only an average Ca^{2+} release of 26.44 ± 4.18 nM (n=9) upon mitochondrial disruption by FCCP (Fig 3.4.2). Compared to the ALS vulnerable and non-vulnerable motoneurons under study, dorsal vagal neuron shows a Ca^{2+} characteristic more similar to the latter. This more or less explains how DVNs are spared at least initially in the neuronal damage associate with ALS.
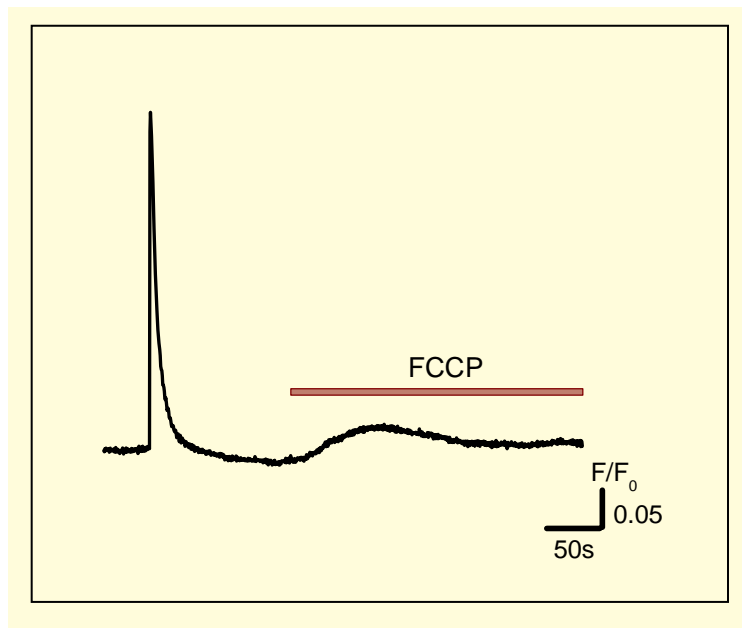
Fig 3.4.2. 2µM FCCP was applied to release the mitochondrially accumulated Ca^{2+} during the short depolarisation induced Ca^{2+} influx (to 10mV for 0.5s). Dorsal vagal neurons had a characteristic low Ca^{2+} release upon FCCP incubation, which was quantified only to be 26.44± 4.18 nM.

3.4.3   No Ca^{2+} transient amplitude increase is observed in DVNs in presence of FCCP

Deleting the mitochondrial participation in Ca^{2+} uptake did not have any significant influence on the K$^+$ induced Ca^{2+} elevation of dorsal vagal neurons. It was also apparent that the presence of FCCP did not affect the recovery of these Ca^{2+} increments (Fig 3.4.3A and B). This was in similarity to what found in oculomotor and trochlear motoneurons where the presence FCCP did not have a huge influence on the propagation and recovery of K$^+$ induced Ca^{2+} up shoot.
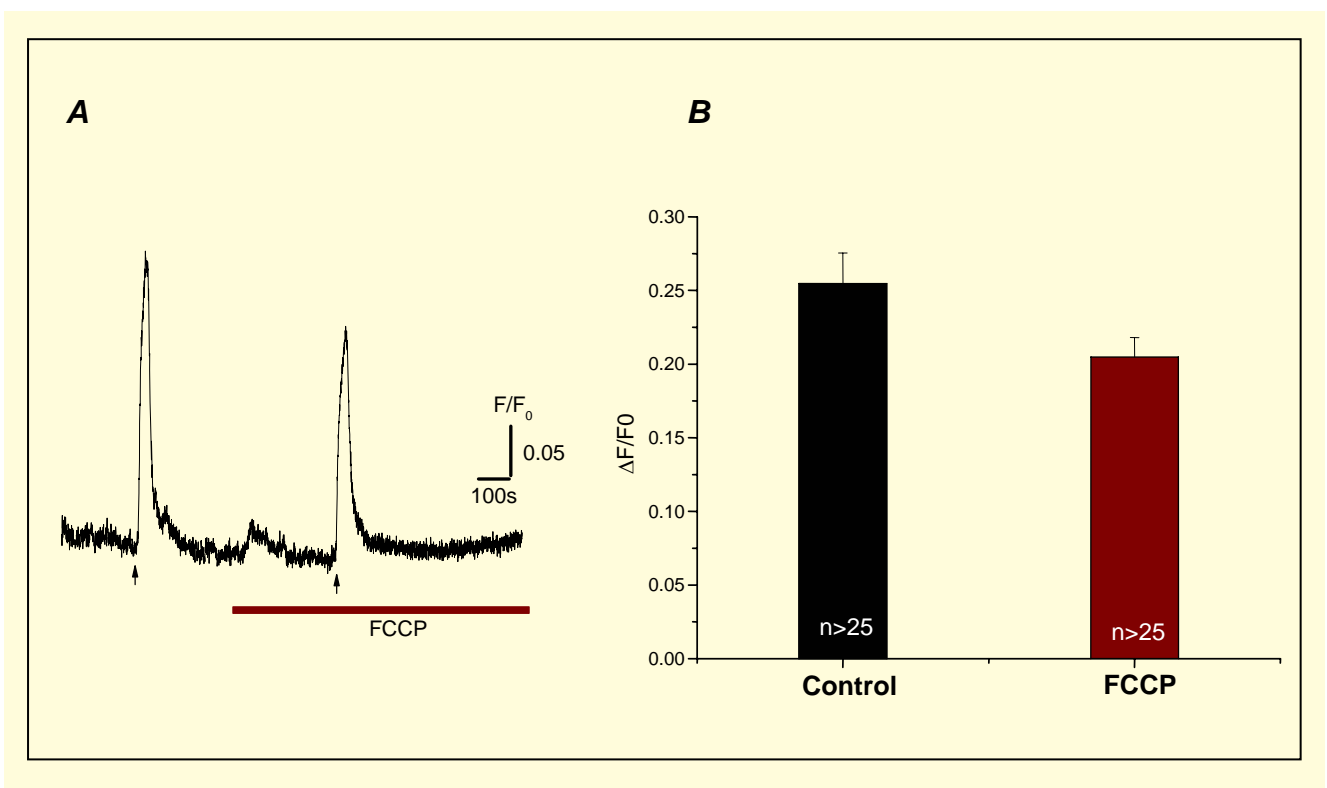
Fig 3.4.3.   Fura-2 AM stained dorsal vagal neurons were stimulated with 30mM K$^+$ to produce Ca^{2+} transients. Arrow indicates the application of 30mM K$^+$ for 30s, (*A*). There was no increase in the amplitude of Ca^{2+} transients in presence of 2µM FCCP in contrast from what was observed in facial and hypoglossal MNs, (B).

3.4.4 DVN's ER seems to be much more calcium loaded than mitochondria after the neuronal activity

Emptying the ER after a controlled voltage stimulus provided an idea on this organelle's efficiency in assimilating Ca^{2+} after an evoked Ca^{2+} inflow through the plasma membrane. When the ER specific Ca^{2+} ATPase blocker CPA (cyclopiazonic acid) was applied to the patch clamped DVNs after a step depolarization of 0.5s duration, they reported an average Ca^{2+} release of 45.62 ± 5.73 nM (n=5) as measured by the increase in the fura-2 ratio(Fig 3.4.4*A* and *B*). This ER release of Ca^{2+} was higher than the mitochondrial Ca^{2+} release after short depolarization.
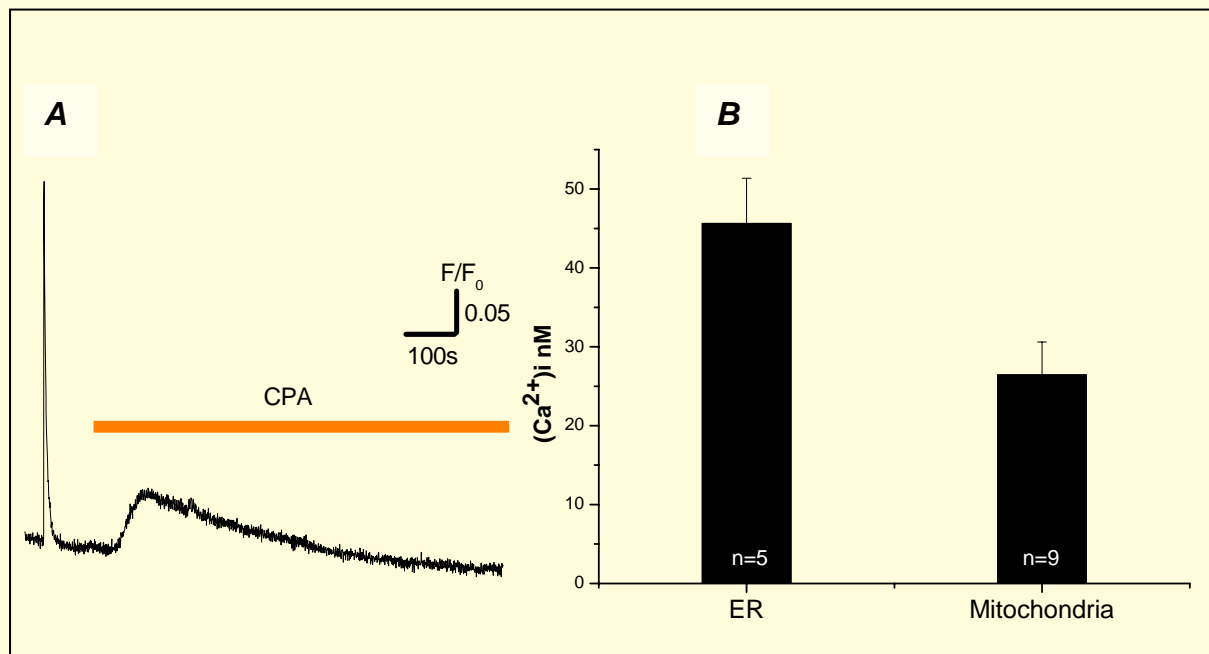
Fig 3.4.4. Dorsal vagal neurons were loaded with 100μM fura-2 and stimulated to fill the intracellular Ca^{2+} stores. 50μM CPA was the applied through the circulation to block the SERCA pumps and cause the Ca^{2+} release (*A*). a comparative analysis revealed that ER of DVNs are in general more Ca^{2+} filled than the mitochondria following a short Ca^{2+} signal (*B*).

3.4.5 DVNs have a high Ca^{2+} buffering capacity value

The same experimental procedure of filling the cells with exogenous Ca^{2+} buffer fura-2, by dialysis from a patch pipette is used to ascertain the buffering capacity of dorsal vagal neurons. Fura-2 concentration used ranged from 50μM to 1000μM and is delivered to the neurons with patch pipettes having resistance higher that 2.5MΩ. Dorsal vagal neurons were identified as the spindle shaped cells with tapering ends lying dorsal to the hypoglossal nucleus. When patch clamped and stimulated with low concentration of fura-2, DVNs had very characteristic slow recovery pattern for the Ca^{2+} transients. The decay time constants of these transients were not very much delayed with an increase in fura-2 concentration from 50μM to 1000μM (Fig 3.4.5*A*). Accordingly theses neurons showed a very high Ks when their decay times to varying $K_{B'}$ of fura-2 was plotted against each other. The linear regression fit traversed the x-axis at a value of 465.69 (Fig 3.4.5*B*). This finding is in agreement with the previously published observations that these neurons have been shown to express high levels of calcium chelating proteins like calretinin and calbindin and moderate concentrations of parvalbumin (Gonzalez et al. 1993, Paxinos et.al 1999).

A
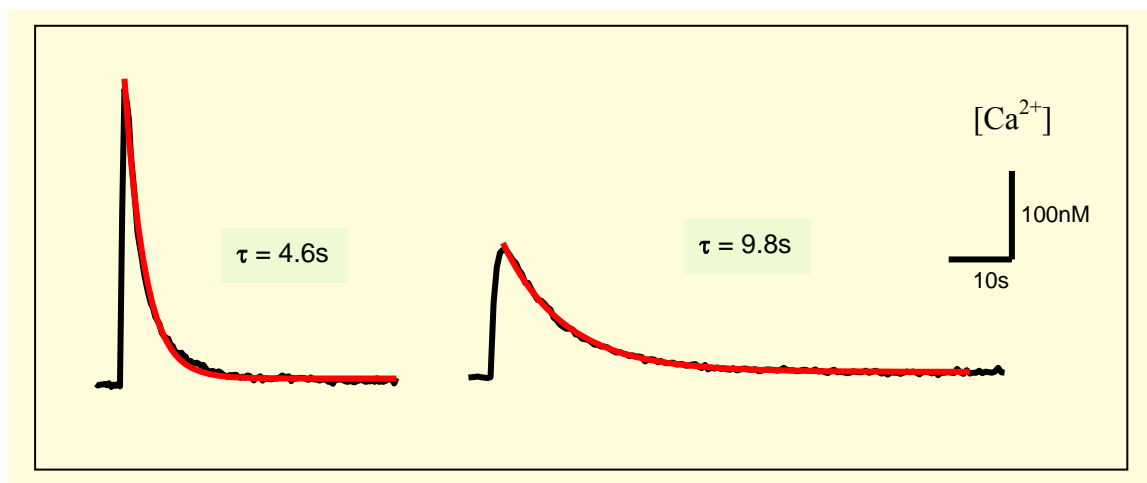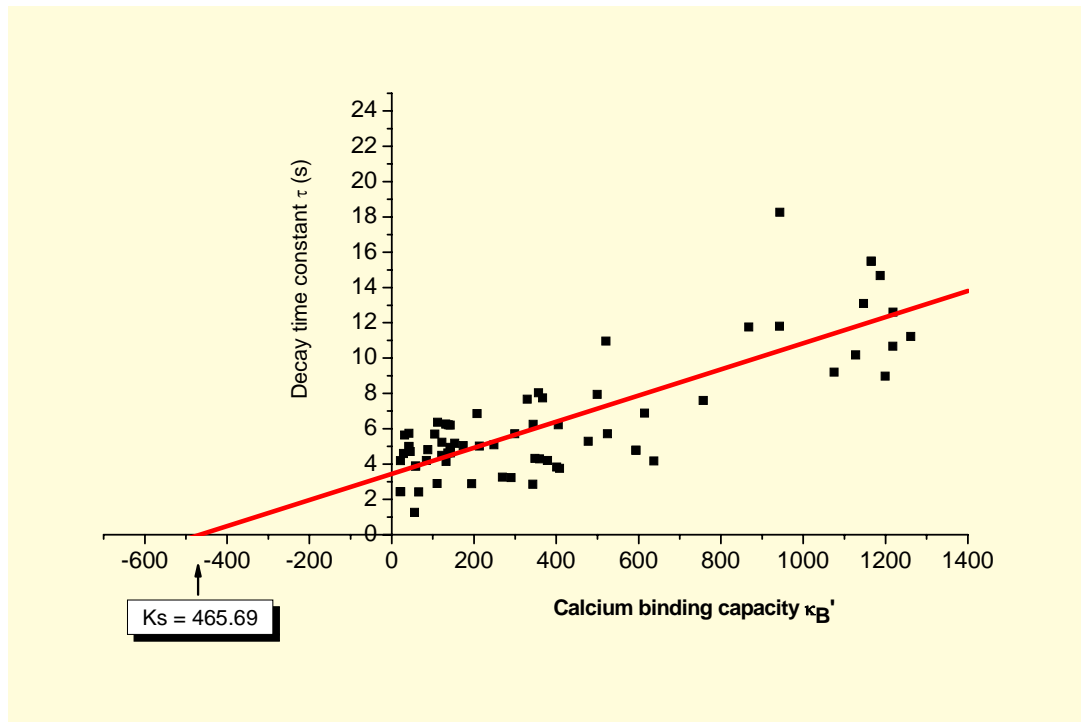
Fig 3.4.5. Ca^{2+} buffering capacity of dorsal vagal neurons were determined through whole cell filling of these neurons with varied concentrations of Ca^{2+} binding dye fura-2 and simultaneous imaging of changes in Ca^{2+} activities. *A*, stimulus evoked Ca^{2+} peaks at a low (left) and high concentration (right) of fura-2. *B*, the obtained calcium transient decay times were plotted against the different calcium binding affinity of fura-2 at different time points during the patch pipette mediated filling of the cell. Linear fit to this graph indicated the molecular concentration of Ca^{2+} buffers in these neurons which was the highest measured in the presented experiments.

Chapter 4

Discussions

The experiments described in the present study have been carried out with the prime objective of understanding the mechanisms which jeopardize specific motoneurons in the motoneuron disease ALS, which has a fatal culmination. The evidence points towards the disturbed calcium handling in motoneurons as a reason for the pathological developments in this disease. The occurrence of Ca^{2+} permeable glutamate channels on motoneurons and the presence of excess glutamate in the extra cellular space due to impaired glutamate uptake by the glial cells lead to excitotoxicity, mediated by uncontrolled Ca^{2+} influx into motoneurons. Another important cellular manifestation of ALS is the damage to mitochondria in motoneurons. It has been proposed that this damage triggers the functional decline of motor neurons and the onset of pathology in ALS. Electron microscopic studies have revealed that massive mitochondrial vacuolation and other abnormalities of mitochondrial structure precede the general muscle weakness symptoms of this disease (Wong et al, 1995; Kong & Xu, 1998; Sasaki et al 2004). The inhibition of enzymes of the electron transport chain is also reported by many groups (Carri et al, 1997; Menzies et al, 2000; Mattiazzi et al, 2002; Jung et al, 2000). Considering the predominant participation of mitochondria, not only in the calcium clearance directly but also in the energy transduction (to operate other Ca^{2+} clearing mechanisms) and in enacting apoptosis, this manifestation is of great significance.

This study has investigated the role of mitochondria in the calcium metabolism of motoneurons which are particularly vulnerable (FMNs & HMNs) or resistant (OMNs & TMNs) in ALS. Dysphagia, dysarthria and difficulty in mastication are major manifestations in human ALS patients as a result of the progressive death of hypoglossal and facial motoneurons. Paralysis of the eye muscles (Ophthalmoplegia) is not generally observed in ALS cases, indicating that oculomotor control is functional during the progress of the disease. The results described provide definite evidence of the distinct role of mitochondria in handling the Ca^{2+} metabolism in the vulnerable motoneurons. These neurons stored a larger amount of calcium in the mitochondria and the disruption of mitochondrial calcium uptake had a marked influence on both the peak amplitude of Ca^{2+} response as well as on the clearance of Ca^{2+} from the cytoplasm. In this report, we studied the Ca^{2+} buffering capacity of some other brainstem neurons where the results show that TMNs are characterized by a very high Ca^{2+} buffering value. This observation categorizes very clearly the neurons studied into

comparatively high-buffered and low-buffered neurons. This is an important characteristic when we consider the survival chance of these neurons in ALS-related insults. FMNs and HMNs which succumb to these pathological conditions are characterized by low support from the intracellular calcium buffering proteins. This scenario probably enables mitochondria in these neurons to actively accumulate Ca^{2+} in order to avoid toxic level Ca^{2+} accumulation in the cytoplasm.

In a disease like ALS where the initial pathophysiological imbalance specifically affects the mitochondria and its metabolic machineries, the neurons, in which mitochondria play this dual role of energy source and calcium-sink, would be placed at the center of the damage.

4.1 FCCP disrupts mitochondrial integrity

The initial experiments clarified that protonophore FCCP could be used as an effective drug to interfere with the mitochondrial Ca^{2+} uptake (Fig. 3.1.1). Under our experimental conditions FCCP did not show any non-specific effect on cell membrane potential. The action of FCCP could be studied very clearly from its effect on the mitochondrial membrane potential (rhodamine-123), NADH autofluorescence and the ensuing $[Ca^{2+}]i$ elevation. When rhodamine-123 loaded hypoglossal motoneurons were treated with 2μM FCCP for 1 minute, there was a sudden and reversible increase in the fluorescence due to ΔΨloss (Fig. 3.1.1A). The application of FCCP also resulted in a sudden decrease in the NADH autofluorescence, indicating its specific action on the mitochondria (Fig. 3.1.1B). The probability of the localization of FCCP on the plasma membrane and any resulting leak of Ca^{2+} ions was also checked. Monitoring the current across the cell membrane in voltage-clamped hypoglossal motoneurons did not reveal any change upon application of FCCP, whereas the application of 2mM sodium cyanide showed an immediate inward current, as previously described (Fig. 3.1.1C). Then simultaneous application of sodium cyanide and FCCP revealed a common target for both the drugs, which are mitochondria (Fig. 3.1.1D). The pre or post application of FCCP to CPA (SERCA pump inhibitor) on HMNs clearly caused a separate Ca^{2+} release. This

indicates the unambiguous action of FCCP in our working model system and the existence of two separate intracellular Ca^{2+} stores in the HMNs (Fig. 3.1.1*E&F*).

4.2 The effect of mitochondrial inhibition on cytosolic calcium clearance rates

Averting the mitochondrial participation in Ca^{2+} uptake, by using FCCP caused a severe delay in the recovery time of $[Ca^{2+}]i$ transients, evoked by 0.5s voltage pulse from $^-$60 to $^+$10mV, only in the vulnerable MN groups (Fig. 3.1.2). This apparently reflects the variability in predominant Ca^{2+} clearing mechanisms of ALS-vulnerable and resistant motoneurons; mitochondria being active part of the Ca^{2+} buffering machinery in FMNs and HMNs (Fig. 3.1.2*A* and *B*). Evidently, in FMNs and HMNs, eliminating the 'mitochondrial calcium buffering' from their naturally low buffered cytoplasm causes the calcium signal to subsist longer, though the plasma membrane Ca^{2+} pumps are evacuating the entered calcium. The probability of cellular energy depletion as a reason for these effects is unlikely, since ATP was supplied to the cells at millimolar concentration via the patch pipette. The effect of FCCP on the ATP depletion could also be compensated by this supply. The additive effect of blocking both mitochondrial Ca^{2+} uptake and the extrusion by plasma membrane channels (by excluding ATP supply) could be visible as severely impaired Ca^{2+} clearance and subsequent secondary Ca^{2+} elevation in the fura-2 AM imaging experiments where ATP is not supplied exogenously (Fig.3.1.4(i) *A &B*).

The delay of τ in FMNs & HMNs and the lack of delay in OMNs & TMNs can be explained in two ways. i) As OMNs and TMNs have comparatively high concentration of calcium binding proteins, the control of calcium transients in these neurons is carried out by these proteins and the plasma membrane extrusion, where mitochondria has little role in terms of calcium buffering. Whereas in the vulnerable neurons, the resident mitochondria has been assigned an additional function of rapid Ca^{2+} uptake at times of neuronal activity. This could be a proficient strategy to control the $[Ca^{2+}]i$, coexisting with the reduced calcium buffering protein population of FMN (Results section) and HMN (Lips & Keller, 1999). ii) There could be even a differential concentration of mitochondria when we compare OMNs & TMNs to the vulnerable MNs; mitochondrial tally being higher in the low buffered FMNs & HMNs and

vice versa. This may provide an explicit localization of mitochondria in to the hotspots of Ca^{2+} entry or a wide spread distribution of these organelles in the low buffer supplied cytoplasm of vulnerable MNs. The localization of mitochondria in the calcium microdomains and the rapid Ca^{2+} uptake and release are well known facts (Rizzuto et al. 2004, Malli et al 2003, Baron et al., 2003). On the other hand mitochondria in the OMNs & TMNs may be majorly attending the role of energy metabolism where calcium buffering proteins are efficiently fulfilling the function of calcium tackling. Supporting evidences are also provided from the experimental results from dorsal vagal neurons which are supplied with ample amount of Ca^{2+} sequestering proteins (de Leon et al, 1993) where the delay in the t of Ca^{2+} transients were not impacted by the mitochondrial permeation caused by FCCP. These experiments also shows the specificity and unambiguous action of FCCP in our system as Ca^{2+} transients are not irreversibly affected by the presence of FCCP, as could be expected if FCCP is non specifically accumulating on the plasma membrane and causing ionic influx, rather effects its specific action intracellularly.

4.3   Mitochondrial function as the Ca^{2+} buffering organelle

It is clear from the above results that mitochondria act as local calcium buffers, thus shaping spatiotemporal aspects of cytosolic calcium signals. As previously described in the results section, mitochondria in facial and hypoglossal motoneurons had a major percentage of the Ca^{2+}, sequestered intracellularly after Ca^{2+} influx through the plasma membrane (Fig. 3.1.3 *A* and *B*). In TMNs, OMNs ((Fig. 3.1.3 *C* and *D*) and DVNs (Fig. 3.4.2) the mitochondrial release was of much less amplitude after the preceding cytosolic Ca^{2+} increase. The bigger load of calcium in HMNs & FMNs could be clearly attributed to the specialization of these cells in employing mitochondria in the major role to seize calcium. This specialized property of mitochondria in HMNs and FMNs could be critical during ALS pathology as the elevated glutamate concentration in synapses, described in ALS clinical samples and animal models, can lead to massive cellular entry and over-accumulation of Ca^{2+} in the mitochondria, which is a well established trigger for mitochondrial swelling and permeability transition. Under such circumstances, motoneurons which employ mitochondria to buffer Ca^{2+} ions are at particular risk than motoneurons which are supplied with abundance of Ca^{2+} chelating proteins. The selective vulnerability of the motoneurons in ALS poses many questions and the

obvious mitochondrial pathology observed in ALS patients and the study models (even before the onset of symptoms) proposes a central role for the degradation of mitochondrial integrity and metabolism. In fact uncontrolled mitochondrial Ca^{2+} accumulation is one of the most important component of the vicious circle of pathological mechanisms in ALS; involving unwanted glutamate accumulation, deregulated Ca^{2+} entry and cytosolic accumulation, mitochondrial damage due to excessive Ca^{2+} entry, production of toxic oxygen radicals, destruction of proteins (membrane channels) and lipids by reactive radicals thus destroying the cellular integrity leading to subsequent undefined entry and intracellular accumulation of ions around the intracellular organelles, and so on, with the lethal cycle.

4.4   Rapid Ca^{2+} accumulation by mitochondria

The rapidness of mitochondrial Ca^{2+} uptake in facial and hypoglossal motoneurons is evident in the experiments where presence of FCCP caused a two fold increase in the amplitude of the $[Ca^{2+}]i$ transients (Fig. 3.1.4(i) *A&B*). The 30mM K^+ induced Ca^{2+} transient in presence of intact mitochondria was smaller in amplitude than the one in presence of FCCP. The excess Ca^{2+} which appears in the second response seems to be hidden by the mitochondrial uptake during the first response. This also proposes a close positioning of mitochondria to the source of Ca^{2+} entry, i.e. to the voltage gated Ca^{2+} channels. Moreover the necessity of mitochondrial uptake for proper recovery of the Ca^{2+} signal is also evident from this experiment, where presence of FCCP causes a rapid and abrupt secondary elevation in the $[Ca^{2+}]i$. Absence of such characteristics in TMNs, OMNs (Fig. 3.1.4(ii) *A&B*) and DVNs (Fig 3.4.3*A* and *B*), implies that in hypoglossal and facial motoneurons mitochondria are serving a pivotal role in controlling the Ca^{2+} entering the cell (even when the neuronal activity and Ca^{2+} entry is underway) and further functional pathways induced by Ca^{2+}.

4.5   ALS vulnerable MNs are characterized by low Ca^{2+} buffering capacity

This study is providing us with an important conclusion derived in connection with our previously published results. i.e. there is a general trend that the MNs which are vulnerable in

ALS are residing only a very small population of calcium binding proteins; for e.g. HMNs, where the Ca^{2+} buffering capacity is 41 (Lips & Keller 1998) & FMNs with Ks value of 46 (from this study, Fig 3.2.2). This is in absolute contrast with that of the ALS non-vulnerable neurons (for e.g. OMNs have Ks of 263). And in this report we have seen that the TMNs which are ALS non-vulnerable motoneurons (Medina et al 1996) have similarly high Ks of 392.71 (Fig 3.2.3). Furthermore the buffering capacity measurements of dorsal vagal neurons, which are known to have an elevated expression of parvalbumin, showed a high Ca^{2+} buffering capacity of 465. This directs us to assume that, the meagre presence of calcium binding proteins in the facial and hypoglossal MNs is a risk factor when considering the huge Ca^{2+} influx during the ALS etiology. Whereas the high buffered neurons are evading the toxic accumulation of free Ca^{2+} in their cytoplasm by effectively buffering it with their high affinity calcium binding proteins.

4.6 Study on ER Ca^{2+} stores

In an attempt to understand more about the Ca^{2+} metabolism of FMNs & HMNs we studied the role of endoplasmic reticulum in calcium handling in these MNs (Fig.3.1.5 *A* and *B*). ER in FMNs & HMNs retained comparatively low quantity of calcium than mitochondria after cytoplasmic Ca^{2+} elevation, indicating its low efficiency to sequester Ca^{2+}. OMNs, TMNs (Fig.3.1.5 *C* and *D*) and DVNs (Fig 3.4.4*A* and *B*) showed slightly higher Ca^{2+} load in the ER than in mitochondria, indicating that the conventional Ca^{2+} storing function of ER is dominating over mitochondrial Ca^{2+} accumulation in these neurons.

4.7 Selective vulnerability of motoneurons in ALS

Despite rigorous research, the precise molecular abnormalities which lead to specific motoneuron damage in ALS are still evading the scientific world. Accumulating evidences suggest uncontrolled Ca^{2+} entry and inefficacy to sequester this calcium as principal cause for the selective damage. The most astonishing feature described, regarding the pathological signs of this disease, is the presence of large vacuoles derived from the degenerating mitochondria and mitochondrial swelling in the motoneurons of the mouse model of ALS (Dal Canto &

Gurney 1994; Wong et al, 1995; Kong & Xu 1998; Kanno et al 2002; Sasaki et al, 2004). In these mice the onset of paralysis is immediately preceded by the degeneration of mitochondria. Muscle biopsies of sporadic ALS patients showed increased mitochondrial volume and mitochondrial calcium levels (Siklos et al, 1996). Alteration in the mitochondrial membrane potential, compromised mitochondrial calcium homeostasis, decreased respiratory chain function (Mattiazzi et al, 2002) and increased susceptibility to mitochondrial toxins is also reported. Since our data suggest an important role for mitochondria in the calcium metabolism of FMNs & HMNs which show pathology in ALS, the above mentioned abnormalities can render these neurons to selective damage and death due to Ca^{2+} mishandling. The cellular specialization in these MNs with regard to the low buffering capacity of the cytoplasm has assigned mitochondria to regulate the calcium entering the cell. As evident from the results, in these neurons which are damaged in ALS, the mitochondria plays a central role to define the Ca^{2+} entry into cells, the propagation of Ca^{2+} signal, and its degeneration. A representation of the differential functional model of the two sets of motoneurons under study has been given in Fig 4.7; where in the vulnerable motoneurons, the calcium buffering machinery is represented by the predominance of mitochondria, and by the calcium binding proteins in the non-vulnerable motoneurons.
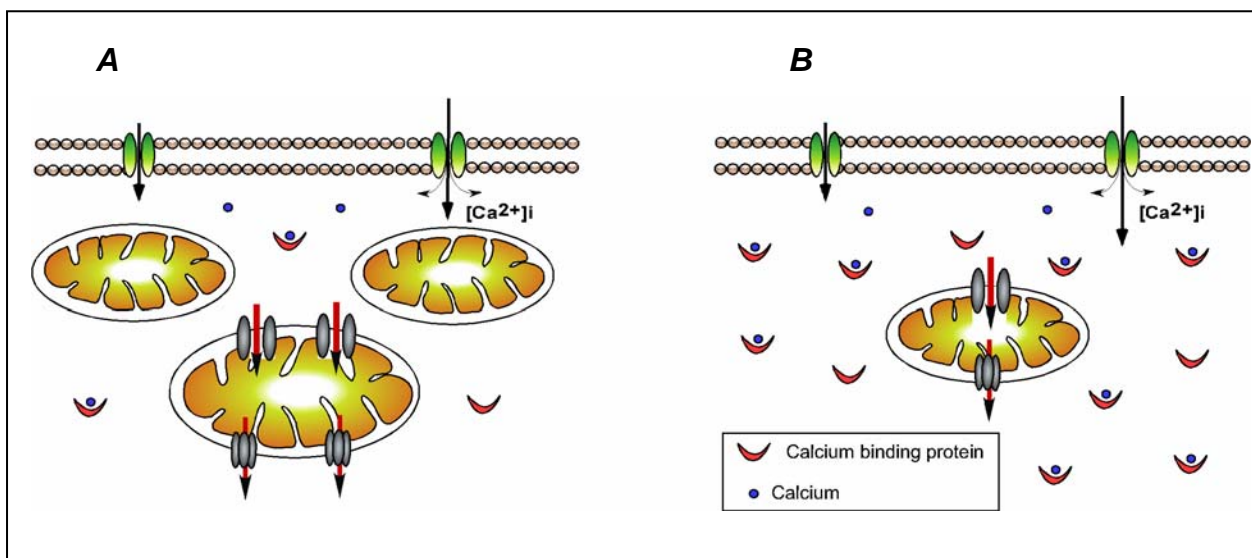
Fig 4.7. Representative model proposed to explain the differential buffering capacity and recruitment of mitochondria in pivotal role in determining the Ca^{2+} dynamics in Facial and hypoglossal motoneurons which are vulnerable to Ca^{2+} mediated insults in ALS. *A*, In FMNs and HMNs the low number of Ca^{2+} buffering proteins are not sufficient to effectively control the Ca^{2+} ions entering during neuronal activity. Consequently these cells have adapted the mitochondria into specialised efficient Ca^{2+} buffering organelles, which take their place very close to the Ca^{2+} entry channels in the neuronal

membrane. *B,* motoneurons like trochlear and oculomotor neurons which are supplied with splendid Ca^{2+} buffering molecules do not apparently need any other mechanisms to tackle the Ca^{2+} molecules entering the cell. In these cells mitochondria is predictably carrying out the primary function of energy production to drive the cellular metabolism, where these organelles are not employed to seize Ca^{2+} in a large way.

Loss of mitochondrial membrane potential, inhibition of molecular respiration & energy production can be very critical in ALS pathophysiology. The risk becomes much higher when mitochondria are placed cardinally to buffer the calcium and to control the subsequent metabolic pathways, since an uncontrolled elevation in the cytosolic Ca^{2+} can lead to immediate cell death.

Summary

Defined motoneuron populations in the brain stem and spinal cord are selectively damaged during pathophysiological conditions such as hypoxia and amyotrophic lateral sclerosis (ALS), which has been linked to perturbed Ca^{2+} metabolism and an exceptional vulnerability to mitochondrial disturbances. In this dissertation, the underlying factors in these pathomechanisms are studied by performing simultaneous patch-clamp recordings and CCD imaging in selectively vulnerable and resistant motoneurons in slice preparations from mouse brainstem. In the case of facial motoneurons (FMNs), which are vulnerable to cell death in ALS, disruption of the mitochondrial electrochemical potential ($\Delta\psi$) by bath application of the mitochondrial "uncoupler" FCCP (Carbonyl cyanide 4-trifluromethoxyphenylhydrazone) provoked a significant retardation of cytosolic calcium clearance rates and substantial Ca^{2+} release from mitochondrial stores. The application of the Sarco-Endoplasmic Reticular Calcium ATPase (SERCA) inhibitor CPA (Cyclopiazonic acid) to empty the endoplasmic reticular Ca^{2+} store, in the presence of FCCP, resulted in a separate, defined Ca^{2+} release, indicating that ER stores are able to operate independently of $\Delta\psi$. These results were similar to the observations from vulnerable hypoglossal motoneurons (HMNs), but were significantly different from observations made in selectively resistant oculomotor neurons (OMNs) and trochlear motoneurons (TMNs) under identical experimental conditions. Both the OMNs and TMNs only displayed minor Ca^{2+} release after FCCP application, where peak amplitudes were ~4-fold smaller compared to those in the FMNs & HMNs. Moreover, FCCP did not significantly affect cytosolic Ca^{2+} clearance rates in TMNs and OMNs.

On the basis of previous studies on Ca^{2+} dynamics of motoneurons, a detailed investigation on the buffering characteristics of FMNs and TMNs revealed their contrasting Ca^{2+} buffering capacities, where FMNs which succumb to death in ALS showed a low Ca^{2+} buffering capacity value of 46 and TMNs which resist the damage in ALS had a value of 392.

Further study of the calcium metabolism of facial motoneurons revealed that the low Ca^{2+} buffering property of facial motoneurons is achieved during the very first few days of post natal development. The basis for this study was the observation that depolarization induced Ca^{2+} transients of FMNs had comparatively slower decay patterns in post-natal day zero (P0) animals than in post-natal day 4 (or higher) animals, when studied under the same conditions of Fura-2 concentration. Accordingly, in P0 animals, facial motoneurons displayed a relatively high calcium buffering capacity value of 132. Furthermore, cytosolic calcium clearance rates were only mildly affected when mitochondria were disrupted by the application of FCCP at this developmental time point. In contrast, FMNs in animals at P4 & P10 displayed substantially lower Ks of 46 and a fast decay time for the voltage induced Ca^{2+} transients. It was obvious that even at the age of P4 itself, these neurons attain this substantially lower calcium buffering value. Furthermore mitochondrial disruption by FCCP provoked a significant retardation of cytosolic calcium clearance rates and prominent Ca^{2+} release from mitochondria at this age. A comparison of Ca^{2+} buffering properties by conducting similar experiments on ALS-resistant oculomotor neurons (OMNs) showed no significant difference in buffering capacity in P0 animals and the previously published value for P2-P6 animals (Vanselow et al, 2000). Taken together, these observations suggest that ALS vulnerable motoneurons are characterized by a low Ca^{2+} buffering capacity, leading to an intimate interaction of mitochondria and $[Ca^{2+}]i$ that optimizes the physiological coupling of metabolic and electrical activity. Under pathophysiological conditions, this specialisation creates a vicious circle where initial mitochondrial disturbances elevate motoneuron excitability and $[Ca^{2+}]i$, and the resulting augmentation in cellular energy demand accelerates deterioration of an already weakened metabolic system. It is also evident from this study that the selectively vulnerable facial motoneurons attain their specialized Ca^{2+} homeostasis in the first post-natal week of development, where the hallmarks of the developed neurons are low cytosolic calcium buffering capacities and a prominent role of mitochondria in the control of $[Ca^{2+}]i$.

Bibliography

Alexianu ME, Ho BK, Mohamed AH, La Bella V, Smith RG, Appel SH (1994) The role of calcium-binding proteins in selective motoneuron vulnerability in amyotrophic lateral sclerosis. *Ann Neurol* 36:846-58

Appel SH, Smith RG, Engelhardt JI, Stefani E (1994) Evidence for autoimmunity in amyotrophic lateral sclerosis. *J Neurol Sci*. 124 Suppl: 14-9. Review

Appel SH, Smith RG, Alexianu M, Siklos L, Engelhardt J, Colom LV, Stefani E (1995-96) Increased intracellular calcium triggered by immune mechanisms in amyotrophic lateral sclerosis. *Clin Neurosci*. 3(6):368-74. Review.

Babcock DF, Herrington J, Goodwin PC, Park YB & Hille B (1997) Mitochondrial participation in the intracellular Ca^{2+} network. *J Cell Biol* 136:833-844

Baron KT, Wang GJ, Padua RA, Campbell C, Thayer SANMDA-evoked consumption and recovery of mitochondrially targeted aequorin suggests increased Ca2+ uptake by a subset of mitochondria in hippocampal neurons. *Brain Res* 993:124-32.

Beckman JS, Beckman TW, Chen J, Marshall PA, Freeman BA (1990) Apparent hydroxyl radical production by peroxynitrite: implications for endothelial injury from nitric oxide and superoxide. *Proc Natl Acad Sci U S A*. 87(4):1620-4.

Borthwick GM, Johnson MA, Ince PG, Shaw PJ, Turnbull DM (1999) Mitochondrial enzyme activity in amyotrophic lateral sclerosis: implications for the role of mitochondria in neuronal cell death. *Ann Neurol*. 46:787-90.

Bowling AC, Schulz JB, Brown RH Jr, Beal MF (1993) Superoxide dismutase activity, oxidative damage, and mitochondrial energy metabolism in familial and sporadic amyotrophic lateral sclerosis. *J Neurochem*. 61(6):2322-5.

Brocard JB, Tassetto M, Reynolds IJ (2001) Quantitative evaluation of mitochondrial calcium content in rat cortical neurones following a glutamate stimulus. *J Physiol* 15:793-805.

Brown RH Jr, Robberecht W (2001) Amyotrophic lateral sclerosis: pathogenesis. *Semin Neurol*. 21:131-9. Review.

Bruijn LI, Houseweart MK, Kato S, Anderson KL, Anderson SD, Ohama E, Reaume AG, Scott RW, Cleveland DW (1998) Aggregation and motorneuron toxicity of an ALS-linked SOD1 mutant independent from wildtype SOD1. *Science* 281:1851–1854

Budd SL, Tenneti L, Lishnak T, Lipton SA (2000) Mitochondrial and extramitochondrial apoptotic signalling pathways in cerebrocortical neurons. *Proc Natl Acad Sci U S A*. 97:6161-6.

Bush AI (2002) Is ALS caused by an altered oxidative activity of mutant superoxide dismutase? *Nat Neurosci* 5:919 –920

Carri MT, Ferri A, Battistoni A, Famhy L, Gabbianelli R, Poccia F & Rotilio G (1997) Expression of a Cu,Zn superoxide dismutase typical of familial amyotrophic lateral sclerosis induces mitochondrial alteration and increase of cytosolic Ca^{2+} concentration in transfected neuroblastoma SH-SY5Y cells. *FEBS Lett* 414:365-8.

Carri MT, Ferri A, Cozzolino M, Calabrese L, RotilioG (2003) Neurodegeneration in amyotrophic lateral sclerosis: the role of oxidative stress andaltered homeostasis of metals. *Brain Res Bull* 61:365–374.

Carriedo SG, Sensi SL, Yin HZ & Weiss JH (2000) AMPA exposures induce mitochondrial $Ca^{(2+)}$ overload and ROS generation in spinal motor neurons in vitro. *J Neurosci* 20:240-50.

Colegrove SL, Albrecht MA, Friel DD (2000) Dissection of mitochondrial Ca^{2+} uptake and release fluxes in situ after depolarization-evoked $[Ca^{2+}](i)$ elevations in sympathetic neurons. *J Gen Physio* 11:351-70.

Cluskey S, Ramsden DB. (2001) Mechanisms of neurodegeneration in amyotrophic lateral sclerosis*. Mol Pathol*. 54(6):386-92. Review.

Darios F, Lambeng N, Troadec JD, Michel PP, Ruberg M (2003) Ceramide increases mitochondrial free calcium levels via caspase 8 and Bid: role in initiation of cell death. *J Neurochem* 84:643-54.

de Leon M, Covenas R, Narvaez JA, Aguirre JA, Gonzalez-Baron S (1993) Distribution of parvalbumin immunoreactivity in the cat brain stem. *Brain Res Bull* 32:639-46.

Duchen MR (2000) Mitochondria and calcium: from cell signalling to cell death. *J Physiol* 15:57-68.

Elliott JL, Snider WD Parvalbumin is a marker of ALS-resistant motor neurons. (1995) *Neuroreport*. 6(3):449-52.

Feeney CJ, Pennefather PS & Gyulkhandanyan AV (2003) A cuvette-based fluorometric analysis of mitochondrial membrane potential measured in cultured astrocyte monolayers. *J Neurosci Methods* 30:13-25.

Figelwicz DA, Krizus A, Martinoli MG, Meiniger V, Dib M, Rouleau GA, Julien JP (1994) Variants of the heavy neurofilament subunit are associated with the development of amyotrophic lateral sclerosis. *Hum Mol Genet*. 3:1757–1761.

Fujita K, Yamauchi M, Shibayama K, Ando M, Honda M, Nagata Y (1996) Decreased cytochrome c oxidase activity but unchanged superoxide dismutase and glutathione peroxidase activities in the spinal cords of patients with amyotrophic lateral sclerosis. *J Neurosci Res*. 1; 45:276-81.

Guegan C, Vila M, Rosoklija G, Hays AP, Przedborski S (2001) Recruitment of the mitochondrial-dependent apoptotic pathway in amyotrophic lateral sclerosis. *J Neurosci.* 1; 21:6569-76.

Guo H, Lai L, Butchbach ME, Stockinger MP, Shan X, Bishop GA, Lin CL (2003) Increased expression of the glial glutamate transporter EAAT2 modulates excitotoxicity and delays the onset but not the outcome of ALS in mice. *Hum Mol Genet.* 12(19):2519-32.

Gunter TE, Yule DI, Gunter KK, Eliseev RA, Salter JD (2004) Calcium and mitochondria. *FEBS Lett* 567: 6-102.

Gurney ME, Pu H, Chiu AY, Dal Canto MC, Polchow CY, Alexander DD, Caliendo J, Hentati A, Kwon YW, Deng H-X, Chen W, Zhai P, Sufit RL, Siddique T (1994) Motor neuron degeneration in mice that express a human Cu, Zn superoxide dismutase. *Science* 264:1772-1775.

Heath PR, Shaw PJ (2002) Update on the glutamatergic neurotransmitter system and the role of excitotoxicity in amyotrophic lateral sclerosis. *Muscle Nerve.* 26(4):438-58. Review.

Henry-Mowatt J, Dive C, Martinou JC, James D (2004) Role of mitochondrial membrane permeabilization in apoptosis and cancer. *Oncogene* 23:2850-60.

Hirano A (1991) Cytopathology of amyotrophic lateral sclerosis .*Adv Neurol.* 56:91-101

Hirano A, Nakano I, Kurland LT, Mulder DW, Holley PW, Saccomanno G (1984) Fine structural study of neurofibrillary changes in a family with amyotrophic lateral sclerosis. J. *Neuropathol. Exp. Neurol.* 43:471–80

Hongpaisan J, Winters CA, Andrews SB (2004) Strong calcium entry activates mitochondrial superoxide generation, upregulating kinase signaling in hippocampal neurons. *J Neurosci* 24:10878-87

Howland DS, Liu J, She Y, Goad B, Maragakis NJ, Kim B, Erickson J, Kulik J, DeVito L, Psaltis G, DeGennaro LJ, Cleveland DW, Rothstein JD (2002) Focal loss of the glutamate transporter EAAT2 in a transgenic rat model of SOD1 mutant-mediated amyotrophic lateral sclerosis (ALS). *Proc Natl Acad Sci U S A.* 99(3):1604-9.

Jackson M, Steers G, Leigh PN, Morrison KE (1999) Polymorphisms in the glutamate transporter gene EAAT2 in European ALS patients. *J Neurol.* 246(12):1140-4.

Jacobson J & Duchen MR (2004) Interplay between mitochondria and cellular calcium signalling. *Mol Cell Biochem* 256-257:209-18.

Kaal EC, Vlug AS, Versleijen MW, Kuilman M, Joosten EA & Bar PR (2000) Chronic mitochondrial inhibition induces selective motoneuron death in vitro: a new model for amyotrophic lateral sclerosis. *J Neurochem* 74:1158-65.

Kahlert S, Zundorf G, Reiser G (2005) Glutamate-mediated influx of extracellular Ca^{2+} is coupled with reactive oxygen species generation in cultured hippocampal neurons but not in astrocytes. *J Neurosci Res* 79:262-71.

Kanno T, Fujita H, Muranaka S, Yano H, Utsumi T, Yoshioka T, Inoue M & Utsumi K (2002) Mitochondrial swelling and cytochrome c release: sensitivity to cyclosporin A and calcium. *Physiol Chem Phys Med NMR* 34:91-102.

Kawamura Y, Dyck PJ, Shimono M, Okazaki H, Tateishi J, Doi H (1981) Morphometric comparison of the vulnerability of peripheral motor and sensory neurons in amyotrophic lateral sclerosis*. J. Neuropathol. Exp. Neurol*. 40:667–75.

Kirichok Y, Krapivinsky G & Clapham DE (2004) The mitochondrial calcium uniporter is a highly selective ion channel. *Nature* 22:360-4.

Kirkinezos IG, Bacman SR, Hernandez D, Oca-Cossio J, Arias LJ, Perez-Pinzon MA, Bradley WG, Moraes CT (2005) Cytochrome c association with the inner mitochondrial membrane is impaired in the CNS of G93A-SOD1 mice. *J Neurosci*. 5; 25:164-72.

Kong J & Xu Z (1998) Massive mitochondrial degeneration in motor neurons triggers the onset of amyotrophic lateral sclerosis in mice expressing a mutant SOD1. *J Neurosci* 18: 3241-50.

Ladewig T & Keller BU (2000) Simultaneous patch-clamp recording and calcium imaging in a rhythmically active neuronal network in the brainstem slice preparation from mouse. *Pflugers Arch* 440:322–332.

Ladewig T, Kloppenburg P, Lalley PM, Zipfel WR, Webb WW & Keller BU (2003) Spatial profiles of store-dependent calcium release in motoneurones of the nucleus hypoglossus from newborn mouse. *J Physiol* 547:775–787.

Leigh PN, Swash M.(1991) Cytoskeletal pathology in motorneuron diseases. *Adv Neurol*. 56:115-24. Review.

Leigh PN, Whitwell H, Garofalo O, Buller J, Swash M, Martin JE, Gallo JM, Weller RO, Anderton BH (1991) Ubiquitin-immunoreactive intraneuronal inclusions in amyotrophic lateral sclerosis. Morphology, distribution, and specificity. *Brain*. 114 (Pt 2):775-88.

Lips MB & Keller BU (1998) Endogenous calcium buffering in motoneurones of the nucleus hypoglossus from mouse. *J Physiol* 511:105–117.

Lips MB & Keller BU (1999) Activity-related calcium dynamics in motoneurons of the nucleus hypoglossus from mouse. *J Neurophysiol* 82:2936–2946

Liu R, Althaus JS, Ellerbrock BR, Becker DA, Gurney ME (1998) Enhanced oxygen radical production in a transgenic mouse model of familial amyotrophic lateral sclerosis. *Ann Neurol*. 44:763-70.

Liu R, Narla RK, Kurinov I, Li B, Uckun FM (1999) Increased hydroxyl radical production and apoptosis in PC12 neuron cells expressing the gain-of-function mutant G93A SOD1 gene. *Radiat Res. Feb*; 151:133-41.

Liu D, Wen J, Liu J, Li L (1999) The roles of free radicals in amyotrophic lateral sclerosis: reactive oxygen species and elevated oxidation of protein, DNA, and membrane phospholipids. *FASEB J* 13:2318-28.

Liu J, Lillo C, Jonsson PA, Velde CV, Ward CM, Miller TM, Subramaniam JR, Rothstein JD, Marklund S, Andersen PM, Brannstrom T, Gredal O, Wong PC, Williams DS, ClevelandDW (2004) Toxicity of familial ALS-linked SOD1 mutants from selective recruitment to spinal mitochondria. *Neuron* 43:5–17.

Llinas R, Sugimori M, Cherksey BD, Smith RG, Delbono O, Stefani E, Appel S (1993) IgG from amyotrophic lateral sclerosis patients increases current through P-type calcium channels in mammalian cerebellar Purkinje cells and in isolated channel protein in lipid bilayer. *Proc Natl Acad Sci U S A*. 90(24):11743-7.

Maragakis NJ, Rothstein JD (2001) Glutamate transporters in neurologic disease. *Arch neurol*. 58(3):365-70. Review.

Malli R, Frieden M, Osibow K, Zoratti C, Mayer M, Demaurex N, Graier WF (2003) Sustained Ca^{2+} transfer across mitochondria is Essential for mitochondrial Ca^{2+} buffering, store-operated Ca^{2+}entry, and Ca^{2+} store refilling. *J Biol Chem* 45:44769-79.

Mattiazzi M, D'Aurelio M, Gajewski CD, Martushova K, Kiaei M, Beal MF, Manfredi G (2002) Mutated human SOD1 causes dysfunction of oxidative phosphorylation in mitochondria of transgenic mice. *J Biol Chem* 277: 29626-33.

Medina L, Figueredo-Cardenas G, Rothstein JD, Reiner A (1996) Differential abundance of glutamate transporter subtypes in amyotrophic lateral sclerosis (ALS)-vulnerable versus ALS-resistant brain stem motor cell groups. *Exp Neurol*. 142:287-95.

Mendonca DM, Chimelli L, Martinez AM (2005) Quantitative evidence for neurofilament heavy subunit aggregation in motor neurons of spinal cords of patients with amyotrophic lateral sclerosis. *Braz J Med Biol Res*. 38(6):925-33.

Menzies FM, Cookson MR, Taylor RW, Turnbull DM, Chrzanowska-Lightowlers ZM, Dong L, Figlewicz DA & Shaw PJ (2002) Mitochondrial dysfunction in a cell culture model of familial amyotrophic lateral sclerosis. *Brain* 125:1522–1533.

Morrison BM, Janssen WG, Gordon JW, Morrison JH (1998) Time course of neuropathology in the spinal cord of G86R superoxide dismutase transgenic mice. *J Comp Neurol*. 391(1):64-77.

Morrison BM, Gordon JW, Ripps ME, Morrison JH. (1996) Quantitative immunocytochemical analysis of the spinal cord in G86R superoxide dismutase transgenic mice: neurochemical correlates of selective vulnerability. *J CompNeurol*.373(4):619-31.

Morrison BM, Morrison JH (1999) Amyotrophic lateral sclerosis associated with mutations in superoxide dismutase: a putative mechanism of degeneration. *Brain Res Brain Res Rev*. 29(1):121-35.

Mostafapour SP, Lachica EA, Rubel EW (1997) Mitochondrial regulation of calcium in the avian cochlear nucleus. *J Neurophysiol* 78:1928-34.

Murphy AN, Fiskum G, Beal MF (1999) Mitochondria in neurodegeneration: bioenergetic function in cell life and death. *J Cereb Blood Flow Metab* 19:231-45.

Neher E (1995) The use of fura_2 for estimating Ca buffers and Ca fluxes. *Neuropharmacology* 34, 1423—1442.

Neher E, & Augustine G J (1992) Calcium gradients and buffers in bovine chromaffin cells. *Journal of Physiology* 450, 273—301.

Oeda T, Shimohama S, Kitagawa N, Kohno R, Imura T, Shibasaki H, Ishii N (2001) Oxidative stress causes abnormal accumulation of familial amyotrophic lateral sclerosis-related mutant SOD1 in transgenic Caenorhabditis elegans. *Hum Mol Genet*. 10:2013-23.

Palecek J, Lips MB & Keller BU (1999) Calcium dynamics and buffering in motoneurones of the mouse spinal cord. *J Physiol* 520:485–502.

Paxinos et al., Chemoarchitectonic atlas of the rat brainstem, Academic Press, 1999

Pivovarova NB, Hongpaisan J, Andrews SB, Friel DD (1999) Depolarization-induced mitochondrial Ca accumulation in sympathetic neurons: spatial and temporal characteristics. *J Neurosci* 19:6372-84.

Pivovarova NB, Nguyen HV, Winters CA, Brantner CA, Smith CL, Andrews SB (2004) Excitotoxic calcium overload in a subpopulation of mitochondria triggers delayed death in hippocampa lneurons. *J Neurosci* 24:5611-22.

Pogun S, Dawson V, Kuhar MJ (1994) Nitric oxide inhibits 3H-glutamate transport in synaptosomes. *Synapse*. 18(1):21-6.

Rao SD, Weiss JH (2004) Excitotoxic and oxidative cross-talk between motor neurons and glia in ALS pathogenesis. *Trends Neurosci*. 27:17-23.

Rizzuto R, Duchen MR, Pozzan T (2004) Flirting in little space: the ER/mitochondria Ca^{2+} liaison. *Sci STKE*.13;2004(215):re1. Review.

Rizzuto R, Bastianutto C, Brini M, Murgia M, Pozzan T (1994) Mitochondrial Ca^{2+} homeostasis in intact cells. *J Cell Biol* 126:1183-94.

Rizzuto R, Brini M, Pozzan T (1993) Intracellular targeting of the photoprotein aequorin: a new approach for measuring, in living cells, Ca^{2+} concentrations in defined cellular compartments. *Cytotechnology* 11:44-6.

Rizzuto R, Simpson AW, Brini M, Pozzan T (1992) Rapid changes of mitochondrial Ca^{2+} revealed by specifically targeted recombinant aequorin. *Nature* 23:325-7.

Rothstein JD, Martin LJ, Kuncl RW. (1992) Decreased glutamate transport by the brain and spinalcord in amyotrophic lateral sclerosis. *N Engl J Med*. 326(22):1464-8.

Rosen DR, Bowling AC, Patterson D, Usdin TB, Sapp P, Mezey E, McKenna-Yasek D, O'Regan J, Rahmani Z, Ferrante RJ, et al. (1994) A frequent ala 4 to val superoxide dismutase-1 mutation is associated with a rapidly progressive familial amyotrophic lateral sclerosis. *Hum Mol Genet*. Jun;3(6):981-7.

Rosen DR, Siddique T, Patterson D, Figlewicz DA, Sapp P, Hentati A, Donaldson D, Goto J, O'Regan JP, Deng HX, et al. (1993) Mutations in Cu/Zn superoxide dismutase gene are associated with familial amyotrophic lateral sclerosis. *Nature*. 362(6415):59-62.

Rosenstock TR, Carvalho AC, Jurkiewicz A, Frussa-Filho R, Smaili SS (2004) Mitochondrial calcium, oxidative stress and apoptosis in a neurodegenerative disease model induced by 3-nitropropionic acid. *J Neurochem* 88:1220-8.

Roy J, Minotti S, Dong L, Figlewicz DA & Durham HD (1998) Glutamate potentiates the toxicity of mutant Cu/Zn-superoxide dismutase in motor neurons by postsynaptic calcium-dependent mechanisms. *J. Neurosci* 18: 9673-9684.

Rutter GA, Burnett P, Rizzuto R, Brini M, Murgia M, Pozzan T, Tavare JM, Denton RM (1996) Subcellular imaging of intramitochondrial Ca^{2+} with recombinant targeted aequorin: significance for the regulation of pyruvate dehydrogenase activity. *Proc Natl Acad Sci USA* 28:5489-94.

Rutter GA, Theler JM, Murgia M, Wollheim CB, Pozzan T, Rizzuto R (1993) Stimulated Ca^{2+} influx raises mitochondrial free Ca^{2+} to supramicromolar levels in a pancreatic beta-cell line. Possible role in glucose and agonist-induced insulin secretion.*J Biol Chem* 25:2385-90.

Said Ahmed M, Hung WY, Zu JS, Hockberger P, Siddique T (2000) Increased reactive oxygen species in familial amyotrophic lateral sclerosis with mutations in SOD1. *J Neurol Sci*. 15; 176:88-94.

Sasaki S, Iwata M (1996) Ultrastructural study of synapses in the anterior horn neurons of patients with amyotrophic lateral sclerosis. *Neurosci Lett*. 204(1-2):53-6.

Sasaki S, Warita H, Abe K, Iwata M.(2005) Impairment of axonal transport in the axon hillock and the initial segment of anterior horn neurons in transgenic mice with a G93A mutantSOD1gene. *Acta Neuropathol* (Berl). 110:48-56.

Sasaki S, Warita H, Murakami T, Abe K & Iwata M (2004) Ultrastructural study of mitochondria in the spinal cord of transgenic mice with a G93A mutant SOD1 gene. *Acta Neuropathol* 107:461-74.

Schinder AF, Olson EC, Spitzer NC, Montal M (1996) Mitochondrial dysfunction is a primary event in glutamate neurotoxicity. *J Neurosci* 16:6125-33.

Shishkin V, Potapenko E, Kostyuk E, Girnyk O, Voitenko N, Kostyuk P (2002) Role of mitochondria in intracellular calcium signaling in primary and secondary sensory neurones of rats. *Cell Calcium* 32:121-30.

Siklos L, Engelhardt J, Harati Y, Smith RG, Joo F, Appel SH (1996) Ultrastructural evidence for altered calcium in motor nerve terminals in amyotropic lateral sclerosis. *Ann Neurol*. 39:203-16.

Vanselow BK & Keller BU (2000) Calcium dynamics and buffering in oculomotor neurones from mouse that are particularly resistant during amyotrophic lateral sclerosis (ALS)-related motoneurone disease. *J Physiol* 525:433-445.

Vielhaber S, Kunz D, Winkler K, Wiedemann FR, Kirches E, Feistner H, Heinze HJ, Elger CE, Schubert W, Kunz WS (2000) Mitochondrial DNA abnormalities in skeletal muscle of patients with sporadic amyotrophic lateral sclerosis. *Brain*. 123 (Pt 7):1339-48.

Wang GJ, Thayer SA (2002) NMDA-induced calcium loads recycle across the mitochondrial inner membrane of hippocampal neurons in culture. *J Neurophysiol* 87:740-9.

Ward MW, Kushnareva Y, Greenwood S, Connolly CN (2005) Cellular and subcellular calcium accumulation during glutamate-induced injury in cerebellar granule neurons. *J Neurochem* 92:1081-90.

Ward MW, Rego AC, Frenguelli BG, Nicholls DG (2000) Mitochondrial membrane potential and glutamate excitotoxicity in cultured cerebellar granule cells. *J Neurosci* 20:7208-19.

Warita H, Hayashi T, Murakami T, Manabe Y, Abe K (2001) Oxidative damage to mitochondrial DNA in spinal motoneurons of transgenic ALS mice. *Brain Res Mol Brain Res*. 89:147-52.

Wiedau-Pazos M, Goto JJ, Rabizadeh S, Gralla EB, Roe JA, Lee MK, Valentine JS, Bredesen DE (1996) Altered reactivity of superoxide dismutase in familial amyotrophic lateral sclerosis. *Science.* 271(5248):515-8.

Wiedemann FR, Winkler K, Kuznetsov AV, Bartels C, Vielhaber S, Feistner H, Kunz WS (1998) Impairment of mitochondrial function in skeletal muscle of patients with amyotrophic lateral sclerosis. *J Neurol Sci*. 156(1):65-72.

Williams TL, Day NC, Ince PG, Kamboj RK, Shaw PJ (1997) Calcium-permeable alpha-amino-3-hydroxy-5-methyl-4-isoxazole propionic acid receptors: a molecular determinant of selective vulnerability in amyotrophic lateral sclerosis. *Ann Neurol* 42: 200-7.

Wong PC, Pardo CA, Borchelt DR, Lee MK, Copeland NG, Jenkins NA, Sisodia SS, Cleveland DW, Price DL (1995) An adverse property of a familial ALS-linked SOD1 mutation causes motor neuron disease characterized by vacuolar degeneration of mitochondria. *Neuron*. 14:1105-16.

Wyatt CN, Buckler KJ (2004) The effect of mitochondrial inhibitors on membrane currents in isolated neonatal rat carotid body type I cells. *J Physiol* 556:175-91.

Acknowledgements

It is my great pleasure to thank the many people who made this thesis possible.

I would like to record my unfathomable gratitude to my Supervisor Prof. Dr. Bernhard Keller for the insightful discussions during the development of the ideas in this thesis. He has constantly helped me to remain focused on achieving my goal. His observations and comments helped me to establish the overall direction of the research and to move forward with the investigation in depth. I also thank him for the technical support, lab-facilities; and in special for the perfect financial support throughout the project period. I express my sincere thanks to Prof. Dr. Reinhold Hustert for agreeing to be the referent and main examiner for my thesis. I am very grateful to Prof. Dr. Friedrich-Wilhelm Schürmann for granting permission to be the co-referent of my thesis. I express my deep gratitude to Prof. Dr. R. Ficner and Priv.-Doz. Dr. M. Hoppert for being my examiners; Prof. Dr. Fritz and Prof. Dr. C. Gatz for agreeing to be the Reviewers for my thesis. I am very grateful to Friederike von Lewinski, MD, PhD, for being a fantastic colleague, and teacher for Fluorescence imaging / Patch clamp technique. The scientific discussions with her nourished the successful completion of this research. I express my Sincere thanks to Prof. Dr. Diethelm W. Richter, Head of the Department for all the support to fulfil my research. I state my gratitude to Prof. Dr. Detlev Schild for the kind support through Graduate college. I thank Dr. Evgeni Ponimaskin for allowing me to use the cell culture facilities, agreeing to be my referee and for the kind help with the manuscript. I also thank Priv.-Doz. Dr. Weiqi Zhang and Prof. Dr. Markus Missler for allowing me to share the lab facilities.

I express my sincere thanks to Susan, Uwe and Axel for their tremendous support through timely supply of the experimental animals. Without their support the successful development of the project would have been impossible. The technical support from Ms. Dagmar Czran and   Ms. Cornelia Hühne is gratefully appreciated and acknowledged. I am thankful to Ms. Regina Sommer-kluß, our Secretary, for her unlimited support with official matters. I extend my gratitude to the workshop members in the Physiology Institute for the

excellent technical support and help with the instruments. Thank you, Manoj for being a nice colleague and helping me in organising the lab. Thank you very much Gaby for the help in the cell culture lab and helping to improve my German. Thanks Gayane for the friendly chats. Thanks to all other colleagues from Physiology Institute for creating a pleasant work environment. Thanks to Peter Funk, Howard Schultens, and Wayne Sidio for the timely help with computers.

Without the support of my loving friends, the completion of the thesis seemed impossible. Thanks beyond words to Dhushan, for supporting, helping, encouraging, caring about me all throughout my stay here and being there for me at extremely difficult times. I very much appreciate his interest in helping to improve the quality of my thesis presentation. Very Special thanks to Davis for his care, countless helps and suggestions to keep me focused. Thanks a lot Smita, for our steady friendship and helpful suggestions to keep me motivated. Thanks a million to Elena for being my best friend and for the relaxing phone calls and long chats; it really helped me in difficult times. Special thanks to Peter and Lila for their deep friendship with me and long conversations and discussions. Thanks to Sujesh and Arun for being there for me. Thank you very much Amme, for your loving emails and prayers. Thanks to Sajeevan and Jaleel for the encouragement. I state my sincere thanks to Malaiyalam for his the timely help with the thesis preparation and submission procedures. Big thanks to Phil for taking time to read and correct my thesis at short notice. Thanks very much too to all my friends from Göttingen Cricket team for keeping my spirits high. Thank you very much Tina, for being a caring friend and constantly helping me to improve my German. Thanks to Ravi and Sarbani for caring about me. Thanks to Tanja for the friendly conversations. Thanks to Wolf Zech for the help with translation.

I express my deep gratitude to Prof. Dr. Babu Philip, Dr. A.V Saramma, and Dr. Rosamma Philip, for helping me to achieve this PhD position.

I express my loving gratitude to my parents and Seena for their love, prayers and moral support to keep myself strong and steady to excel in my PhD study.

Above all I thank God for everything.

Manuscripts

1,   Ute Renner, Konstantin Glebov, Ekaterina Papoucheva, **Saju Balakrishnan**, Bernhard U. Keller, Thorsten Lang, Reinhard Jahn, Diethelm Richter, Evgeni Ponimaskin (2006) Localization of the 5-HT1A receptor in lipid rafts is important for the receptor interaction with heterotrimeric Gi protein and is dependent on receptor palmitoylation. *In Review* (EMBO)

2,   **Saju Balakrishnan**, Bernhard U. Keller (2006) Mitochondria differentially regulate $[Ca^{2+}]i$ in brain stem motoneurons that are selectively vulnerable or resistant in ALS-related motoneuron disease. *In preparation.*

3,   **Saju Balakrishnan**, Bernhard U. Keller(2006) Developmental changes in $[Ca^{2+}]i$ homeostasis in facial motoneurons that are selectively vulnerable in ALS-related motoneuron disease. *In preparation.*

4   Miriam Lotz, Wolf-Dieter Zech, Manoj K Jaiswal, **Saju Balakrishnan**, Sandra Ebert, Maria Teresa Carri, Bernhard U. Keller and Roland Nau. (2006) Expression of a Cu Zn superoxide dismutase typical for familial amyotrophic lateral sclerosis increases the vulnerability of neuroblastoma cells to infectious injury. *In preparation.*

Meetings attended and presentations:

German Neuroscience meeting (2003) Goettingen, Germany.
Intracellular calcium signalling in motoneuron and a non-motoneuron cell line: potential implications for amyotrophic lateral sclerosis (ALS): *Poster*.

German Physiology meeting (2004) Leipzig, Germany
Two - photon NADH imaging in the hypoglossal nucleus – implications for differential neuronal and astrocytic metabolism: *Poster*.

SFN International neuroscience meeting (2004) San Diego California, USA.
Mitochondria differentially regulate $[Ca^{2+}]i$ in brainstem motoneurons from mouse: implications for selective motoneuron vulnerability: *Poster*.

German Neuroscience meeting & German Physiology meeting (2005) Goettingen, Germany.
Mitochondria differentially regulate $[Ca^{2+}]i$ in ALS vulnerable and resistant brainstem motoneurons from mouse: implications for selective motoneuron vulnerability: *Poster*.

SFN International neuroscience meeting (2005) Washington DC, USA.
Developmental changes of cytosolic Ca^{2+} homeostasis of Facial Motoneurons from mouse: implications for selective motoneuron vulnerability in ALS: *Slide presentation*.

German Physiology meeting (2006) Munich, Germany

Developmental changes of cytosolic Ca^{2+} homeostasis of Facial Motoneurons from mouse: implications for selective motoneuron vulnerability in ALS: *Poster selected for young FEPS (Federation of European Physiological Societies) award presentation*.

Curriculum Vitae

Name: Saju Balakrishnan.

Date of Birth: 21.02.1977.

Father's Name: E. K. Balakrishnan

Mother's Name: Santha Balakrishnan

Place of Birth: Ollur, Kerala, India.

1992 - 1994:   Pre-University, Sacred Heart College, Cochin, India.

1994 - 1997:   Bachelor of Science in Zoology, Sacred Heart College, Cochin, India.

1997 - 2000:   Master of Science in Marine Biology, Cochin University of Science & technology, India.

           M.Sc Dissertation: Distribution of fish eggs and larvae in Indian waters.

2000 - 2002:   Worked as Junior Research Fellow (CSIR) Indian Institute of Chemical Biology, Calcutta, India.

2002 - 2006   Doctorate student under Prof. Dr. Bernhard U. Keller, Zentrum Physiologie & Pathophysiologie, University of Goettingen, Germany.